HEINRICH HEINE
UNIVERSITÄT DÜSSELDORF

# Therapeutic Knockdown of the Prion Protein

Inaugural-Dissertation

zur Erlangung des Doktorgrades der
Mathematisch-Naturwissenschaftlichen Fakultät
der Heinrich-Heine-Universität Düsseldorf

vorgelegt von
**Julian Victor**
aus Hamburg-Bergedorf

Düsseldorf, Dezember 2017

aus dem Institut für Physikalische Biologie
der Heinrich-Heine-Universität Düsseldorf

Gedruckt mit der Genehmigung der
Mathematisch-Naturwissenschaftlichen Fakultät der
Heinrich-Heine-Universität Düsseldorf

Berichterstatter:

1. Prof. Dr. Dieter Willbold

2. Prof. Dr. Dr. h.c. Detlev Riesner

Tag der mündlichen Prüfung: 23. Januar 2018

# Eidesstattliche Erklärung

Ich versichere an Eides Statt, dass die Dissertation von mir selbständig und ohne unzulässige fremde Hilfe unter Beachtung der „Grundsätze zur Sicherung guter wissenschaftlicher Praxis an der Heinrich-Heine-Universität Düsseldorf“ erstellt worden ist.

Düsseldorf, den 18. April 2018

Julian Victor

# Summary

Prion diseases are debilitating, fatal brain disorders in humans and animals. They are caused by misfolding of the endogenous prion protein (PrP) from a soluble conformational isomer $PrP^{C}$ to the insoluble aggregation-prone $PrP^{Sc}$ conformation. The process culminates in the formation of large, pathogenic protein aggregates which requires the constant production of $PrP^{C}$. It is for this reason that the knockdown of prion protein expression has been regarded as a viable therapeutic option. This work explores the use of the RNA-cleaving 10-23 DNAzyme as a new type of knockdown agent for the treatment of prion diseases. Similarly to ribozymes, DNAzymes consist of a catalytic core and flanking DNA segments which form double strands with the regions of the RNA adjacent to a cleavage site.

Accessible target sites for DNAzyme-mediated cleavage in the prion protein mRNA were predicted *in silico* with the use of a sequential folding algorithm. Specifically designed DNAzymes cleave short RNA substrates with high sequence specificity. Rational adjustments to the DNAzymes enable them to perform multiple turnover cleavage. Furthermore, highly structured PrP RNA transcripts are cleaved by DNAzymes according to their *in silico* predicted accessibility. Unexpectedly, treatment of WAC 2 neuroblastoma cells with DNAzymes introduced into the cells did not result in an effective knockdown of prion protein expression. However, specific siRNA molecules for the same target sites lowered $PrP^{C}$ levels substantially. Analysis of cleavage kinetics revealed that DNAzyme activity is highly sensitive to changes in $Mg^{2+}$ concentrations in the submillimolar range. The data suggest that binding of at least three $Mg^{2+}$ ions is required for sizeable DNAzyme activity and the low intracellular concentration of free $Mg^{2+}$ ions is most probably responsible for the failure of DNAzymes in cells.

The initial aim of this work involved the delivery of DNAzymes into brain-derived cells with the use of virus-like particles (VLPs) derived from the John Cunningham virus which were prepared by NEUWAY Pharma AG in cooperation with Dr. Manninga. Because of the lacking DNAzyme activity *in vivo* it was attempted to deliver siRNA molecules and shRNA expression plasmids into WAC 2 cells via VLPs. However, it had to be concluded that JC virus-derived VLPs are at the present not suitable for the targeted delivery of therapeutic nucleic acids into WAC 2 cells.

Although a DNAzyme-mediated knockdown of prion protein expression in cells could not be achieved the work at hand provides valuable information about the characteristics and mode of action of DNAzymes, especially in respect to their $Mg^{2+}$ ion dependency. Furthermore, highly potent siRNAs and shRNA expression plasmids were developed. These knockdown agents could serve as a basis for therapeutic strategies for the treatment of prion diseases. In this regard, future efforts should be directed at developing DNAzymes with a lower $Mg^{2+}$ ion dependency and combining siRNAs and

shRNA expression plasmids with the plethora of techniques that are being developed for the targeted delivery of therapeutics to the brain.

# Zusammenfassung

Prionenerkrankungen sind neurodegenerative Leiden mit tödlichem Verlauf bei Mensch und Tier. Sie werden durch die Fehlfaltung des körpereigenen Prion-Proteins (PrP) von einer löslichen Konformation ($PrP^C$) in eine unlösliche Konformation ($PrP^{Sc}$) ausgelöst. Das fehlgefaltete Protein aggregiert zu pathogenen Protein-Ablagerungen. Da für das Ausbilden dieser Ablagerungen die anhaltende Produktion weiterer $PrP^C$-Monomere unabdingbar ist, wurde eine Reduktion der Prion-Protein-Expression als therapeutische Maßnahme vielfach in Betracht gezogen. Die vorliegende Arbeit befasst sich mit dem RNA-spaltenden 10-23 DNAzym, welches ähnlich wie Ribozyme Doppelstränge mit einer RNA-Zielsequenz ausbildet und diese mithilfe eines katalytischen Zentrums zwischen den beiden Segmenten spaltet.
Potenzielle DNAzym-Schnittstellen innerhalb der mRNA des Prion-Proteins wurden *in silico* auf ihre Zugänglichkeit hin untersucht. In einer ersten Serie wurden kurze RNA-Substrate von speziell konzipierten DNAzymen sequenzspezifisch gespalten. Die DNAzyme können für eine katalyische Verwendung angepasst werden, sodass die Spaltung von RNA-Substraten im Überschuss gewährleistet ist. Auch strukturierte PrP-RNA-Transkripte werden durch diese DNAzyme gespalten. Dabei stimmt die Effizienz der Spaltung mit der zuvor ermittelten Zugänglichkeit der Schnittstellen überein. Die Behandlung der Zelllinie WAC 2 mit eingeschleusten DNAzymen resultiert unerwarteterweise nicht in einer Reduktion des exprimierten $PrP^C$, während der Einsatz entsprechender siRNA und von einem Plasmid exprimierter shRNA den $PrP^C$-Spiegel beträchtlich senkt. Kinetische Untersuchungen zeigen dass die Aktivität des DNAzyms drastisch von der $Mg^{2+}$-Konzentration abhängt. Für die Aktivität des DNAzyms ist die Bindung von mindestens drei $Mg^{2+}$-Ionen notwendig. Diese Ergebnisse legen den Schluss nahe, dass unter anderem die geringe Konzentration an freiem $Mg^{2+}$ für die geringe Aktivität der DNAzyme in Zellen verantwortlich ist.
Ein weiteres Ziel dieser Arbeit war es, in Zusammenarbeit mit Dr. Manninga (NEUWAY Pharma AG) virusartige Partikel (VLPs) auf ihre Fähigkeit hin zu untersuchen, therapeutische Nukleinsäuren in Zellen einzuschleusen. Dabei wurden anstatt der ursprünglich vorgesehenen DNAzyme hochpotente siRNA-Moleküle und shRNA-Expressions-Plasmide eingesetzt. Umfangreiche Versuche mit den von der NEUWAY Pharma AG präparierten VLPs waren für das vorliegende Zellmodell zur Zeit noch nicht erfolgreich.
Die in dieser Arbeit durchgeführten Experimente erlauben einen detaillierten Einblick in die Prinzipien die der Aktivität des DNAzyms zugrunde liegen. Insbesondere wurden wertvolle Daten bezüglich der Abhängigkeit des DNAzyms von $Mg^{2+}$-Ionen erhalten. Die siRNA-Moleküle und shRNA-Expressions-Plasmide, die in dieser Arbeit entwickelt wurden, bilden eine Grundlage für zukünftige Behandlungsmöglichkeiten

für Prionenerkankungen. DNAzyme müssten so modifiziert werden, dass sie eine geringere Abhängigkeit von $Mg^{2+}$-Ionen ausweisen. Eine umfangreiche Methodik zum gehirnspezifischen Wirkstofftransport muss mit diesen Molekülen kombiniert werden.

# Table of contents

# 1 Introduction

## 1.1 Transmissible spongiform encephalopathies

Creutzfeldt-Jakob disease (CJD) is a debilitating brain disorder that was first described independently by Hans Gerhard Creutzfeldt and Alfons Maria Jakob in the early 1920s (Creutzfeldt, 1920; Jakob, 1921). Patients suffering from CJD present with a range of neurological and psychological symptoms such as ataxia, speech impediments, impaired vision, irritability, anxiety, depression, dementia, and insomnia. Over the course of disease physical and mental capabilities steadily decline. Within months, patients become confined to bed and lose the ability to interact with their surroundings. CJD is a terminal condition and death at later stages is usually due to pneumonia or respiratory failure. To this day no cure for CJD exists and treatment of patients is restricted to palliative care.

The discovery of a disease similar to CJD would lead to important insights into the nature and transmission of the two pathologies even though their connection was not noted at the time (see Hörnlimann et al (2001) for a detailed historical description). By the 1950s, a catastrophic epidemic affected the Fore people, an ethnic group of about 11,000 people in Papua New Guinea, killing more than 2,500 individuals. The natives named the sickness kuru, which means shivering or trembling in their language, to reflect the characteristic tremor that victims suffered from. Kuru progresses over an average of 12 months from headaches and pains in limbs and joints to unprovoked laughter, speaking difficulties, severe ataxia and tremors that further deteriorate until the eventual death of the patient.

American virologist D.C. Gajdusek was determined to systematically characterize kuru and identify its cause. While spending several years as head of a hospital in Fore territory, he examined hundreds of kuru patients, collected clinical histories and samples and conducted autopsies (Hörnlimann et al, 2001). Tissue samples were transported to Australia and the US for histological analysis. The pathologist I. Klatzko, who worked closely together with Gajdusek, soon noted that kuru resembled CJD. Based on pathological studies, Gajdusek concluded that kuru was a degenerative disease that exclusively affects the brain. He was unable to find external risk factors or evidence for an infectious etiology. This led him to believe in a genetic cause for kuru (Gajdusek and Zigas, 1959). When Gajdusek published his hypothesis, epidemiologist L.T. Kurland and colleagues raised doubts about this explanation (Williams et al, 1964). A hereditary cause could not explain the abrupt rise in incidence and the similar manifestation of kuru in children and adults. Furthermore, cases of women from kuru-free tribes that contracted kuru after moving into Fore territory due to marriage argued against a gene-

tic cause. While the Fore themselves firmly believed witchcraft to be the cause of kuru, contemporary accounts by outsiders blamed the spread of kuru on the Fore peoples' practice of endocannibalism. The Fore consumed their dead as a funerary practice. The brains of the deceased were usually eaten by women and children, who where also more likely to contract the disease than adult males. This argued for an infectious agent in the brain which is passed on. But Gajdusek's colleague C.J. Gibbs jr. carried out many failed attempts to transmit the disease to laboratory animals. When Gajdusek organized an exhibition on kuru in London, microscopic pictures of histological samples that were acquired by Klatzko were displayed. These prompted W.J. Hadlow to draw the connection between kuru and scrapie, a neurodegenerative disease in sheep and goats which had been known for centuries (Hadlow, 1959). Not only did the two diseases share a similar pathology, researchers had also been able to show that scrapie was transmissible. Hadlow suggested experimental transmission of kuru to apes and pointed out the long incubation time between exposure and disease outbreak that was known for scrapie. Following Hadlow's advice, Gajdusek was able to prove that kuru was transmissible by inoculating primates with brain matter from a confirmed case of kuru (Gajdusek et al, 1966). This procedure successfully transmitted the disease and led to kuru-like symptoms after more than one and a half years. In their earlier attempts, Gibbs and Gajdusek simply did not wait long enough for symptoms to appear. Experimental transmission was later repeated with brain homogenate from patients that died as a result of CJD or Gerstmann-Sträussler-Scheinker syndrome, a condition with similar, but slower, disease progression (Gibbs et al, 1968; Masters et al, 1981). His work on kuru later earned Gajdusek the Nobel Prize in Physiology or Medicine.

By the 1960s, kuru incidence began to markedly decrease (Hörnlimann et al, 2001). This was due to the Australian legislature banning the practice of endocannibalism, which however was not motivated by the kuru epidemic since the connection was not known at the time. It later turned out that parenteral exposition to infectious material was a more likely explanation for the disparate risks in women and children than the actual consumption of brains. Since women and children carried the responsibility for preparing meals, also from the bodies of deceased family members, their hands were exposed to infectious material that was often passed to small cuts or the conjunctiva when the natives applied substances to their skin and faces to protect from cold and insects.

Today, the term transmissible spongiform encephalopathies (TSEs) is used to summarize several diseases in humans and animals with a common etiology (Collinge, 2001). Among them are CJD and kuru, fatal familial insomnia (FFI), and Gerstmann-Sträussler-Scheinker syndrome (GSS) in humans, scrapie in sheep and goats, bovine spongiform encephalopathy in cattle (BSE, also known as mad cow disease), and chronic wasting disease (CWD) in elk and other Cervidae. Progression of TSEs is accom-

panied by profound histological changes. The brain undergoes spongiform change due to neurodegeneration which in turn leads to astrogliosis. Manifestation and severity of symptoms may vary greatly between cases. The term transmissible spongiform encephalopathy highlights both the transmissible nature and the brain tissue degeneration that occurs during disease progression. Besides that, TSEs also share an uncommonly long incubation period between exposition and the first onset of symptoms. It must be noted that the search for the causative agent has almost exclusively been carried out in scrapie models. It was only later discovered that the disorders that are now summarized as TSEs share a common etiology. But, as the scrapie kuru connection indicated early on, all TSEs are linked by a common transmissible agent. However, the nature and identity of this infectious agent remained elusive for years to come.

## 1.2 The prion

Historically, most scientists and veterinarians believed scrapie to be the consequence of a slow virus infection (Sigurdsson, 1954). In addition, a plethora of alternative explanations existed that placed hypothetical replicating agents at the heart of scrapie, such as polysaccharides in membranes (Gibbons and Hunter, 1967), replicating proteins, etc. (Pattison and Jones, 1967; Griffith, 1967).

The long incubation time after exposure to the transmissive agent is in accordance with what is known of lentivirus infections. However, attempts to inactivate the alleged scrapie virus revealed a high resistance to ultraviolet and ionizing irradiation (Latarjet et al, 1970; Alper et al, 1978; Gibbs et al, 1978). This led to the suggestion that nucleic acids might not be an active component of the infectious agent, which makes the viral hypothesis unlikely. On the contrary, methods that inactivate or modify proteins markedly reduced scrapie infectivity (Prusiner et al, 1981). From there it was not much later that Stanley Prusiner developed the prion hypothesis in which proteins are the causative agent of disease (Prusiner, 1982). He coined the term prion for a **pro**teinacous **in**fectious particle that is able to amplify and cause disease. Shortly after, the protein that makes up major portions of the prion was isolated from infected Syrian golden hamster brains and given the name prion protein (PrP) (Bolton et al, 1982; Prusiner et al, 1982, 1984). At that time, the Syrian golden hamster (*Mesocricetus auratus*) was an important model organism for the study of scrapie because of the short incubation time for the disease in these animals which is in the range of months. Prusiner's idea was met with great criticism for many years. But today the more strictly formulated, so-called protein-only hypothesis, which states that a protein is the sole causative agent of TSEs, is the most widely accepted explanation for TSE pathogenesis. It should be noted that the correlation between $PrP^{Sc}$ and infectivity did not finally exclude an ad-

ditional compound that was not detected, possibly a hidden nucleic acid. In rigorous and quantitative analyses, however, it could be shown that in highly infectious samples more infectious units than nucleic acid molecules (larger than 25 nt) were present. Consequently, infectious units exist without a single nucleic acid molecule (Safar et al, 2005; Kellings et al, 1992).

With the discovery of the prion protein, an illness-specific molecule was found that is present in characteristic deposits in the brains of animals and patients with TSEs (Bockman et al, 1985; Brown et al, 1986). The prion protein is expressed from a single copy gene and comprises about 250 amino acids depending on the species. It forms a disulfide bond and carries a glycosyl-phosphatidylinositol anchor (GPI) by which it is attached to the extracellular surface of the plasma membrane. Two positions can be N-glycosylated before the protein leaves the endoplasmic reticulum. Importantly, the prion protein occurs in a cellular isoform $PrP^{C}$ which is not pathogenic but also as the disease-associated $PrP^{Sc}$ isoform (where C and Sc denote cellular and scrapie, respectively). Although both isoforms have identical amino acid sequences, they differ markedly in secondary and tertiary structure. While $PrP^{C}$ contains roughly 40 % $\alpha$-helices and few $\beta$-sheets $PrP^{Sc}$ is characterized by an increased $\beta$-sheet content (Pan et al, 1993). While $PrP^{C}$ is the soluble, cellular isoform, $PrP^{Sc}$ represents an abnormal, misfolded conformer that is not only partially protease-resistant but also insoluble and therefore prone to aggregation into large amyloid fibrils. TSE pathogenesis involves the constant conversion of $PrP^{C}$ to $PrP^{Sc}$ which forms large aggregates in the process (Prusiner, 1998). Importantly, $PrP^{Sc}$ serves as a template for $PrP^{C}$ misfolding and greatly accelerates the process.

Different models have been used to explain prion propagation. Prusiner himself proposed a heterodimer model in which a single $PrP^{Sc}$ binds to one $PrP^{C}$ molecule and causes its conversion into $PrP^{Sc}$. Theoretical considerations by Eigen (1996) led him to conclude that this explanation was unlikely given the narrow window of kinetic rate parameters that would be necessary for such a mechanism to work in the observed manner. Instead, Eigen approved of the Lansbury mechanism of nucleated plaque formation. In this model two conformations of the prion protein exist in equilibrium: the $PrP^{C}$ conformer and a partially unfolded $PrP^{U}$ monomer in a pre-prion conformation which is non-pathogenic (Fig. 1.1). Several consecutive binding events lead to the formation of a nucleus where the prion protein adopts the scrapie conformation. These nuclei accelerate further conversion of $PrP^{C}$ to $PrP^{Sc}$ thus leading to rapid $PrP^{Sc}$ fibril growth. $PrP^{C}$ binds to the ends of $PrP^{Sc}$ fibrils where it is converted to $PrP^{Sc}$. Fibril fragmentation doubles the amount of growing ends, speeding up the process exponentially (Come et al, 1993). In the case of infection, $PrP^{Sc}$ is introduced as nuclei from an exogenous source and the need for an otherwise slowly occurring nucleus formation is circumvented.

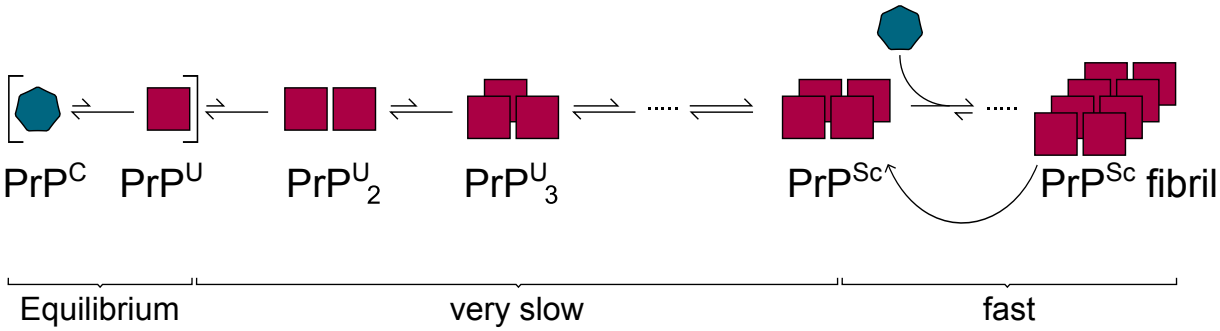


**Figure 1.1 – Mechanism of $PrP^{Sc}$ formation.** In this model, different PrP conformations exist in equilibrium, namely $PrP^{C}$ (teal) and a partially unfolded form $PrP^{U}$ (red) which is a non-pathogenic PrP monomer in a pre-prion conformation. A series of cooperative binding events leads to the formation of $PrP^{Sc}$ nuclei. More $PrP^{C}$ monomers bind to these nuclei where they are converted to $PrP^{Sc}$, leading to the formation of $PrP^{Sc}$ fibrils. Endogenously expressed $PrP^{C}$ can bind to the fibril ends where it is converted to $PrP^{Sc}$. The fragmentation of fibrils increases the number of fibril ends thus accelerating the aggregation process exponentially. The formation of nuclei is very slow but in the case of prion infection these nuclei are introduced from an exogenous source. Based on Come et al (1993) and Eigen (1996)

A number of reasons can lead to the presence of initial $PrP^{Sc}$ seeds. Several mutations in the *Prnp* gene are known that destabilize the soluble conformation and lead to conversion of $PrP^{C}$ to $PrP^{Sc}$ (Prusiner, 1998). These genetic causes explain the existence of familial, inherited prion disease, such as FFI, GSS, and fCJD. Prion infection can be iatrogenic (iCJD) due to contaminated instruments or a consequence of exposure to contaminated brain, for example during ritual cannibalism as is the case for kuru or due to the consumption of infected animals as in variant CJD (vCJD), respectively. However, only a relatively small proportion of all manifestations of prion disorders are inherited or due to infection. Most cases are believed to be due to the accumulation of sporadic nucleation events or somatic mutations in the PRNP locus (Prusiner, 1998).

An important discovery was that mice devoid of $PrP^{C}$ due to gene ablation were protected from prion infection. Moreover, they did not show a distinct histological or behavioural phenotype (Büeler et al, 1992, 1993). These observations, however, have also made it difficult to decipher the physiological function of $PrP^{C}$. The protein is highly expressed in neurons which indicates that it might fulfil an important role in the central nervous system (CNS). Many suggestions exist in the literature. For example, a neuroprotective function has been attributed to $PrP^{C}$ (Roucou et al, 2004). Only recent work shows that neuronal $PrP^{C}$ expression is essential for the maintenance of peripheral myelin and $PrP^{C}$ ablation leads to late-onset chronic demyelinating polyneuropathy (CDP) (Bremer et al, 2010). Other recent studies have described $PrP^{C}$ as a surface receptor that binds oligomeric amyloid-$\beta$ with deleterious effects on synaptic plasticity and dendritic spine integrity (Laurén et al, 2009; Um et al, 2012). These investigations would provide a direct link between $PrP^{C}$ and Alzheimer's disease. In light of recent research it is safe to conclude that $PrP^{C}$ has a dual role, it has a physiological function

without being vital and it is also a key player in several debilitating neurodegenerative diseases.

## 1.3 Therapeutic approaches against TSEs

Today, the prion is widely believed to be the causative and transmissive agent of TSEs. Because of that, efforts to combat TSEs are also mainly directed at the prion protein. Therapeutic approaches target prionopathies from different angles (Korth and Peters, 2006). Since conversion of $PrP^{C}$ to $PrP^{Sc}$ is a major hallmark of prion disease, several studies have attempted to halt prion replication. This can for example be achieved by shielding $PrP^{C}$ from conversion with the use of monoclonal antibodies (White et al, 2003). Treatment with anti-$PrP^{C}$ antibodies without specificity for $PrP^{Sc}$ prevents prion propagation *in vitro* by sequestration of $PrP^{C}$. When administered to mice, these antibodies are able to markedly reduce $PrP^{Sc}$ levels and prolong survival times, but only after peripheral prion infection.

A similar strategy is the shielding of $PrP^{Sc}$ with compounds that inactivate its ability to convert $PrP^{C}$. This can be achieved with polyanionic compounds such as Congo red, dextran sulfate, heparin and pentosan polysulfate (PPS), the latter of which was tested in clinical trials in the United Kingdom (Forloni et al, 2013). However, these trials assessing the therapeutic potential of intraventricular PPS infusion fell short of expectations (Bone et al, 2008; Whittle et al, 2006). Sequestration of $PrP^{Sc}$ with specific antibodies is also a feasible strategy. Because antibodies do not readily traverse the blood-brain barrier, a recent study investigated the use of single-chain variable fragments (scFvs) linked to the cell-penetrating peptide (CPP) penetratin. This approach led to the successful delivery of the scFv-CPP into mouse brain after intravenous administration (Škrlj et al, 2013). But to this date, passive immunization against prion disease has not made the leap to clinical application.

The antimalarial drug quinacrine prevents the conversion of $PrP^{C}$ to $PrP^{Sc}$ *in vitro* but a trial in humans did not show improved survival of CJD patients. Similarly, tetracyclines were reported to reduce prion toxicity *in vitro* but in a recent phase 2 trial doxycyclin failed to significantly affect the course of CJD (Haïk et al, 2014). The aggregation inhibitors anle138b and cpd-B greatly increased survival times of prion-infected animals but are possibly neurotoxic themselves, which limits the dose that can be administered (Berry et al, 2013; Kawasaki et al, 2007; Wagner et al, 2013).

It has been reasoned that the neuroprotective properties of the non-opioid analgesic flupirtin could alleviate the neurotoxic effects of prion replication. $PrP^{Sc}$ toxicity is likely evoked via cellular signalling pathways, although a detailed understanding is currently

lacking. Treatment of CJD patients with flupirtin indeed proved to have beneficial effects on cognitive function (Otto et al, 2004).

Gene silencing techniques offer an alternive way of combating TSEs. Since ablation of the *Prnp* gene protects animals from prion disease without major side-effects, except at a higher age, it is reasonable to assume that even a reduction in $PrP^{C}$ expression levels could be beneficial for patients (Büeler et al, 1992, 1993). Indeed, the concentration of $PrP^{C}$ is one important factor that determines the growth rate of $PrP^{Sc}$ fibrils (Masel et al, 1999). Furthermore, up to 96-99 % of inoculated prions are rapidly cleared from the brain (Safar et al, 2005). Only after 96 h do $PrP^{Sc}$ levels increase again, indicating the accumulation of newly formed $PrP^{Sc}$ from endogenous $PrP^{C}$ that is accelerated by the remaining prions. These results indicate that patients could be treated by short-term depletion of $PrP^{C}$ expression until $PrP^{Sc}$ is cleared from the brain. A post-infection neuron-specific knockout effectively reverses spongiosis and neurological symptoms (Mallucci et al, 2003). Treatment with small interfering RNA (siRNA), short hairpin RNA (shRNA), and antisense oligodeoxynucleotides (AS-ODNs) showed promising outcomes in cell and mouse models (Tilly et al, 2003; Daude et al, 2003; White et al, 2008; Pfeifer et al, 2006; Friberg et al, 2012). It is not clear, however, how these molecules should be delivered to the site of action. Friberg et al (2012) implanted osmotic pumps into animals for the intraventricular administration of AS-ODNs, which would be a strongly invasive intervention for patients. Lentivector-mediated RNA interference (RNAi) proved to be very effective in prolonging survival time after prion infection (Pfeifer et al, 2006). However, transgenic approaches cannot be considered viable treatment options at the moment. Delivery of siRNA to the brain via CPP-coated liposomes and water-in-oil microemulsions are promising strategies that could reach their full potential in the future (Lehmann et al, 2014; Pulford et al, 2010; Bender et al, 2016). More delivery methods will be discussed in Chapter 1.6: *Targeted delivery of nucleic acids*.

A novel approach for the treatment of prion diseases comes in the form of deoxyribozymes. These biomolecules have the ability to lower RNA levels, which could be exploited to reduce $PrP^{C}$ expression. Although functionally related to siRNA, miRNA, and AS-ODNs, deoxyribozymes have some potential advantages over these more familiar approaches.

## 1.4 Deoxyribozymes

Deoxyribozymes (or DNAzymes) are single-stranded DNA molecules that are able to catalyze chemical reactions (Silverman, 2016). Intramolecular base pairing allows them to adopt three-dimensional structures which are a prerequisite for their reactivity.

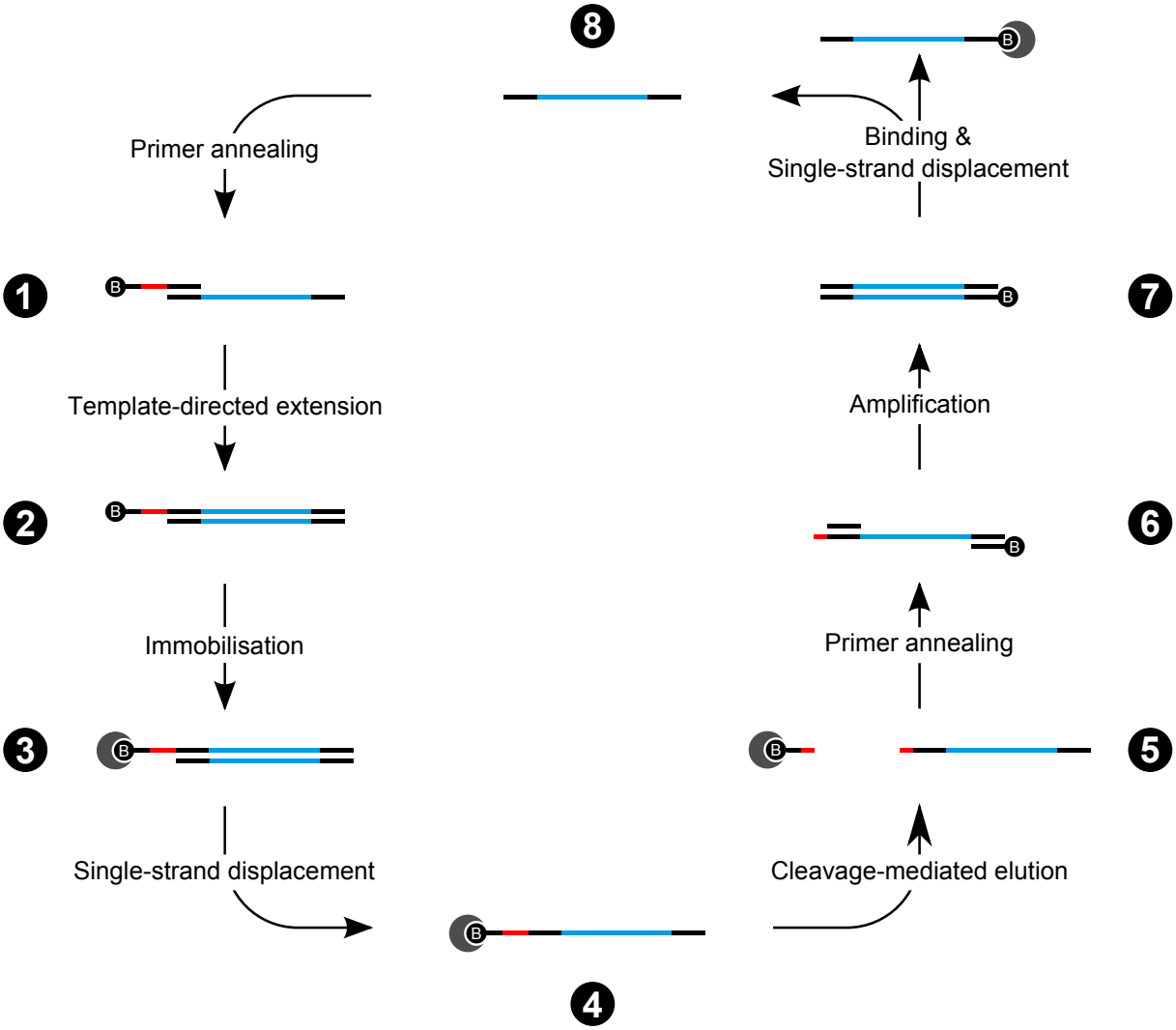


**Figure 1.2 – Selection of RNA-cleaving DNAzymes.** A library of $10^{14}$ different DNA strands is used. Each strand comprises a randomized sequence of 50 nucleotides (light blue) flanked by two constant primer binding sites (black). (1) These DNA strands are annealed to a chimeric primer that contains an RNA stretch (red). Binding of the partially complementary primer to the library DNA results in an overhang of the RNA stretch and a 5'-biotin-labeled DNA portion. (2) Template-directed extension yields double stranded products with the overhang preserved. (3) These double strands are immobilized on streptavidin columns. (4) Washing steps with NaOH denature the double strand thereby removing the non-biotinylated strand from the column. (5) The desired reaction buffer is added. Some DNA sequences within the randomized pool form a catalytically active nucleic acid fold capable of cleaving the intramolecular RNA stretch. They thereby release their covalent link to the solid support and are eluted from the column. (6 & 7) A separate set of primers is used to amplify the eluted sequences via PCR. The reverse primer carries a biotin moiety. (8) The PCR products are captured on streptavidin columns and subsequently treated with NaOH. The alkaline conditions release the non-biotinylated DNA strands, thereby replenishing the pool. This pool is decreased in its sequence diversity when compared to the initial library. RNA-cleaving DNA sequences are greatly enriched while the fraction of catalytically inactive strands is reduced. Consecutive cycles of selection continually favour active DNA sequences. Therefore, the pool is eventually dominated by families of RNA-cleaving DNAzymes that can be isolated and characterized. Based on Santoro and Joyce (1997) and Silverman (2005)

In this regard they resemble ribozymes, which are their RNA counterparts. However, in contrast to ribozymes, which can be either natural or artificial, DNAzymes have not been identified in nature and need to be isolated via *in vitro* selection.

The *in vitro* selection of DNAzymes (and artificial ribozymes) is in many ways similar to that of aptamers (Wilson and Szostak, 1999). Aptamers are short, single-stranded DNA or RNA molecules that bind a given target structure with high affinity and specificity (Ellington and Szostak, 1990; Tuerk and Gold, 1990). For the selection of both aptamers and DNAzymes, a vast library of up to $10^{16}$ different sequences is gradually narrowed down to a few sequence motifs that exhibit the desired properties (Silverman, 2005). This is based on the following assumptions: (i) different nucleic acid sequences adopt different three-dimensional structures, (ii) structure determines function, and (iii) virtually any structure feasible would be present in a large, randomized library – at least if it is within the structural boundaries of nucleic acids of the used length (Silverman, 2016). Therefore it is possible to find sequences in the library that perform the desired function. The task is then to partition those sequences from the bulk of sequences without that functionality. The problem of separating nucleic acid strands based on their functionality can be solved in many ways. For aptamers, the key lies in exposing the nucleic acid pool to target molecules where the strands will compete for binding. Binders are retained on a solid support or separated from non-binders based on a mobility shift. They are subsequently eluted and amplified to regenerate the nucleic acid pool. Ideally, iterative cycles decrease the sequence diversity and enrich binders within the pool. This process is referred to as SELEX (**S**ystematic **E**volution of Ligands by **EX**ponential enrichment).

Selection protocols for catalytic nucleic acids depend on the nature of the chemical transformation they are required to perform. Catalysts that form or break chemical bonds, for example, can covalently attach or detach themselves from a suitable label that may be immobilized on a solid support (Breaker and Joyce, 1994; Cuenoud and Szostak, 1995; Santoro and Joyce, 1997). For instance, Santoro and Joyce (1997) used chimeric molecules containing a randomized DNA stretch linked to biotin via a set of ribonucleotides in order to isolate general-purpose RNA-cleaving DNAzymes (Fig. 1.2). The chimeric nucleic acids were first generated and then immobilized on streptavidin columns. Catalytically active sequences were eluted with a reaction buffer containing $Mg^{2+}$ and collected for the next cycle of selection. Only if the random DNA stretch cleaved the RNA part was the sequence released from the solid support. Inactive sequences remained attached to the streptavidin column and would thus be excluded from the next round of selection. Santoro's and Joyce's attempts yielded two particular RNA-cleaving DNAzyme motifs that would be often used in following studies: the 8-17 DNAzyme and the 10-23 DNAzyme, thus named because they derive

from the 17$^{th}$ clone that was isolated after eight selection cycles and the 23$^{rd}$ clone after ten cycles, respectively.

The catalytical repertoire of DNAzymes is not restricted to RNA cleavage. Other reactions performed by DNAzymes include: reactions of peptides and small molecules, photoreversion of thymine dimer formation in DNA, nucleic acid ligation, and more (Silverman, 2016). However, the prospect of using RNA-cleaving DNAzymes for the therapeutic knockdown of disease-associated genes has put especially the 10-23 DNAzyme in the center of attention.

## 1.5 The 10-23 DNAzyme

The 10-23 DNAzyme is a *trans*-acting deoxyribozyme with ribonuclease activity (Santoro and Joyce, 1997). It contains a fixed sequence of 15 nt that makes up the catalytic core. This catalytic core is flanked on both sides by variable sequences that allow the DNAzyme to hybridize with a complementary RNA sequence, leaving a single ribonucleotide unpaired (Fig. 1.3 A). The catalytic core then brings about the cleavage of the RNA between an unpaired purine and a paired pyrimidine nucleotide.

RNA cleavage by the 10-23 DNAzyme is dependent on the presence of divalent cations. Although Magnesium is used in *in vitro* assays that resemble *in vivo* conditions, Manganese, Cobalt, and other ions are able to compensate for $Mg^{2+}$ to various extent (Santoro and Joyce, 1998). When designed properly, the 10-23 DNAzyme is a true catalyst that performs multiple turnover cleavage of RNA. Multiple turnover cleavage involves three obligatory steps (Fig. 1.3 B): (i) The DNAzyme and RNA first associate with each other. (ii) The DNAzyme then cleaves the RNA strand into two fragments in a metal ion-dependent manner. (iii) Afterwards, the reaction products dissociate from the DNAzyme, restoring it to its initial, unbound state. The DNAzyme is then available for the association with the next, intact RNA. The association and dissociation steps are of particular importance for multiple turnover RNA cleavage. These steps depend on the composition and length of the target recognition arms since they determine duplex stability. If the duplex stability is too low the association of RNA and 10-23 DNAzyme is impaired, too high a duplex stability prevents the dissociation of the cleaved RNA fragments and thereby stalls multiple turnover catalysis. Naturally, for the DNAzyme to catalyze multiple turnover RNA cleavage inside the human body, each binding arm needs to have a melting temperature ($T_m$) of about 37 °C. This corresponds to a binding free energy $\Delta G^\circ_{37}$ of $-8$ to $-10\ \mathrm{kcal\,mol^{-1}}$ for each arm (Fokina et al, 2012). Depending on the GC content and the sequence in general this translates to an approximate length of 7 – 14 nt per binding arm (Sugimoto et al, 1995).

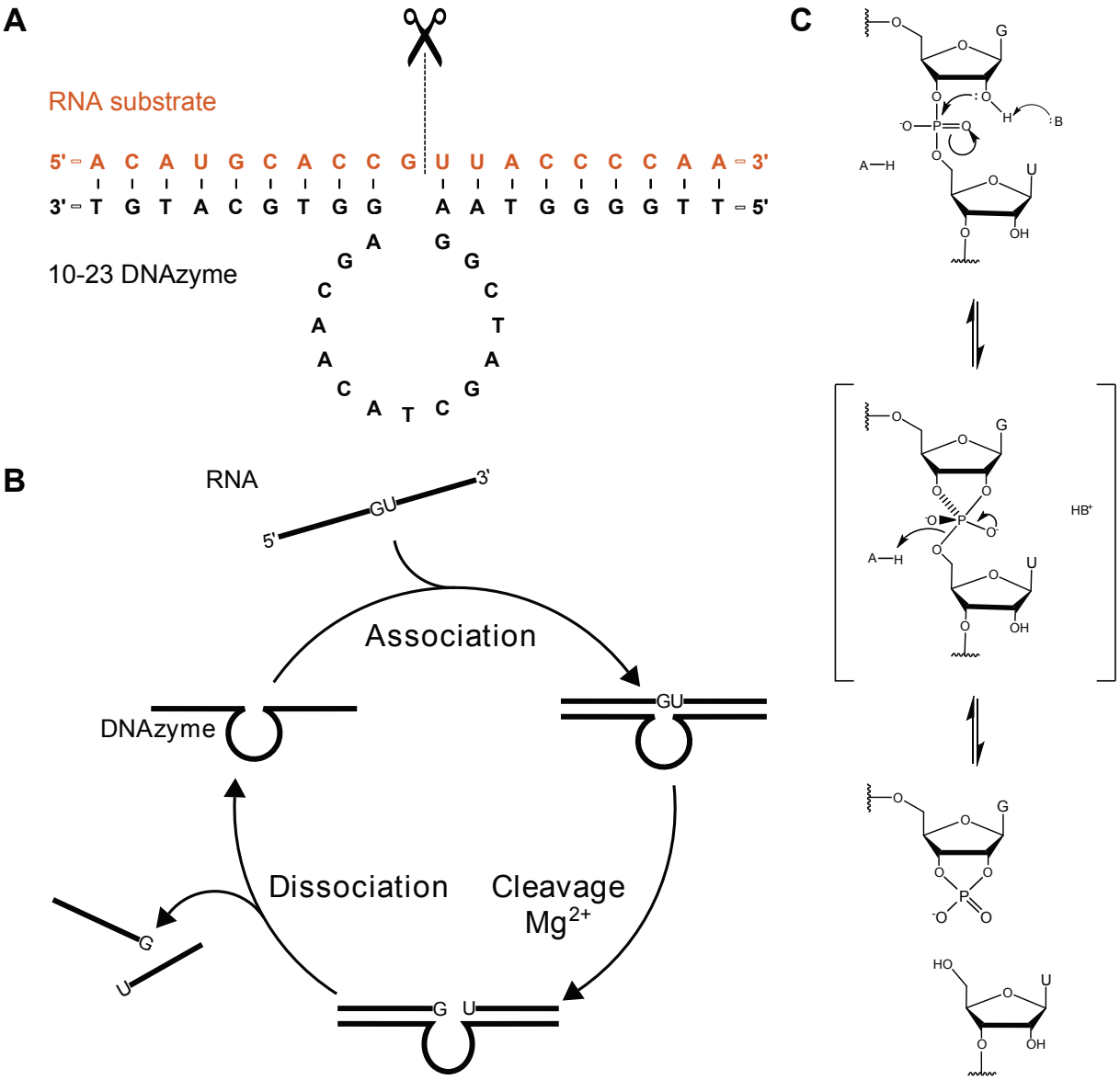


**Figure 1.3** – **Composition and function of the 10-23 DNAzyme. (A)** Secondary structure of the 10-23 DNAzyme in complex with its RNA target. The DNAzyme (black) comprises a fixed catalytic core sequence that is flanked by variable target recognition arms. These arms bind to a complementary RNA target sequence (orange) via Watson-Crick base pairing. Thus, the sequences of the binding arms can be adjusted to allow a specific binding of the DNAzyme to virtually any RNA of interest. The catalytic core catalyzes the cleavage of the bound RNA between an unpaired purine and a paired pyrimidine nucleotide. **(B)** Reaction scheme. The DNAzyme and its RNA target associate via intermolecular base pairing, followed by $Mg^{2+}$-dependent cleavage of the RNA. The ternary complex dissociates and the DNAzyme can bind another RNA target. From: (Victor et al, in press). **(C)** Proposed reaction mechanism. A proton is abstracted from the 2'-hydroxyl group on the ribose of the unpaired purine nucleotide. The resulting oxyanion performs a nucleophilic attack on the phosphorus center of the phosphodiester bond thus generating a pentacoordinated phosphorane intermediate. The intermediate degrades into two RNA fragments that are terminated by a 2'-3'-cyclic phosphate and a 5' hydroxyl group, respectively. G = guanine; U = uracil. Based on: Breaker et al (2003)

It is assumed that the catalytic core adopts a three-dimensional structure which allows the DNAzyme to cleave the phosphodiester bond that strings RNA nucleosides together. That very structure, however, is still unknown. Earlier attempts at solving the structure via X-ray crystallography resulted instead in the crystallization of a catalytically irrelevant nucleic acid fold (Nowakowski et al, 1999). Other groups have mutated the catalytic core sequence as well as introduced or removed functional groups in order to elucidate their involvement in catalysis (Nawrot et al, 2007; Wang et al, 2010; Robaldo et al, 2012; Yang et al, 2016). However, in absence of conclusive structural data, the exact mode of action of the 10-23 DNAzyme remains poorly understood. The reaction mechanism is believed to be a transesterification similar to that performed by the hammerhead ribozyme (Breaker et al, 2003; Santoro and Joyce, 1998). An unknown Brønsted base in the catalytic core of the DNAzyme abstracts a proton from the 2'-hydroxyl group of the ribose that is located 3' of the scissile bond, thus creating an oxyanion (Fig. 1.3 C). The nucleophile performs an in-line attack on the phosphorus center of the phosphodiester bond. The result is a pentacoordinated phosphorane intermediate which hydrolyzes into the reaction products, namely two RNA fragments that are terminated by a 5'-hydroxyl and a 2'-3'-cyclic phosphate, respectively.

Conceptually, the 10-23 DNAzyme is particularly attractive as a therapeutic agent (Fokina et al, 2015). Its ability to cleave RNA could be exploited to knockdown mRNA levels and thereby the amount of disease-associated proteins themselves. Advantages it shares with most other nucleic acid-based therapeutics are its high versatility and specificity. The hybridization arms, which confer substrate specificity, can be freely modified to recognize any RNA of interest. A pyrimidine purine dinucleotide at the center of the RNA target sequence remains the only prerequisite in terms of sequence. Moreover, nucleic acid hybridization relies on more or less strict complementarity of sequential information that fundamentally guarantees high sequence specificity. Unlike RNA interference (RNAi) and antisense oligodeoxynucleotides (AS-ODNs), the 10-23 DNAzyme represents a self-sufficient catalyst that does not rely on cellular proteins for its function.

As of yet, DNAzymes for different mRNA targets have been regarded for their use as therapeutic agents. 10-23 DNAzymes specific for the vanniloid receptor subtype I have been examined extensively in *in vitro* studies but have not made the leap to use in cell culture, yet (Kurreck et al, 2002). Others have applied 10-23 DNAzymes for the treatment of basal cell carcinoma (Cho et al, 2013). A GATA3-specific DNAzyme is currently in phase II clinical trials for the therapy of $T_h2$-driven asthma (Krug et al, 2015). Up to this point, however, DNAzyme or even ribozyme-based therapeutics have not moved beyond clinical trials.

## 1.6 Targeted delivery of nucleic acids

It is not sufficient for a drug candidate to show effectiveness *in vitro*. The bioavailability of the compound will ultimately determine its pharmacological activity. Simply put, for a drug to unfold its therapeutic potential it needs to reach the site of action in sufficient amounts. The same holds true for nucleic acid-based therapeutics. Whether the compound will accumulate in the target tissue for an adequate length of time depends on its pharmacokinetic properties. Those properties include (i) the absorption of the compound into the blood stream, (ii) its distribution throughout the body, (iii) metabolism of the compound into (inactive or even harmful) products, and (iv) its eventual excretion from the body. A possible liberation of the active ingredient is important if the compound is a prodrug that needs to be metabolized into an active drug after its administration or if the compound is part of a formulation and needs to be released. The (**L**iberation,) **A**bsorption, **D**istribution, **M**etabolism, and **E**xcretion phases are summarized under the acronym (L)ADME. In terms of these criteria nucleic acid therapeutics face several obstacles that they need to overcome on their way into clinics.

The stability in biological fluids and tissues is a particularly important factor for nucleic acid therapeutics. RNA is generally prone to hydrolytic degradation of the backbone. In addition, near ubiquitous ribonucleases rapidly digest single-stranded or double-stranded RNA, either beginning from the 5' or 3' end or via cutting internally (Houseley and Tollervey, 2009). While the delicate nature of RNA provides the organism with effective means to regulate protein levels via RNA turnover, it also complicates the use of unmodified RNA molecules as therapeutics. DNA is generally more stable than RNA. The lack of the 2'-hydroxyl group of the ribose makes the sugar phosphate backbone stable over a large pH range. The most important pathway for ssDNA degradation comes in the form of 3' $\longrightarrow$ 5' exonucleases (Ortigão et al, 1992). Since extensive work has been done on the chemical modification of nucleic acids a plethora of unnatural nucleotides can be used for the stabilization of DNA and RNA against nucleolytic digestion. The use of 2'-fluoro ribose, 2'-amino ribose, 2'-methoxy ribose, locked nucleic acid (LNA), phosphothioate, and other backbone modifications is now standard practice and greatly enhances the stability of nucleic acids in biological fluids without disturbing the specificity of base pairing (Kanasty et al, 2013). Additionally, some backbone modifications reduce Toll-like receptor (TLR)-mediated activation of the immune system, which is a possible side effect of treatment with nucleic acids. For ssDNA it is common to attach a 3'-3'-linked inverted thymidine nucleotide to the 3' end of the molecule (Ortigão et al, 1992; Sun et al, 1999). This effectively creates a strand with two 5' ends thereby avoiding the recognition by 3' $\longrightarrow$ 5' exonucleases altogether. An elegant way of stabilizing nucleic acids against degradation is the use of DNA or RNA in L-configuration instead of the naturally favoured D-configuration. Use of the

L-enantiomer greatly increases the half life due to general avoidance of the substrate specificity of nucleases (Ashley, 1992; Klussmann et al, 1996; Vater and Klussmann, 2015).

Efforts to achieve the absorption of nucleic acid-based therapeutics and to guide their distribution throughout the organism to the effector site have largely focused on the delivery of siRNA and AS-ODNs. In principle, though, all following strategies can be adapted to a use with similar molecules, such as DNAzymes. Nucleic acid therapeutics can be administered locally or topically if the target tissue is easily accessible, which is for example the case for the skin, eyes, and mucous membranes (Whitehead et al, 2009). Intranasal or intratracheal application brings nucleic acids into direct contact with lung epithelial cells (Bitko et al, 2005; de Fougerolles and Novobrantseva, 2008). Another example for the local delivery of nucleic acid therapeutics is a recent attempt at reducing $PrP^C$ levels by intraventricular infusion of an AS-ODN via implanted osmotic pumps (Friberg et al, 2012). Direct injection into tumors was also shown to be a suitable method of administration (Niu et al, 2006). Certain delivery methods however, such as the aforementioned intraventricular infusion, carry risks and contraindications for patients. Moreover, many organs and tissues might not be accessible to local application. In these cases, intravenous (IV) injection can be chosen as a suitable route for systemic administration. After IV administration, nucleic acid formulations must navigate the circulatory system to the effector site while avoiding renal clearance, phagocytic uptake, binding to serum proteins, and degradation. In addition, it is obligatory that they pass several barriers in order for them to reach their effector site, i. e. the cytoplasm of the target cell. These barriers include the blood vessel endothelium, the extracellular matrix (ECM), and the plasma membrane, which is charged and amphipathic, and thus essentially impermeable for nucleic acids via passive diffusion (Whitehead et al, 2009). As a consequence, internalization must occur via endocytosis which leaves the drug entrapped inside endosomes. Therefore, endosomal escape is obligatory. If the brain is the target tissue, the highly selective blood-brain barrier presents another obstacle that prevents nucleic acids from reaching their site of action.

In light of these major obstacles, great effort continues to be directed at developing a number of delivery systems. Those can be divided into carrier-free and carrier-mediated targeting systems (Dovydenko et al, 2016). Carrier-free systems make use of targeting ligands that are covalently attached to their nucleic acid payload and shuttle them to their destination. Among those are conjugates with carbohydrates such as N-acetyl galactosamine, cell-targeting and cell-penetrating peptides, aptamers, and lipids such as cholesterol, $\alpha$-tocopherol, phospholipids, fatty acids, and bile acids (Nair et al, 2014; Prakash et al, 2014; Hoyer and Neundorf, 2012; Aaldering et al, 2015; Raouane et al, 2012). Depending on the nature of the conjugate, nucleic acids are either internalized via receptor-mediated endocytosis, targeted to the cell membrane because of

their increased lipophilicity or guided through the circulatory system by binding to high-density or low-density lipoprotein. Attaching polyethylene glycol (PEG) to nucleic acids further allows them to avoid aggregation with serum proteins and glomerular filtration (Watson et al, 2000).

Carrier-mediated delivery systems can be further divided into polymeric systems, lipid-based systems, and inorganic carriers (Dovydenko et al, 2016). In polymeric delivery systems, nucleic acids are condensated by positively charged functional groups of a polymer (Sunshine et al, 2011). Lipidic systems encapsulate nucleic acids in leaflets, vesicles or stable nucleic acid lipid particles (SNALPs) for their delivery (Whitehead et al, 2009). Targeting ligands such as CPPs or carbohydrates can be bound to the lipid surface to grant the vesicle cell type or tissue specificity. Finally, inorganic carriers bind nucleic acids and facilitate their uptake through different mechanisms (Sunshine et al, 2011). Inorganic materials that have been used for nucleic acid delivery include gold nanoparticles, carbon nanotubes, silica and others.

A special case is the use of cell-penetrating peptides for targeted delivery of nucleic acids (Hoyer and Neundorf, 2012). They often derive from viral systems and greatly increase uptake, often in a specific cell type or even across the blood-brain barrier. CPPs can be conjugated to nucleic acids either via covalent attachment or non-covalently through charge-charge interactions between a positively charged binding domain (e. g. arginine repeats) and the negatively charged DNA or RNA backbone. In addition, polymeric systems, vesicles and nanoparticles can be decorated with CPPs in order to increase their uptake and specificity. Prominent examples of CPPs include the HIV protein tat (trans-activator of transcription) and the rabies virus glycoprotein (RVG) which has for example been successfully used for targeted delivery of AS-ODNs to the brain for the treatment of Huntington's disease in a mouse model (Wender et al, 2000; Kumar et al, 2007; Kordasiewicz et al, 2012). A combination of these virus-derived vectors with particulate systems comes in the form of virus-like particles (VLPs). These particles are assembled from viral capsid proteins but instead of containing the viral genome they can be loaded with a cargo of choice. A prime example that is especially relevant for this work is the use of VLPs derived from the John Cunningham virus (JCV). The JC virus is an opportunistic pathogen that infects between 70 and 90 percent of the population. Infection is usually not problematic but in immunocompromised individuals, the virus can cause progressive multifocal leukoencephalopathy (PML), a rare but deadly brain disorder. Several studies have focused on repurposing the JCV capsid protein VP1 for drug delivery. So far, plasmids and siRNA molecules have successfully been transported to mouse tissues and osteoblasts using VLPs assembled from VP1 capsomers (Chen et al, 2010; Chang et al, 2011; Hoffmann et al, 2016). Since VLPs circumvent a number of obstacles for nucleic acid delivery - they shield their cargo from nucleases, avoid renal clearance, navigate the circulation, and release their con-

tents into the cytosol - they also promise to be useful for delivering DNAzymes to their effector site.

## 1.7 Aim of the work

The objective of the following work is to explore the therapeutic potential of using 10-23 DNAzymes for the treatment of Creutzfeldt-Jakob disease. At the center of CJD and all other prionopathies lies the eponymous prion protein. Not only is the prion the transmissive agent, the accumulation of neurotoxic aggregates can only occur if sufficient amounts of endogenously expressed $PrP^{C}$ are converted to the $\beta$ sheet-rich $PrP^{Sc}$ isomer. Many studies have demonstrated that a complete lack or substantial reduction of $PrP^{C}$ expression either makes animals immune to infection or prolongs the onset of prion disease and overall survival times. Besides transgenic approaches, several knockdown techniques, such as RNA interference (RNAi) and AS-ODNs, have been studied for the possible treatment of TSEs. While the compounds proved to be robust and promising gene silencing agents, the targeted delivery to the brain remains a major obstacle.

The use of DNAzymes may offer several advantages over other knockdown techniques. DNAzymes are self-sufficient biocatalysts that do not rely on the presence of other biomolecules the way that RNAi relies on argonaut proteins and antisense oligodeoxynucleotides on the action of RNase H. Compared to RNA, single-stranded DNA is inherently more stable and cost-effective. A recent study delivered experimental evidence that mirror-image hammerhead ribozymes and DNAzymes, where the backbone contains L-enantiomeric ribose or deoxyribose instead of the naturally favoured D-(deoxy)ribose, are also able to cleave natural RNA. If verified, this would offer a completely novel knockdown agent with superior stability since these so-called Spiegelzymes are not recognized by nucleases (Wyszko et al, 2014). The claim by Wyszko et al (2014) is to be investigated first. Otherwise, the regular 10-23 DNAzyme in D-configuration will be tested for its ability to cut the human *Prnp* mRNA and lower protein levels.

Since mRNA is characterized by secondary structure formation, many possible cleavage sites in the human *Prnp* mRNA will likely be inaccessible for DNAzyme hybridization. A sequential folding algorithm will be used to determine target sites that have a higher probability to be accessible than others. The cleavage of short, unstructured RNAs by a selection of DNAzymes will be attempted first before the predictions of the sequential folding algorithm will be tested by cleaving long, structured RNA during *in vitro* transcription (IVT). Afterwards, promising candidates will be tested in cell culture. Human neuroblastoma cells are to be transfected with DNAzymes in an attempt to

reduce $PrP^C$ expression. RNA interference will serve as a positive control during these proof-of-concept experiments.

If suitable DNAzymes are obtained, the attempt to establish a brain-specific delivery vector will follow. The company NEUWAY Pharma AG (Bonn, Germany) focuses on developing JCV-based virus-like particles into a drug delivery platform for the central nervous system and offered a cooperation. According to their method, virus-like particles (VLPs) will be assembled from capsomers that derive from the main capsid protein of the JC virus. These particles will be loaded with the DNAzyme cargo. Besides their ability to pass the blood brain barrier and deliver compounds to the brain, VLPs also shield their payload from serum nucleases and avoid renal filtration. Thereby, unfavourable pharmacokinetic properties of nucleic acids can be circumvented and the DNAzymes can be directed to the effector site. The goal of this cooperation will be to achieve a successful delivery of DNAzymes in a cell culture model.

The methods and techniques investigated in this work have the possibility to evolve into therapeutics not only aimed at treating Creutzfeldt-Jakob disease. Because of the universality of the prion hypothesis, they offer the prospect of treating all debilitating prion-like disorders in one generalized approach.

# 2 Results

## 2.1 Accessibility of cleavage sites

Post-transcriptional gene silencing (PTGS) can be achieved by several techniques. Among them are the use of RNA interference (RNAi), antisense oligodeoxynucleotides (ASO-ODNs), ribozymes, and DNAzymes. All of these approaches require the hybridization of a short oligo(ribo- or deoxy)nucleotide to the mRNA of interest. After that, they bring about the degradation of this mRNA by different means. It is a well-established fact that different knockdown agents fluctuate highly in their efficacy to reduce the same mRNA. Naturally, the individual mechanisms influence effectiveness to a certain degree. However, efficacy will also vary greatly between for instance just siRNAs specific for the same mRNA. The reason for this is that not all target sites on the mRNA are equally accessible for siRNA hybridization. Single-stranded RNAs such as mRNA adopt a complex secondary structure due to short- and long-range intramolecular base-pairing. Therefore large parts of the mRNA sequence are actually present in a double-stranded form, leaving these locations blocked from hybridizing with siRNAs. The same can be expected for other knockdown agents, including ribozymes and DNAzymes.

In contrast to siRNA and ASO-ODNs, which can be designed for any RNA sequence, ribozymes and DNAzymes require a consensus sequence for cleavage. Because of that, the number of possible ribozymes and DNAzymes that cleave a given mRNA is lower than the number of possible siRNAs or ASO-ODNs. Still, the abundance of cleavage sites in any given mRNA is typically very high. For instance, the PrP mRNA from Syrian golden hamster (*Mesocricetus auratus*, SHa), an important animal model for prion disease, has a length of 2808 nt and contains 451 RY dinucleotides that could be cleaved by 10-23 DNAzymes. Testing all of these possible cleavage sites would be very laborious and cost-intensive. Instead it is reasonable to reduce this number based on criteria that correlate with knockdown efficacy. Those criteria could be used in bioinformatics to determine the most promising cleavage sites. In an approach to provide such a selection tool for siRNA, Tafer et al (2008) used the sequential folding program RNAPLFOLD to predict local RNA structure formation. Essentially, base pairing probabilities are calculated in a window $W$ of 80 nt that is slid over the whole mRNA sequence. Also, the maximum base-pair span $L$ is set to 40 nt. Within these constraints, the probability of a region $u$ with adjustable length to be base-paired is determined. Importantly, the value for $L$ does not permit any structures with base-pairs that span more than 40 nt. This is based on the rationale that longer structures are disentangled in actively translated mRNA by the helicase activity of the ribosome and that they are slow to reform. Indeed, they found that the silencing efficiency of siRNAs correlated

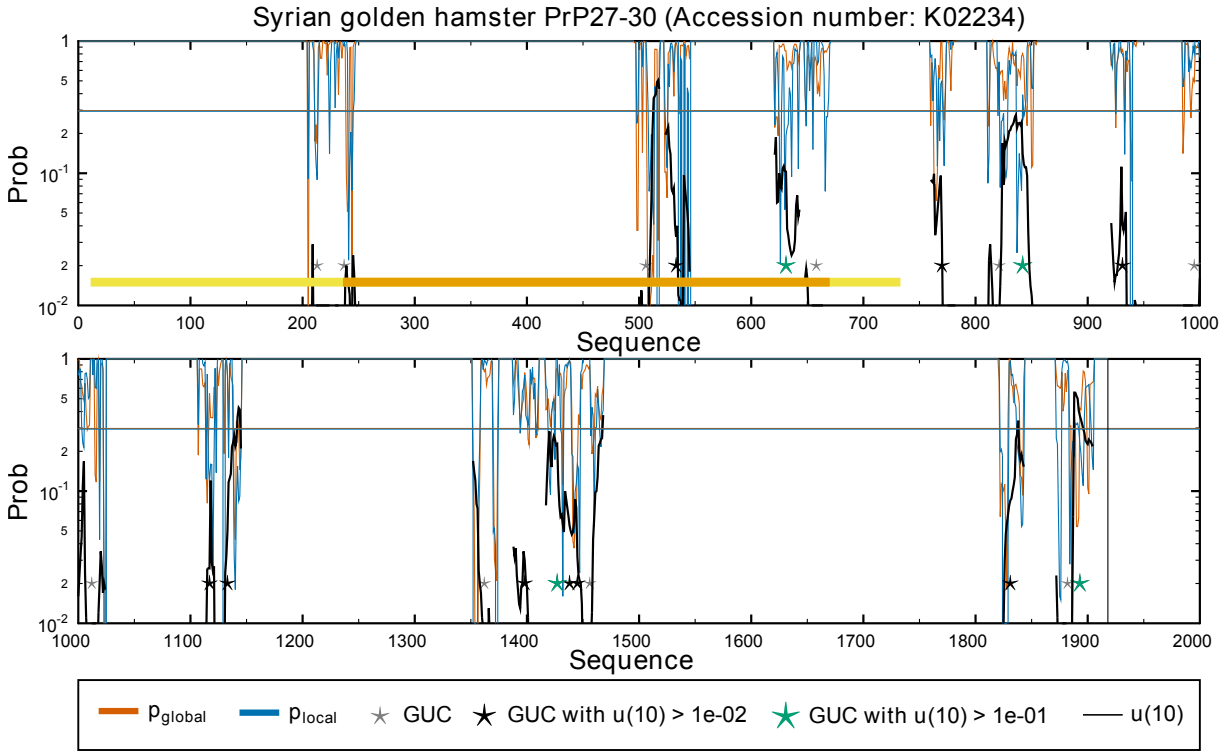


**Figure 2.1 – Accessibility of GUC cleavage sites in the SHa PrP mRNA.** The x-coordinate represents the position in the mRNA sequence. The pairing probability is displayed on the y-axis. The local base-pairing probability $p_{local}$ for each nucleotide is presented by blue lines. The black lines represent the probability $u_{10}$ that a sequence of length $l = 10$ centered at this position is not base-paired as an indicator of target site accessibility. The value of $u_{10}$ is dependent on $p_{local}$ and correlates well with the knockdown efficacy of knockdown agents that bind to this region. The global base-pairing probability $p_{global}$ is shown by orange lines. All GUC sequences are represented by stars. Those sequence serve as cleavage sites for hammerhead ribozymes and 10-23 DNAzymes. Grey stars show GUCs with $u_{10} < 0.01$, which are cleavage sites that are inaccessible. Black stars indicate GUCs with $u_{10} > 0.01$ and therefore medium accessibility, and green stars are considered the most accessible cleavage sites with $u_{10} > 0.1$. $p_{local}$ and $p_{local}$ are only shown for the ten nucleotides surrounding each GUC cleavage site. The yellow bar indicates the open reading frame (11 to 733) and the orange bar the sequence that corresponds to the mature protein after post-translational modification (236 to 673).

significantly with the target site accessibility as determined by their calculations. The exact values for $W$ and $L$ were empirically determined: out of all tested values the calculations with $W = 80$ and $L = 40$ allowed the best separation of functional siRNAs from non-functional siRNAs.

Wyszko et al (2014) claimed that hammerhead ribozymes and 10-23 DNAzymes in L-configuration are able to cleave D-RNA. In order to investigate whether these mirror-image enzymes could be used for PrP mRNA knockdown suitable cleavage sites had to be determined first. In an effort to rank cleavage sites for hammerhead ribozymes and 10-23 DNAzymes in mRNA sequences Gerhard Steger adjusted the algorithm by Tafer et al (2008) to return sequences of length $l = 10$ with cleavage sites at their center. It is important to note that the hammerhead ribozyme and the 10-23 DNAzyme

have different requirements concerning the consensus cleavage site in their RNA substrates. The hammerhead ribozyme cleaves its substrate RNA after an NHH consensus sequence where N can be any nucleotide and H can be A, U or C (the symbols that are used for nucleotide nomenclature are based on the IUPAC-IUB recommendations, which are summarized in Table 4.2 on page 115). Out of all possible triplets, cleavage after GUC shows the highest rate constant. The 10-23 DNAzyme on the other hand requires a RY dinucleotide in its substrate, where R is any purine (G or A) and Y is any pyrimidine ribonucleotide (C or U). GU and AU dinucleotides are cleaved with the highest rate constant (Kore et al, 1998). It is for that reason that calculations were carried out for GUC cleavage sites since the GUC triplet overlaps the substrate specificities of both the hammerhead ribozyme and the 10-23 DNAzyme while it is also expected to be most rapidly cleaved. The SHa PrP mRNA was initially chosen for a proof-of-concept study, since the Syrian golden hamster is traditionally an important animal model for prion disease. This strategy will later be abandoned in favour of the human PrP mRNA sequence because accessibility calculations are not necessarily transferable from the SHa to the human PrP mRNA sequence and mouse strains with humanized PrP can be used as appropriate model organisms. When calculating the local secondary structure formation in the SHa PrP mRNA the algorithm returns the probability $u_{10}$ that a sequence of 10 nt length is not base-paired. Based on thresholds for this value that correlate with knockdown efficacy, the 23 possible GUC cleavage sites can be narrowed down to 13 sites with $u_{10} > 0.01$ (Fig. 2.1). These are considered cleavage sites with at least medium accessibility. Out of these, 4 sites have a $u_{10} > 0.1$ which are regarded as highly accessible. Three of those latter cleavage sites were chosen for proof-of-concept studies with hammerhead ribozymes and 10-23 DNAzymes in L-configuration. The first experiments were carried out with RNA substrates that are too short to form higher-ordered structures. Later in this work experiments with longer *in vitro* transcibed RNA will be presented. These transcripts mimic actual mRNA more closely and are therefore suitable to validate the predicted cleavage site accessibility.

## 2.2 RNA cleavage by Spiegelzymes

In a recent publication, Wyszko et al (2014) provided evidence that RNA cleavage by hammerhead ribozymes and 10-23 DNAzymes is irrespective of their chirality. In other words, according to their data RNA in (natural) D-configuration could be cleaved by hammerhead ribozymes and 10-23 DNAzymes in L-configuration and L-RNA could be cleaved by D-ribozymes and D-DNAzymes, respectively. These L-enantiomeric nucleic acid enzymes were named Spiegelzymes in reference to Spiegelmers, which are L-enantiomeric aptamers that had been developed earlier. The terms derive from

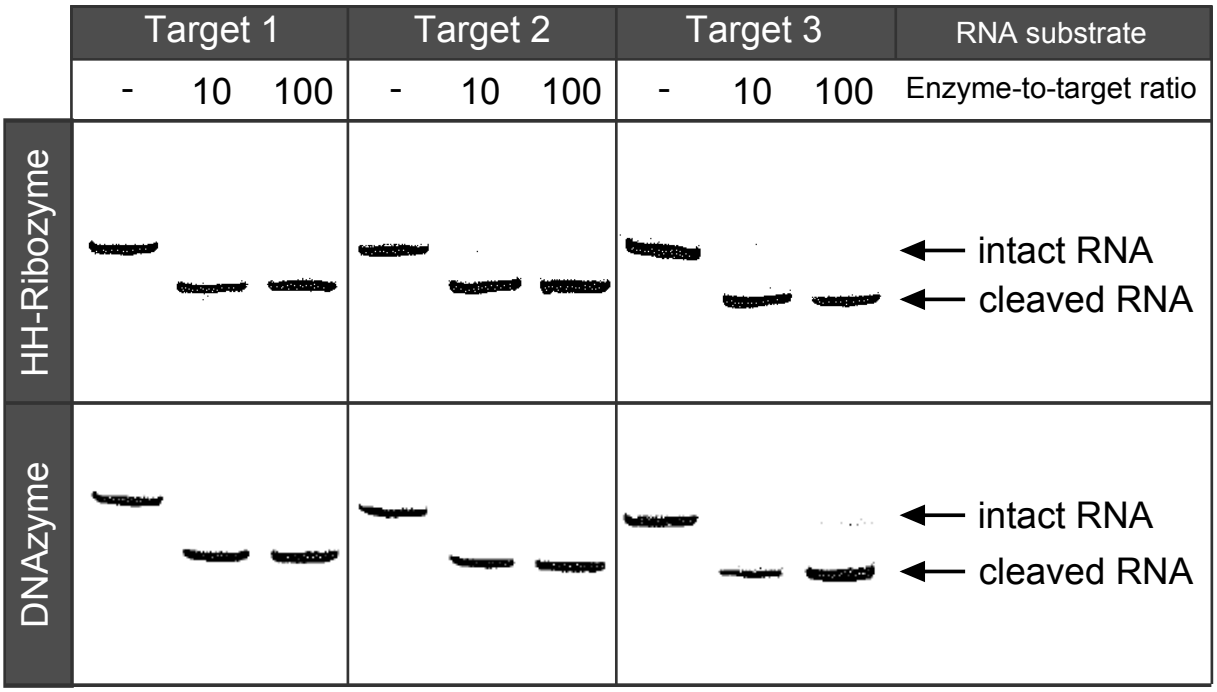


**Figure 2.2 – RNA cleavage by 10-23 DNAzymes and hammerhead ribozymes.** Three different RNA substrates were incubated together with specific 10-23 DNAzymes and hammerhead ribozymes in the indicated molar ratios. The reaction was started by adding $MgCl_2$ to a final concentration of 10 mmol $l^{-1}$. Incubation proceeded at 37 °C. Afterwards, the samples were separated by size via 18 % denaturing polyacrylamide gel electrophoresis (dPAGE). During the 3 h incubation all three RNA substrates were cleaved to completion by both the respective hammerhead ribozymes and 10-23 DNAzymes. HH-Ribozyme = hammerhead ribozyme; DNAzyme = 10-23 DNAzyme

the German word for mirror (Spiegel) which reflects the fact that L-RNA and L-DNA are mirror images of their naturally occurring D-enantiomeric counterparts. Since Spiegelmers had already been shown to be non-toxic, non-immunogenic, and highly stable in biological fluids similar qualities could be assumed for Spiegelzymes. Therefore, mirror-image nucleic acids possibly outperform D-RNA or D-DNA-based pharmaceuticals even though they are not as cost-effective.

The potential applicability of Spiegelzymes for targeted knockdown of the prion protein was to be tested first. Suitable cleavage sites in the SHa PrP mRNA sequence were determined based on sequential folding calculations which were performed by Gerhard Steger (see chapter 2.1). Based on these calculations short target RNAs of 14 nt length with a GUC at their center were designed that resemble stretches of the SHa PrP mRNA with high accessibility for hammerhead ribozyme or 10-23 DNAzyme hybridization. Those RNAs contain a GUC triplet at their center. Complementary hammerhead ribozymes and 10-23 DNAzymes were designed for each target sequence. The RNA substrate is labelled with a fluorescein molecule conjugated to the 5' end and can therefore be detected by fluorescence-based methods. Cleavage of the RNA produces two RNA fragments, one of which retains the fluorescein label. Therefore,

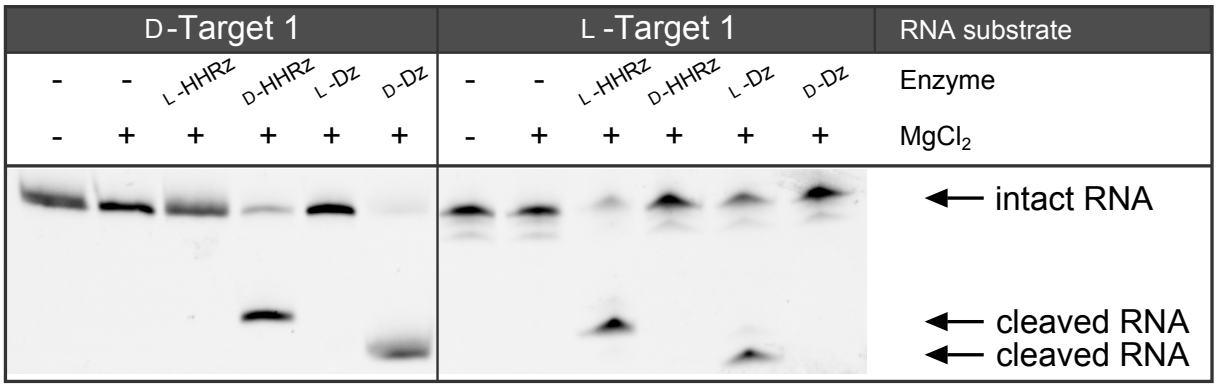


**Figure 2.3 – L-DNAzymes and L-hammerhead ribozymes exclusively cleave L-RNA.** The RNA substrate in D- or L-configuration was incubated together with specific 10-23 DNAzymes or hammerhead ribozymes in either a homochiral or a heterochiral manner. Afterwards the samples were separated by 18 % dPAGE. During a 3 h incubation at 37 °C the D-RNA substrate was only cleaved by the hammerhead ribozyme and 10-23 DNAzyme in D-configuration. The respective hammerhead ribozyme and 10-23 DNAzyme in L-configuration only cleaved the L-RNA substrate, proving that they work in a homochiral but not a heterochiral system. HHRz = hammerhead ribozyme; Dz = 10-23 DNAzyme

RNA cleavage can be monitored by the appearance of a fluorescently labelled fragment that can be distinguished from the labelled full-length substrate based on its shortened length. As a proof of concept, the cleavage reaction was first tested in a homochiral setup with substrate RNA and nucleic acid enzyme both in D-configuration (Fig. 2.2). Three different substrate RNAs were incubated together with their complementary hammerhead ribozymes and 10-23 DNAzymes in a tenfold or a hundredfold molar excess. The cleavage reaction was started by adding $MgCl_2$ and stopped after 3 h by adding sample buffer with an excess of EDTA. For all three RNA substrates the cleavage reaction proceeded until completion, proving that the specifically designed hammerhead ribozymes and 10-23 DNAzymes are able to cleave RNA.

After establishing the general RNA cleavage activity of hammerhead ribozymes and 10-23 DNAzymes in D-configuration the activity of Spiegelzymes was investigated next. For that purpose, RNA substrates in both D- or L-configuration were used. These RNA substrates were incubated with hammerhead ribozymes and 10-23 DNAzymes of either the same or the opposite chirality, i. e. in homo- or heterochiral setups (Fig. 2.3). While the D-RNA substrate was cleaved to completion by the D-hammerhead ribozyme and the D-DNAzyme both the L-hammerhead ribozyme and the L-DNAzyme were incapable of cleaving D-RNA. They did, however, cleave a complementary L-RNA substrate. It is evident from these results that Spiegelzymes are indeed active nucleic acid enzymes but only in homochiral setups. In accordance with these data, the hammerhead ribozyme and 10-23 DNAzyme in D-configuration were also unable to cleave the L-RNA substrate.

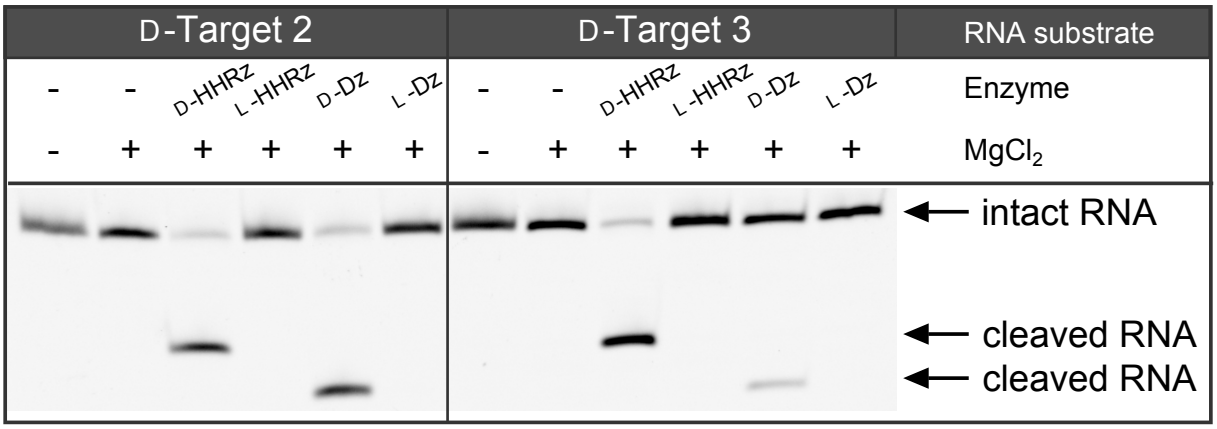


**Figure 2.4 – No evidence for heterochiral RNA cleavage.** The D-RNA substrates Target 2 and Target 3 were incubated together with specific hammerhead ribozymes and 10-23 DNAzymes in D- or L-configuration. Incubation proceeded at 37 °C for 3 h. The samples were separated by 18 % dPAGE. Cleavage activity was only observed for homochiral systems. Both L-hammerhead ribozymes and L-DNAzymes completely failed to cleave D-RNA. HHRz = hammerhead ribozyme; Dz = 10-23 DNAzyme

It is possible that the particular RNA substrate that was used did not allow for heterochiral interaction while other RNA and nucleic acid enzyme sequences exhibit this behaviour. In order to test this, the D-RNA substrates Target 2 and Target 3, which resemble other stretches of the SHa PrP mRNA, were incubated with hammerhead ribozymes and 10-23 DNAzymes in D- or L-configuration (Fig. 2.4). Both RNA substrates were only cleaved by nucleic acid enzymes in D-configuration. Interestingly, in the case of Target 3, the D-DNAzyme activity was markedly reduced when compared to the respective hammerhead ribozyme. Again, L-hammerhead ribozymes and L-DNAzymes did not show cleavage activity that would be evidence for a heterochiral interaction.

The influence of several reaction parameters was extensively explored in order to determine whether other reaction conditions allow the cleavage of D-RNA by Spiegelzymes. Those parameters include: (i) The substrate-to-enzyme ratio, (ii) the concentration of $MgCl_2$, (iii) the addition of other metal ions such as potassium, (iv) the reaction time, (v) the influence of initial denaturation and renaturation steps under different conditions, and more. None of these variations led to heterochiral Spiegelzyme activity, and since the focus of this work lies on examining the therapeutic potential of DNAzymes the results will not be discussed in detail.

The fact that none of the tested Spiegelzymes was able to cleave D-RNA is in discrepancy with the data of Wyszko et al (2014). To exclude that the experimental execution differs the authors of the original paper provided the samples that were used to produce the published data. The substrate sequence is derived from the GFP mRNA sequence for simple proof-of-concept experiments in cell culture. Incubating a tenfold molar excess of these Spiegelzymes with their respective D-RNA substrate indeed revealed some cleavage activity of the L-hammerhead ribozymes (Fig. 2.5). Intriguingly,

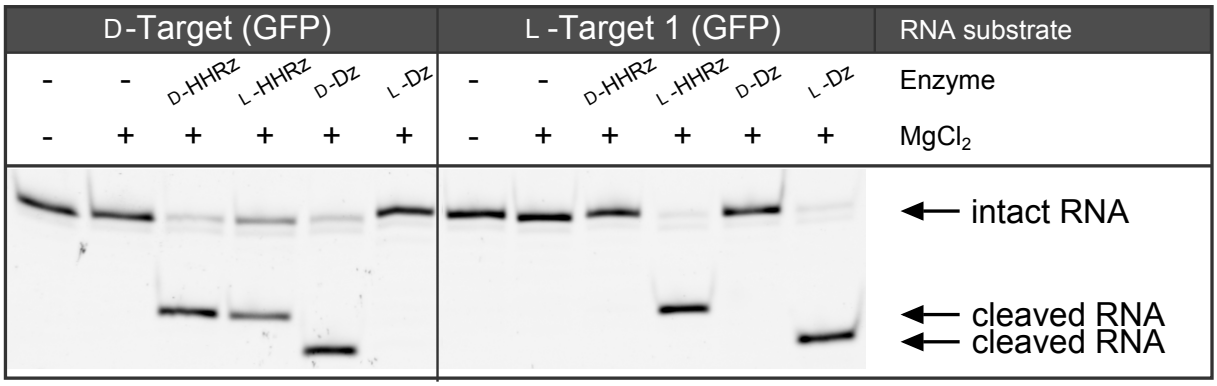


**Figure 2.5 – Heterochiral cleavage of GFP RNA substrates.** The samples that Wyszko et al (2014) used to obtain their published data were used for this experiment. The RNA substrates in D- and L-configuration resemble stretches of the GFP sequence. These substrates were incubated together with a tenfold molar excess of specific hammerhead ribozymes and 10-23 DNAzymes in D- or L-configuration. Incubation proceeded at 37 °C for 3 h. The samples were separated by 18 % dPAGE. Cleavage activity was observed for all homochiral systems. L-hammerhead ribozymes exhibited cleavage activity for the RNA target D-configuration L-DNAzymes completely failed to cleave D-RNA. HHRz = hammerhead ribozyme; Dz = 10-23 DNAzyme

this was not the case for the opposite setup: when incubating the L-RNA substrate together with the D-hammerhead ribozyme no cleavage was observed. This raises doubts as to the validity of the authors' conclusions. It is feasible that the L-hammerhead ribozyme sample was at one point contaminated with D-hammerhead ribozymes, possibly during synthesis or purification. Due to the enzymatic nature and high processivity of the hammerhead ribozyme, even trace amounts of D-hammerhead ribozymes could result in detectable cleavage over time. Contrary to the data of Wyszko et al (2014) the L-DNAzyme in this study also did not cleave the D-RNA substrate but only its L-RNA substrate. Since Spiegelzyme-mediated cleavage of PrP mRNA-related sequences could not be achieved this line of work was abandoned in favour of regular 10-23 DNAzymes in D-configuration.

## 2.3 DNAzymes cleave short RNA substrates

In the previous experiments, Spiegelzyme treatment was ruled out as an approach for the reduction of PrP mRNA levels since they did not cleave PrP-related D-RNA. Hammerhead ribozymes and 10-23 DNAzymes in D-configuration, however, cleaved RNA effectively. When comparing the two, it becomes evident that hammerhead ribozymes and 10-23 DNAzymes have different advantages and disadvantages. Hammerhead ribozymes consist of RNA that can be transcribed from a plasmid. The delivery of this plasmid to the target tissue could result in the constant production of hammerhead ribozymes for a certain time period after administration. Such an approach could in

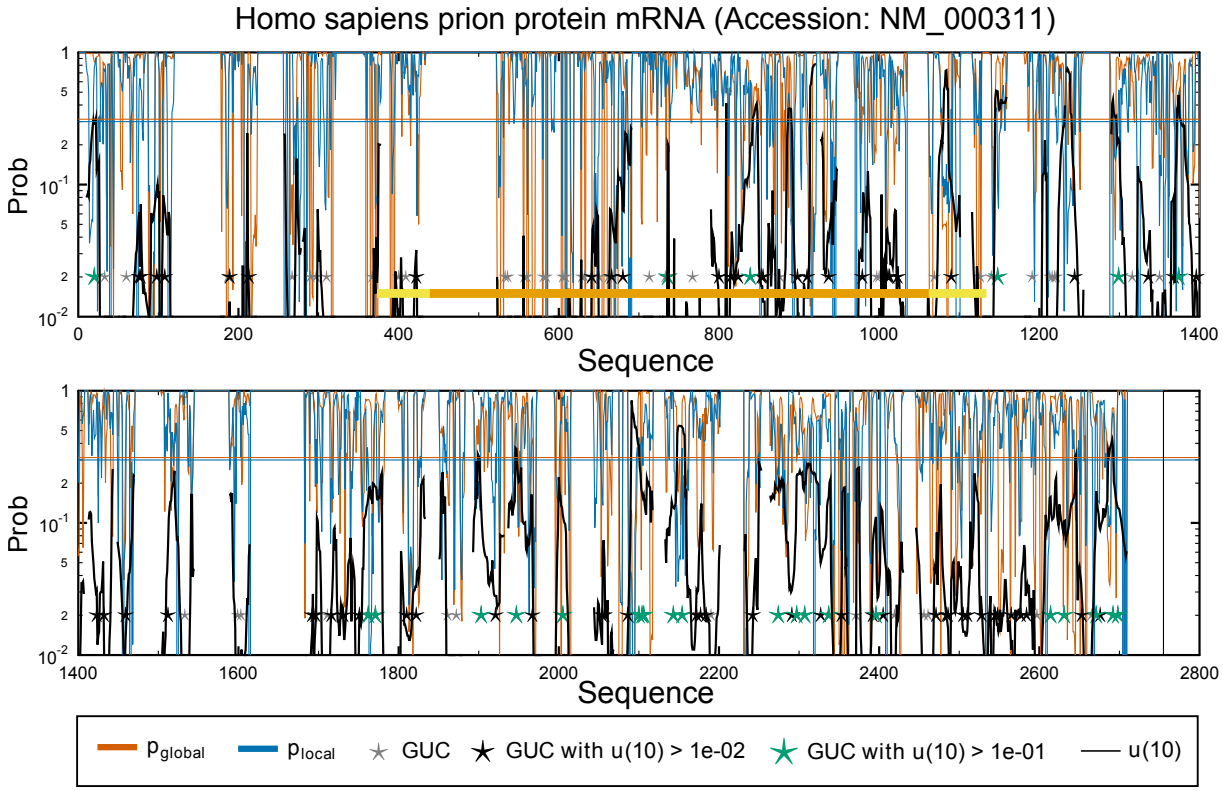


**Figure 2.6 – Accessibility of GU cleavage sites in the human PrP mRNA.** The x-coordinate represents the position in the mRNA sequence and the pairing probability is displayed on the y-axis. The local base-pairing probability $p_{local}$ for each nucleotide is represented by blue lines. It was calculated with the sequential folding program RNAPLFOLD. The black lines represent the propability $u_{10}$ that a sequence of length $l = 10$ centered at this position is not base-paired. The global base-pairing probability $p_{global}$ is shown by orange lines. GU sequences are represented by stars. Those sequence serve as cleavage sites for 10-23 DNAzymes. Grey stars show inaccessible GUs with $u_{10} < 0.01$. Black stars show medium accessible GUs with $u_{10} > 0.01$, and green stars indicate the most accessible cleavage sites with $u_{10} > 0.1$. The yellow bar indicates the open reading frame from position 373 to position 1134. The orange bar represents the sequence that corresponds to the mature protein after post-translational modification (439 to 1062).

theory limit the initial dose that needs to be administered. However, short nucleic acid strands are generally more well-defined than entire plasmids since a smaller number of factors need to be considered when estimating possible side effects. DNAzymes are inherently more stable in biological fluids than RNA and their chemical synthesis is more cost-effective. It is for these reasons that the following work focused exclusively on 10-23 DNAzymes.

With the focus on 10-23 DNAzymes instead of hammerhead ribozymes the previous cleavage site accessibility calculations become incomplete. Instead of the GUC cleavage sequence that was used before, any RY dinucleotide can be cleaved by the 10-23 DNAzyme. Even when only GU sequences are considered, the human PrP mRNA already contains 144 possible cleavage sites. 92 GUs have a $u_{10} > 0.01$ out of which 28 have a $u_{10} > 0.1$. Four cleavage sites were chosen that are located in the

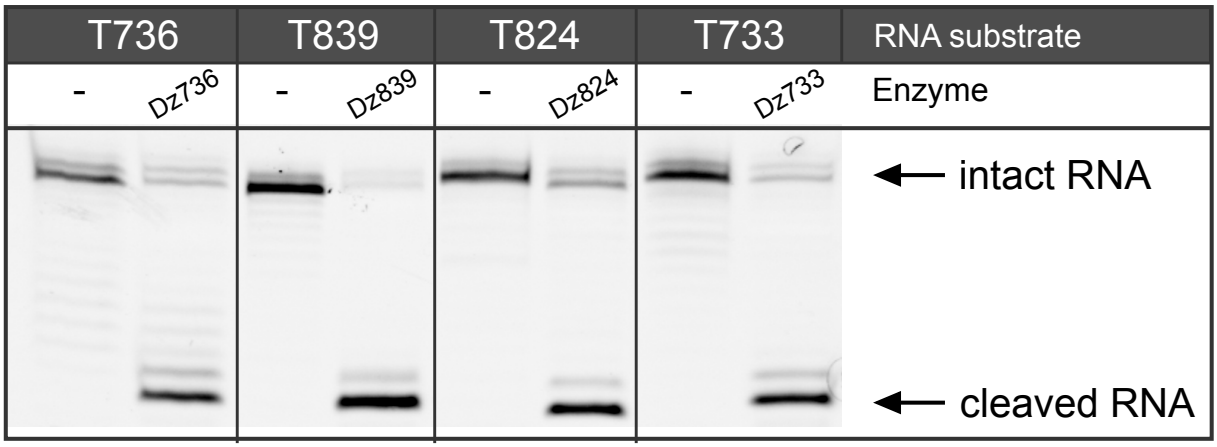


**Figure 2.7 – 10-23 DNAzymes cleave their respective targets.** The RNA substrates T736, T839, T824, and T733 were incubated for 3 h at 37 °C in absence or presence of a tenfold molar excess of the respective DNAzymes Dz736, Dz839, Dz824, and Dz733. Each substrate was cleaved nearly to completion by its respective DNAzyme, while the RNAs remained intact in the absence of catalysts. T = target; Dz = 10-23 DNAzyme

open reading frame (ORF) of the human prion protein mRNA (Fig. 2.6, yellow bar). The four cleavage sites that were selected are at positions 736, 839, 824, and 733. Positions 736 and 839 are highly accessible ($u_{10} = 0.198$ and $u_{10} = 0.309$, respectively). Position 824 has a medium accessibility ($u_{10} = 0.024$) and position 733 is considered inaccessible ($u_{10} = 0.002$). Those four target sites were chosen because they allow for testing whether the value of $u_{10}$ in fact has an influence on how well a respective DNAzyme performs. Initially, however, short RNA substrates were designed that are identical to the 25 nucleotides in the mRNA that contain the cleavage site at the center. These substrates were named after the position of the cleavage site in the mRNA sequence. For instance, the substrate T839 (T for target) is identical to nucleotides 827 to 851 of the prion protein mRNA which contains the GU cleavage site at positions 839 and 840. Cleavage in the mRNA would occur between those two positions. 10-23 DNAzymes were designed that are specific for these four targets: Dz736 specifically recognizes T736 and Dz839, Dz824, and Dz733 were named in the same manner.

In order to evaluate DNAzyme performance the four RNA substrates T736, T839, T824, and T733 were incubated together with a tenfold molar excess of the respective DNAzyme (Fig. 2.7). All four targets were cleaved nearly to completion after 3 h.

The following experiments aimed at monitoring the sequence specificity of each DNAzyme. Dz736 was incubated together with either of the four substrates T736, T839, T824 or T733 (Fig. 2.8). While T736 was effectively cleaved by Dz736, targets T839 and T824 remained intact when incubated together with Dz736 and were only cleaved by Dz839 and Dz824, respecively. T733, on the other hand, was cleaved by both Dz733 and Dz736. This is due to the fact that the targets T736 and T733 represent two mRNA stretches that overlap by 22 nt since the respective cleavage sites are only 3 nt apart.

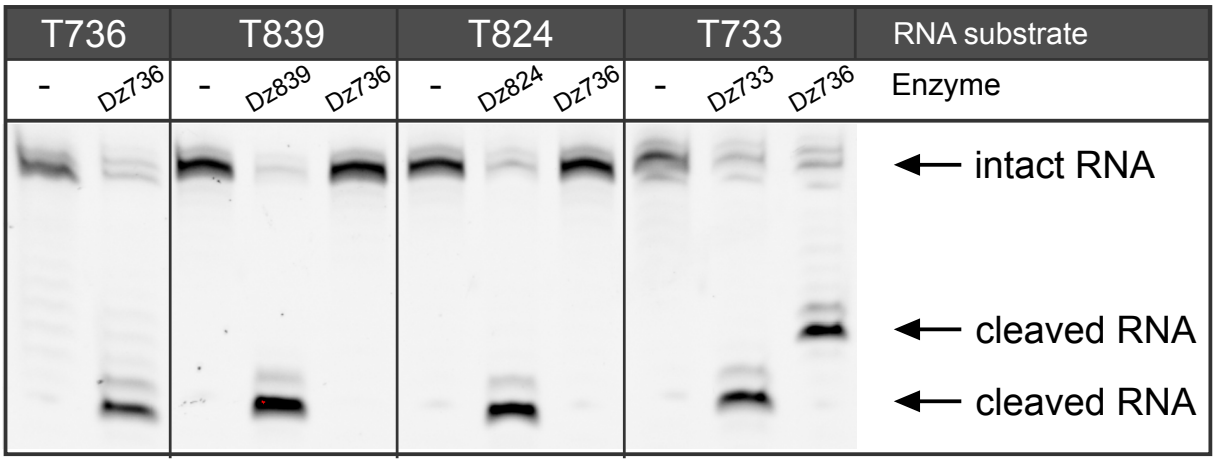


**Figure 2.8 – Dz736 is specific for substrates T736 and T733.** The four RNA substrates T736, T839, T824, and T733 were incubated together with their respective DNAzyme and additionally with Dz736. After 3 h at 37 °C, each target was cleaved exclusively by its specific DNAzyme with the exception of T733 which was cleaved by both Dz733 and Dz736. T736 and T733 overlap by 22 nt, therefore they are both recognized by Dz736. However, Dz736 still cleaves its specific cleavage site in T733. For that reason the cleavage product is larger than what is observed for the T733:Dz733 combination. T = target; Dz = 10-23 DNAzyme

Therefore, Dz736 also recognizes T733. Importantly, Dz736 still cleaves its respective cleavage site in T733. Because of that, the labelled reaction product is larger than that for Dz733-mediated cleavage and the two display a different running behaviour in denaturing RNA gel electrophoresis. It can be concluded that Dz736, even though it cleaves both T736 and T733, is specific for its cleavage site.

The same experiment was performed with the remaining DNAzymes to analyse their sequence specificity. As expected, Dz839 only cleaves the substrate T839 and was unable to recognize T736, T824, or T733 (Fig. 2.9). A similar result was observed with Dz824, which only cleaved T824 but not T736, T839, or T733 (Fig. 2.10). When the substrate specificity of Dz733 was tested a similar pattern as was observed for Dz736 emerged. While targets T839 and T824 again remained intact in the presence of Dz733, the combinations T733:Dz733 and T736:Dz736 both resulted in detectable RNA cleavage. The reason for the cleavage of T736 by Dz733 is the same as for the cleavage of T733 by Dz736: the two RNA substrates overlap by 22 nt and both can hybridize to each DNAzyme.

These results clearly demonstrate the effectiveness of DNAzyme-mediated RNA cleavage but they do not show the reaction kinetics. Also, since the DNAzymes were used in a molar excess over the RNA substrates, the experiments do not demonstrate multiple-turnover catalysis. The multiple-turnover behaviour of the selected DNAzymes will be explored in the following chapter.

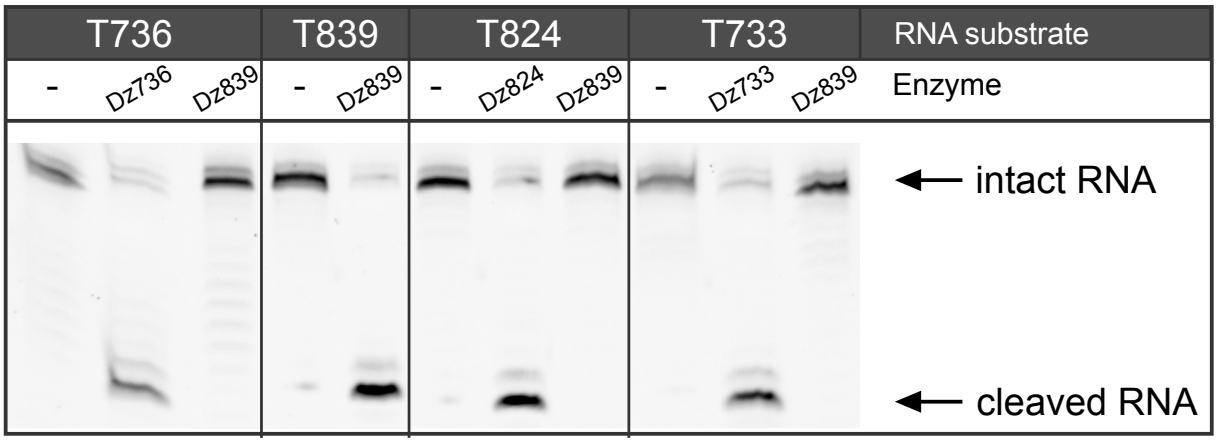


**Figure 2.9** – **Dz839 cleaves only its designated substrate.** T736, T839, T824, and T733 were incubated together with their respective DNAzyme and additionally with Dz839. Dz839-mediated cleavage only occured in the T839:Dz839 combination. All other substrates remained intact in the presence of Dz839 but were cleaved by their specific DNAzymes.

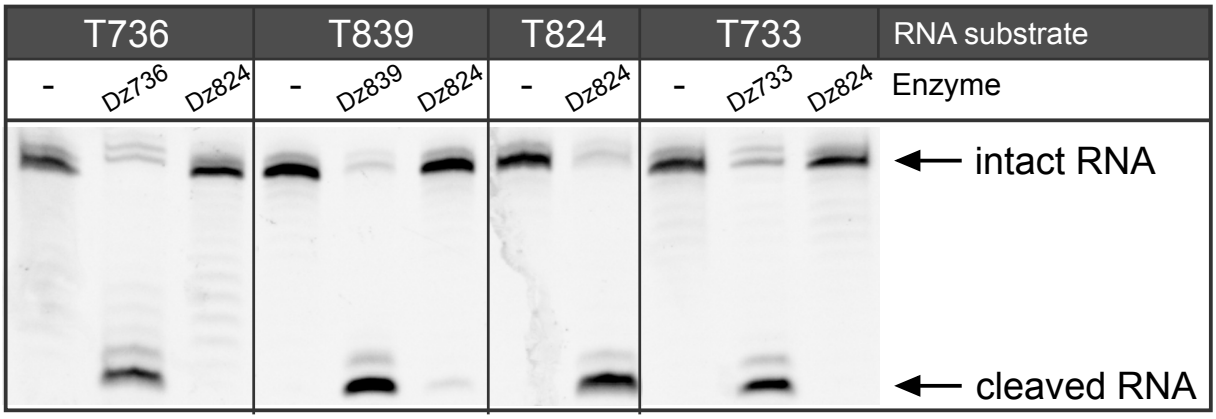


**Figure 2.10** – **Dz824 only cleaves T824.** When incubating T736, T839, T824, and T733 together with Dz824, only T824 is cleaved while the other targets are cleaved by their respective DNAzymes.

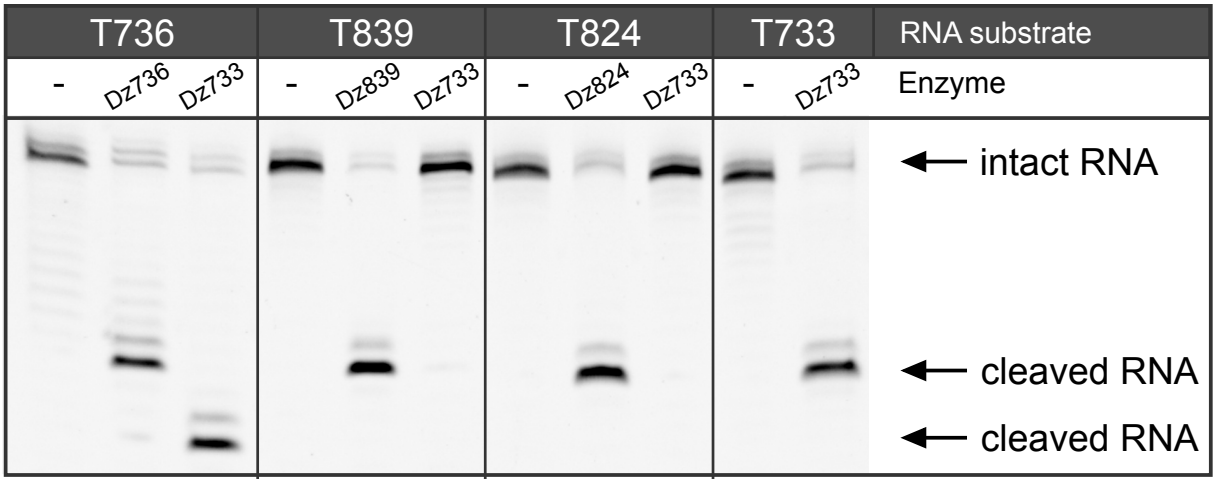


**Figure 2.11** – **Dz733 is specific for substrates T733 and T736.** The RNA substrates T736, T839, T824, and T733 were used in cleavage reactions with Dz736, Dz839, Dz824, and Dz733. Dz733 was used in combination with all four targets. While T839 and T824 were only cleaved by Dz839 and Dz824, respectively, Dz733 was able to cleave both T736 and T733 since the two substrates overlap by 22 nt. T = target; Dz = 10-23 DNAzyme

## 2.4 Multiple turnover RNA cleavage by DNAzymes

### 2.4.1 10-23 DNAzymes display multiple-turnover behaviour

From the previous experiments it is evident that specifically designed 10-23 DNAzymes cleave respective RNA targets that are identical to stretches of the human PrP mRNA. They do so in a sequence-specific manner. It is important to note that all experiments were performed with a tenfold molar excess of DNAzyme over RNA substrate and the reaction products were separated after a 3 h incubation time. Under these conditions two assumptions can be made: (i) almost all RNA strands are hybridized to a DNAzyme, (ii) the reaction is given enough time to proceed even if $k_{cat}$ is uncharacteristically low. The phosphodiester bond between two RNA nucleosides undergoes spontaneous transesterification with a rate constant of $10^{-8}\,\mathrm{min}^{-1}$ at 23 °C and neutral pH (Li and Breaker, 1999). Even a modest rate enhancement of $10^5$ practically guarantees cleavage within 180 min. By comparison, self-cleaving ribozymes typically approach maximum observed $k_{obs}$ values of $10\,\mathrm{min}^{-1}$, which is equivalent to a rate enhancement of $10^9$. Since this value is four orders of magnitude higher than what would be necessary for complete cleavage of the substrate RNA within a time frame of 3 h it is reasonable to assume that this is also possible with DNAzymes.

The previous experiments, however, do not display the reaction kinetics. The data are also not sufficient to classify these particular 10-23 DNAzymes as true catalysts which, by definition, emerge from a reaction unaltered and are therefore able to act repeatedly. In order to test whether the DNAzymes that were used in the previous experiments are truly catalytic the four RNA substrates T736, T839, T824, and T733 were incubated together with the respective DNAzymes in a 0.1:1 enzyme-to-substrate ratio (Fig. 2.12). In such an experimental setup complete RNA cleavage can only occur if every single DNAzyme molecule cleaves on average ten RNA substrate molecules. Interestingly, only Dz839 cleaves a tenfold molar excess of its substrate to completion. Dz839 is thus a true catalyst that works in a multiple turnover fashion, i. e. a single DNAzyme molecule catalyzes the cleavage of RNA substrate molecules multiple times. DNAzymes Dz736, Dz824, and Dz733 do not cleave more than 10 % of their respective substrates. Therefore, it must be concluded that in these instances DNAzymes act stoichiometrically, i. e. every DNAzyme molecule cleaves only one RNA molecule.

The discrepancy between the behaviour of Dz839 on one hand and that of the DNAzymes Dz733, Dz824, and Dz733 on the other hand can be comprehended in light of the multiple turnover process. Multiple turnover activity necessitates a cycle of three steps: (i) association of DNAzyme and RNA substrate, (ii) RNA cleavage, and (iii) release of the products which is immediately followed by step (i) again. A brief description of these steps can be found in Chapter 1.5: *The 10-23 DNAzyme* and in Figure 1.3 B

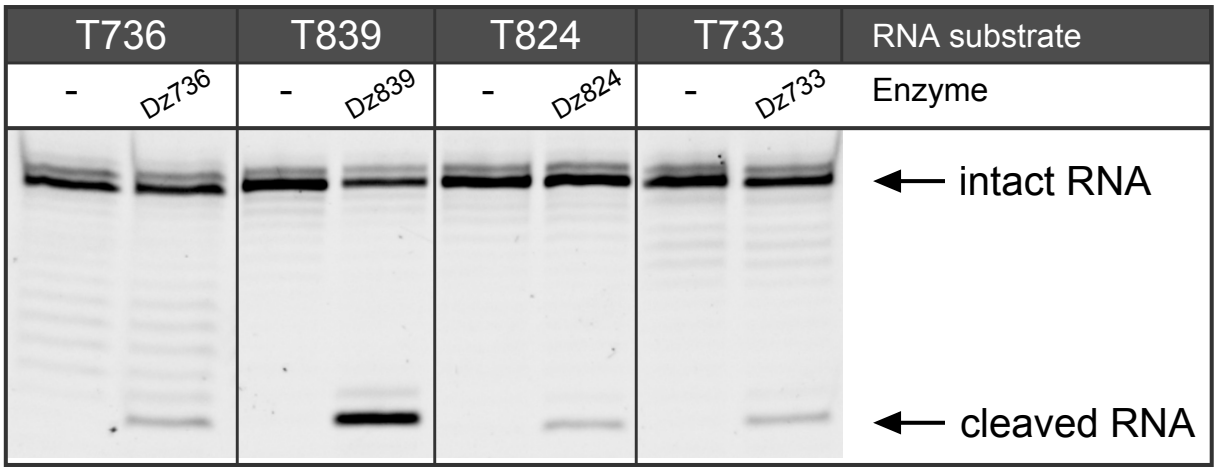


**Figure 2.12 – Single and multiple turnover behaviour of 10-23 DNAzymes.** The RNA substrates T736, T839, T824, and T733 were incubated together with a tenfold lower concentration of their respective DNAzymes. For complete RNA cleavage to occur, each DNAzyme needs to cleave a tenfold molar excess of RNA. After 3 h at 37 °C only Dz839 was able to cleave more than 10 % of its substrate. The other DNAzymes do not display multiple turnover behaviour. T = target; Dz = 10-23 DNAzyme

on page 11. It is evident that all three steps are performed when incubating Dz839 together with T839 but for the other combinations at least one of the steps is perturbed.

The association step (i) can be perturbed if the duplex of DNAzyme and RNA substrate has a thermal stability that is lower than required for its formation at the incubation temperature of 37 °C. It is clear though that the complex of DNAzyme and RNA forms at least once in all instances, otherwise no cleavage would be observed at all. But it is also possible that the samples reach a temperature that is lower than 37 °C before the reaction is initiated. This would enable the formation of a complex and RNA cleavage up to a point at which the incubation temperature of 37 °C is reached. Duplex stability is also crucial for the dissociation step (iii). In this case, however, it is the complex of DNAzyme and RNA cleavage products that is critical. If the thermal stability of these complexes is too high, the product strands will not dissociate from the DNAzyme or be displaced by a full-length substrate. In these instances, every DNAzyme molecule would cleave only one RNA molecule. Since the DNAzyme is not able to associate with another substrate, the reaction cycle is interrupted at this point. The actual cleavage of RNA (ii) could be a rate-limiting step of the reaction as well. For a reaction time of 3 h a rate enhancement of approximately $10^6$ would be necessary for complete cleavage of a tenfold molar excess of RNA. However, the data show that this is well within the limits of Dz839 performance and since all 10-23 DNAzymes share a common core sequence it is unlikely, although not impossible, that the actual cleavage steps proceed at different speeds.

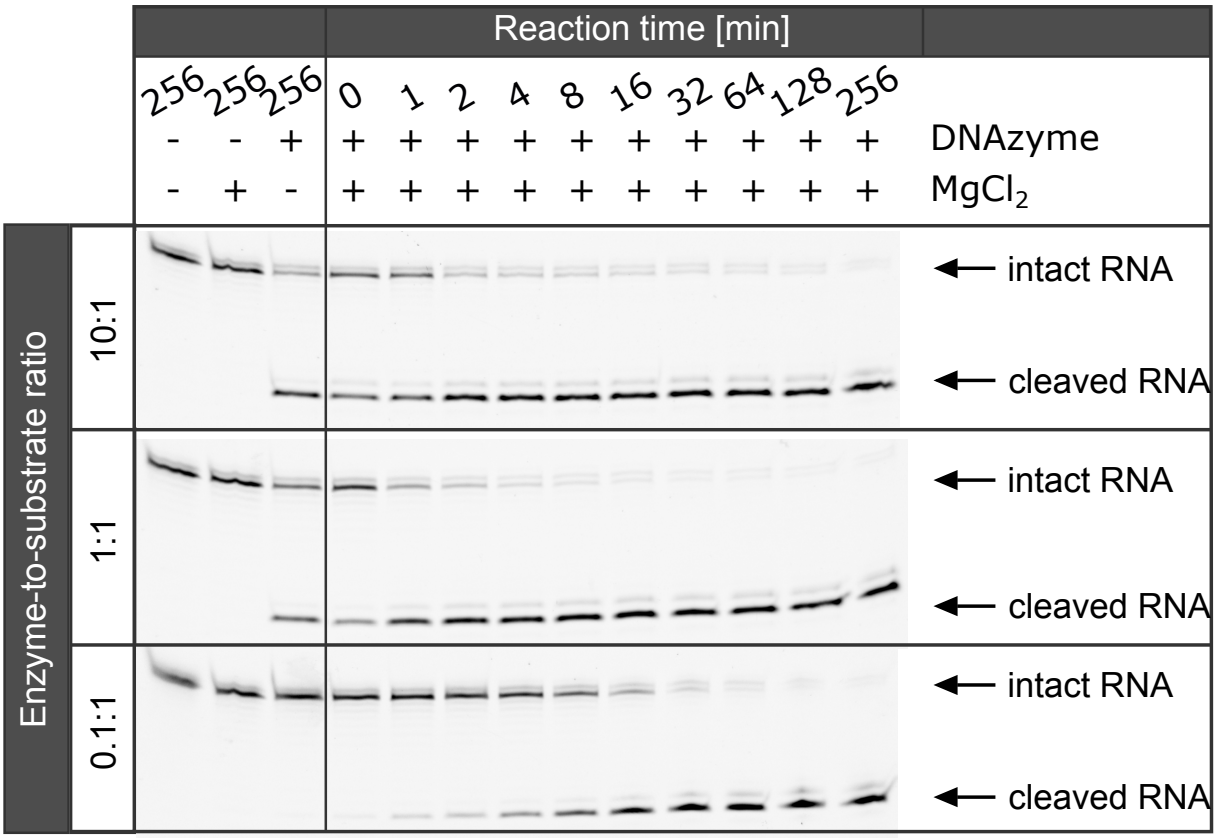


**Figure 2.13 – Single and multiple turnover kinetics of Dz839-mediated RNA cleavage.** The RNA substrate T839 was incubated with Dz839 in a 10:1, 1:1, or 0.1:1 enzyme-to-substrate molar ratio. Samples were taken at the indicated time points. The reaction kinetics are similar between the samples with tenfold molar excess of DNAzyme and the samples with equimolar concentrations of substrate and DNAzyme. In both cases cleavage is complete after 1 to 2 min. At an enzyme-to-substrate ratio of 0.1:1 DNAzyme-mediated cleavage reaches completion after 16 to 32 min, i. e. ten times slower.

### 2.4.2 DNAzyme kinetics

To gain an understanding of DNAzyme reaction kinetics Dz839 and T839 were incubated at different molar ratios and samples were taken at different points in time (Fig. 2.13). The concentration of T839 in these experiments is constant while the Dz839 concentration is altered. The data show that a tenfold molar excess of DNAzyme cleaves its RNA substrate to completion after 1 to 2 min. At a 1:1 molar ratio the reaction kinetics are remarkably similar. In fact, while the experimental procedure certainly leaves some room for error, the kinetic profiles are almost identical. The conclusion that can be drawn from these data is that even at a 1:1 molar ratio the RNA substrate is almost completely saturated with DNAzymes. Apparently, in the absence of cleavage, the equilibrium between non-hybridized RNA and DNAzymes and hybridized complexes strongly favours the latter to a point at which the population of non-hybridized sequences can be disregarded.

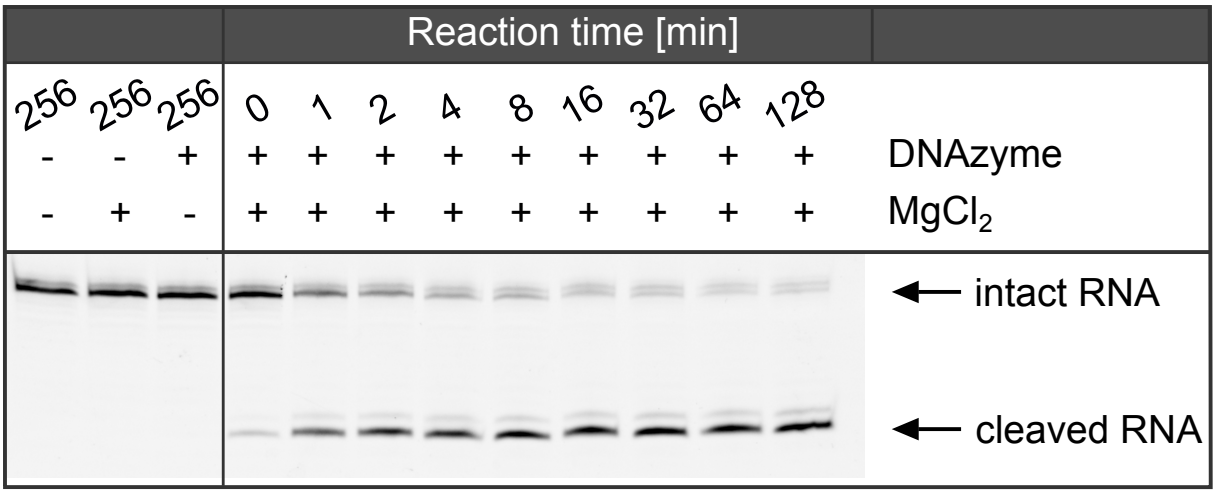


**Figure 2.14** – **Single turnover kinetics of Dz824-mediated RNA cleavage.** The RNA substrate T824 was incubated together with a tenfold molar excess of Dz824. Samples were taken at the indicated time points. The reaction kinetics are similar to those observed for Dz839 in combination with T839. Cleavage is complete after 2 to 4 min.

When comparing the single turnover kinetics of Dz839 to those of Dz824-mediated T824 cleavage the profiles are very similar (Fig. 2.13 and Fig. 2.14). Dz824 cleaves T824 to completion within 2 to 4 min. The Dz824 data were acquired with a 10:1 molar enzyme-to-substrate ratio since Dz824 was already shown to be incapable of multiple turnover catalysis (Fig. 2.12). The modest deviation from the observations that were made for Dz839 can be explained by slight variabilities that are introduced by the experimental procedure. Small differences notwithstanding, the $k_{obs}$ values for both DNAzymes are within the same order of magnitude. It is therefore highly unlikely that the rate of RNA cleavage prohibits Dz824 from performing multiple turnover catalysis.

### 2.4.3 Influence of $Mg^{2+}$ impurities

Surprisingly, in the case of Dz839, DNAzyme-mediated RNA cleavage could also be observed without the addition of $MgCl_2$ (Fig. 2.13). The existing literature has made it abundantly clear, though, that divalent metal ions are absolutely required for the activity of the 10-23 DNAzyme. Also, Dz736-mediated RNA cleavage was not observed without the addition of $MgCl_2$ (Fig. 2.14). Divalent metal ion contaminations in the Dz839/T839 samples are a possible explanation for this observation. In order to test this hypothesis, samples of the RNA substrate T839 were incubated together with a tenfold molar excess of Dz839 without adding any $MgCl_2$ (Fig. 2.15). Instead, the chelating agent EDTA (ethylenediaminetetraacetic acid) was added in different concentrations. EDTA binds metal cations with a charge number of $+2$ or higher and is thus well suited to sequester $Mg^{2+}$ or other divalent ions and prevent them from binding to the DNAzyme:RNA complex. Indeed, the presence of at least 1 mM EDTA completely

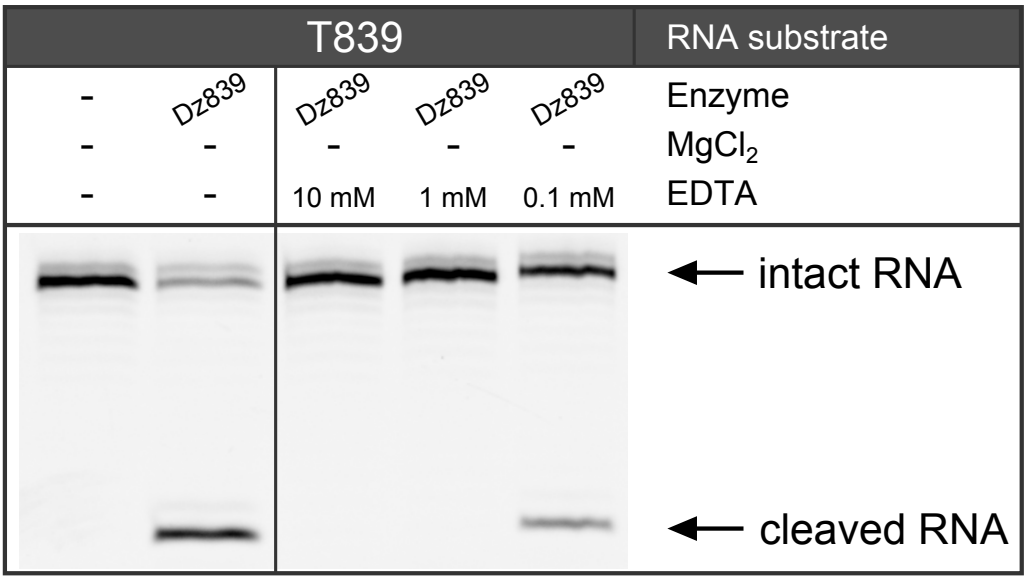


**Figure 2.15** – **Nucleic acid samples contain divalent cations.** The RNA substrate T839 was incubated together with Dz839 without addition of $MgCl_2$. After 3 h at 37 °C cleavage occured even when no $MgCl_2$ was added to the sample (slot 2). Addition of 10 or 1 mM EDTA to the reaction completely abolished cleavage while 0.1 mM EDTA led to a marked reduction. These data demonstrate that the initial samples contain divalent metal ions in a concentration range between 0.1 and 1 mmol $l^{-1}$. T = target; Dz = 10-23 DNAzyme

abolished DNAzyme activity. This result makes it clear that the activity that is observed without the addition of $MgCl_2$ is due to metal ion contamination. In the presence of 0.1 mM EDTA, activity is greatly reduced but not completely inhibited. EDTA binds its ligands stoichiometrically. Therefore, it can be assumed that the background contamination of divalent metal ions in these samples amounts to a concentration between 0.1 and 1 mM. The previously performed kinetics experiments give a hint as to which of the reaction components is contaminated (Fig. 2.13). At a 10:1 molar enzyme-to-substrate ratio Dz839 cleaves T839 to completion without the addition of $MgCl_2$. At a 1:1 ratio, however, only about 50 % are cleaved even after approx. 4 h. At a 0.1:1 enzyme-to-substrate ratio, Dz839-mediated T839 cleavage without the addition of $MgCl_2$ is undetectable. Importantly, only the Dz839 concentration differs between these experiments while RNA and buffer concentrations are kept constant. Taken together, these data point towards a contaminated DNAzyme sample. The concentration of divalent metal ions in this sample are sufficient to promote complete RNA cleavage at a 10:1 enzyme-to-substrate ratio. When the DNAzyme is diluted by a factor of 10 the background contamination is diluted likewise and only allows for minimal DNAzyme activity. If one of the other reaction components was contaminated the background concentration of divalent metal ions in these two experiments would be identical and thus DNAzyme activity could be expected to be more similar. Although it can be concluded that the Dz839 sample contains divalent metal ions, whether the contamination happened during synthesis, purification, or at a later time can only be speculated. When studying

the metal ion-dependency of DNAzymes these contaminations have to be taken into consideration.

### 2.4.4 Multiple turnover and thermal stability

The kinetics experiments show that RNA cleavage by DNAzymes occurs rapidly. They provide evidence that the actual cleavage reaction is not the rate-limiting step in multiple turnover catalysis. Different rate constants are likely not the reason why Dz839 is capable of multiple turnover RNA cleavage while Dz736, Dz824, and Dz733 are not true catalysts. It is more probable that impaired substrate association or product release cause this inability. To explore these possibilities the $T_m$ values for all DNAzyme:RNA duplexes were calculated (Table 2.1). For the duplexes formed by the DNAzyme and full-length RNA a single mismatch was assumed for the RNA position that is not base-paired. The $T_m$ value of the complex between Dz839 and its full-length RNA substrate T839 is at 47 °C and therefore higher than 37 °C (the human core body temperature) while both reaction products hybridize with Dz839 with $T_m$ values of 28.5 °C and 31 °C, respectively, i. e. lower than 37 °C, and therefore dissociate after cleavage. It is conspicuous that the complexes formed by Dz736, Dz824, and Dz733 with the respective RNA sequences do not have these properties. While the Dz736:T736 duplex indeed has a $T_m$ of 73 °C, which is higher than 37 °C, the $T_m$ values of the duplexes formed by Dz736 and its reaction products (51 °C and 63 °C, respectively) are still higher than 37 °C. For this reason, a product inhibition can be assumed because both reaction products may block Dz736 from binding to another full-length RNA substrate. For the combination of Dz824 and T824 the opposite is the case. The complex between DNAzyme and full-length RNA substrate already has a $T_m$ value that is lower than 37 °C, namely 31 °C. Therefore it can be expected that the Dz824:T824 duplex is not stable in the reaction conditions that were used. It is possible that Dz824:T824 complexes form before the incubation temperature of 37 °C is reached. RNA cleavage will occur up to

**Table 2.1** – $T_m$ values for DNAzyme:RNA duplexes

| Complex with | Dz736 | Dz839 | Dz824 | Dz733 |
|---|---|---|---|---|
| Full-length RNA substrate | 73 °C | 47 °C | 31 °C | 70 °C |
| 5' reaction product | 51 °C | 28.5 °C | 22 °C | |
| 3' reaction product | 63 °C | 31 °C | 17 °C | |

| Complex with | Dz736_6/7 | Dz824_10/11 |
|---|---|---|
| Full-length RNA substrate | 49 °C | 42 °C |
| 5' reaction product | 26.5 °C | 30 °C |
| 3' reaction product | 35.5 °C | 26 °C |

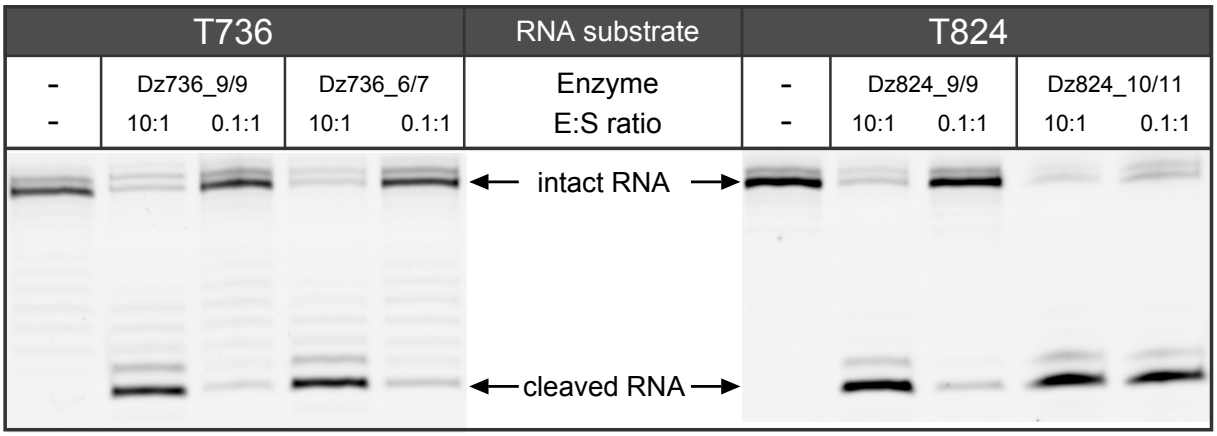


**Figure 2.16 – Single and multiple turnover behaviour of DNAzyme variants.** The RNA substrates T736 and T824 were incubated with Dz736 and Dz824 variants with shortened or lengthened substrate recognition arms in a 10:1 or a 0.1:1 enzyme-to-substrate molar ratio. During 3 h at 37 °C T736 was cleaved by both Dz736 variants but complete cleavage was only observed with a tenfold molar excess of DNAzyme. Multiple turnover cleavage could not be achieved. T824 was cleaved by both Dz824 variants. While Dz824_9/9 did not display any multiple turnover behaviour, Dz824_10/11 cleaved a tenfold molar excess of substrate to completion. T = target; Dz = 10-23 DNAzyme; E:S ratio = enzyme-to-substrate ratio

this point in time but afterwards no more complex formation takes place. Naturally, the $T_m$ values of the duplexes between Dz824 and its reaction products, with 22 °C and 17 °C, respectively, are also lower than 37 °C.

These calculations support the hypothesis that unfavourable duplex stability inhibits multiple turnover catalysis. Incidentally, Dz839 features the right characteristics. It is feasible to use rational design in order to bestow similar characteristics upon other DNAzymes. The $T_m$ value of a nucleic acid duplex is a function of both its length and nucleotide sequence. The nucleotide sequence is predefined by the desired target specificity of the DNAzyme and thus cannot be altered. Instead, altering the length of the hybridization arms of a DNAzyme can be used to manipulate duplex stability. When Dz736 is shortened by 3 nt beginning from the 5' end and by 2 nt from the 3' end the calculated $T_m$ for a complex with T736 decreases from 73 °C to 49 °C (Table 2.1). More importantly, the $T_m$ values for the duplexes of the 5' reaction product and the 3' reaction product with the new Dz736_6/7 drop below 37 °C, namely to 26.5 °C and 35.5 °C, respectively. For a Dz824 variant in which the hybridization arms are lengthened to 10 and 11 nt for the 5' and 3' arm, respectively, the $T_m$ value for the Dz824_10/11:T824 increases from 31 °C to 42 °C while the values for the reaction products with the DNAzyme (30 °C and 26 °C, respectively) are still below 37 °C. These two variants resemble Dz839 more closely in terms of duplex stability and, if the hypothesis is correct, are thus more likely capable of multiple turnover catalysis.

In order to test whether these rationally designed DNAzymes are able to perform multiple turnover cleavage the RNA substrates T736 and T824 were incubated with dif-

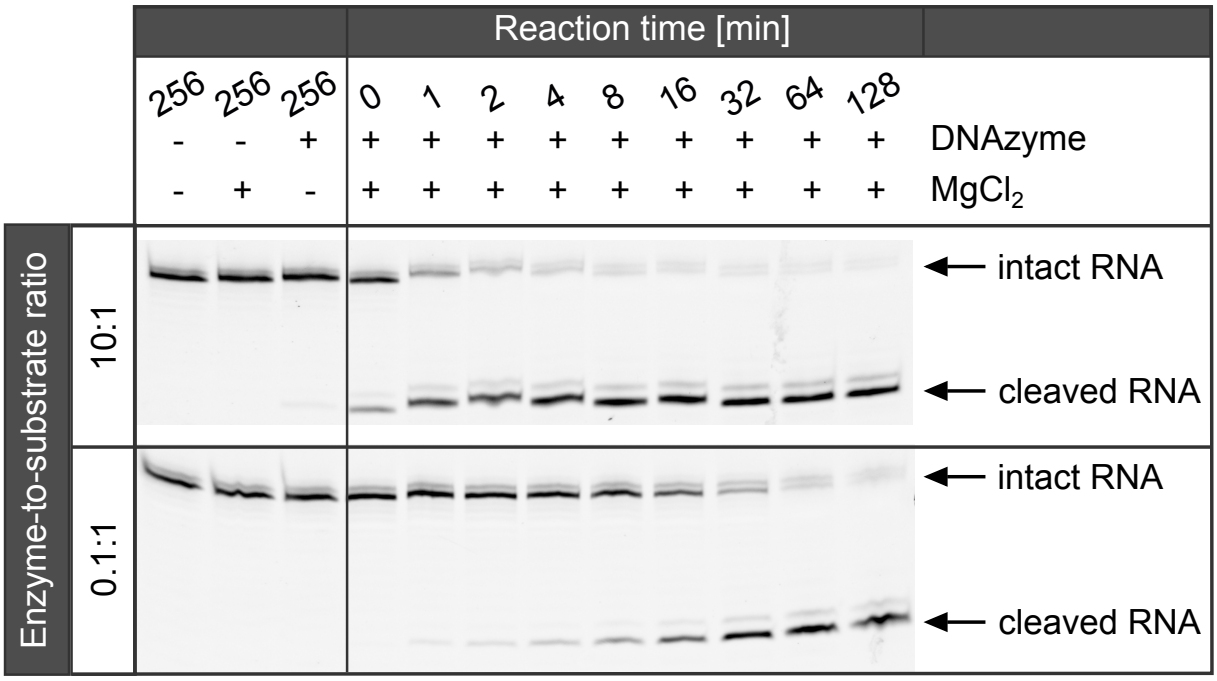


**Figure 2.17 – Single and multiple turnover kinetics of Dz824_10/11-mediated RNA cleavage.** The RNA substrate T824 was incubated together with Dz824_10/11 in a 10:1 or 0.1:1 molar enzyme-to-substrate ratio. Samples were taken at the indicated time points. A tenfold molar excess of DNAzyme cleaves the substrate to completion within 2 min. A tenfold lower concentration of DNAzyme cleaves its substrate to completion after 16 to 32 min. The reaction kinetics are similar to those observed with Dz839.

ferent DNAzyme variants in either a 10:1 or 0.1:1 molar enzyme-to-substrate ratio (Fig. 2.16). As before, a tenfold molar excess of Dz736 cleaves T736 to completion within 3 h but at a substrate-to-enzyme ratio of 0.1:1 Dz736 does not cleave more than 10 %. The Dz736_6/7 variant exhibited only a slightly higher extent of cleavage, but more favourable properties were expected. In the case of Dz824, however, the Dz824_10/11 variant is clearly able to cleave a tenfold molar excess of RNA to completion while its 9/9 counterpart did not perform multiple turnover catalysis. Although the approach was only successful for Dz824 and not for Dz736, the results show that it is feasible to alter existing DNAzymes in such a way that they gain multiple turnover capabilities.

To test whether the reaction kinetics of Dz824_10/11 are similar to those observed for Dz839, the RNA substrate T824 was incubated together with Dz824_10/11 in either a 10:1 or a 0.1:10 molar enzyme-to-substrate ratio. A tenfold molar excess of DNAzyme cleaves T824 to completion within 1 to 2 min. At a 0.1:1 enzyme-to-substrate ratio, T824 is completely cleaved after 32 to 64 min. This kinetic profile is similar to that of Dz839. The single turnover kinetics are nearly identical between the two DNAzymes. As for multiple turnover catalysis, Dz824_10/11 is slightly slower than Dz839 by a factor of approximately 2. These data support the notion that the substrate association and product release steps are indeed rate-limiting. The slight difference between the two

DNAzymes is possibly due to the slightly higher $T_m$ value for the Dz839:T839 duplex (47 °C) when compared to that formed by Dz824_10/11 and T824 (42 °C).

In conclusion, the data that were accumulated up to this point demonstrate that it is feasible to design 10-23 DNAzymes that cleave the human PrP mRNA. These specifically designed DNAzymes perform rapid RNA cleavage and can be fine-tuned to perform this reaction in a multiple turnover fashion.

## 2.5 DNAzyme activity during *in vitro* transcription

In the previous experiments 10-23 DNAzymes were established that cleave RNA substrates which resemble stretches of the human prion protein mRNA. These target stretches have different calculated accessibilities. Ultimately, the efficacy of a DNAzyme-mediated knockdown depends on the reactivity of the respective DNAzyme but also on whether it can reach its target stretch in the mRNA. Up to this point, however, all experiments were performed with short RNA molecules as a model. These short RNA molecules are suitable for studying reaction kinetics. But they are naturally not large enough to form the long-range contacts and secondary structures that could make cleavage sites inaccessible. Therefore, this experimental setup provides no information about the actual accessibility of the RNA target in the prion protein mRNA.

In order to test whether the accessibility calculations accurately describe if a particular DNAzyme cleaves structured RNA transcripts, the DNAzymes are to be tested on the human PrP23-230 RNA (which codes for the prion protein amino acids 23-230) while it is *in vitro* transribed from a plasmid. This experimental model was chosen because it mimics the situation *in vivo* that was described by Tafer et al (2008). Their calculations consider the situation of actively translated mRNA in the cell. During translation the helicase activity of the ribosome breaks down secondary structures as it scans across the mRNA. Local base pairing leads to restructuring of the mRNA while long-range contacts are slow to reform. Correspondingly, during *in vitro* transcription stretches of the transcripts adopt local secondary structures immediately after they are transcribed. Long-range interactions that lead to more complex folding are disfavoured. It is because of these similarities that *in vitro* transcription is considered an appropriate model for dynamic mRNA structure *in vivo*. But before DNAzyme activity in this model could be tested a suitable labelling method had to be established that would allow easy detection of the *in vitro* transcribed RNA and all cleavage products.

### 2.5.1 Fluorescent labelling of *in vitro* transcripts

The short RNA substrates that were used in the previous experiments were end-labelled with fluorescent moieties during synthesis by the manufacturer. Since the

*in vitro* transcripts will be produced enzymatically their visualization is not as simple. The use of dyes that intercalate between nucleobases, such as ethidium bromide, GelRed, or SYBR dyes, is standard procedure for nucleic acid visualization. However, the detection limit of these dyes for double-stranded nucleic acids is in the low nanogram range and sensitivity is usually much lower with single-stranded nucleic acids. The sensitivity of silver staining protocols does not depend as much on whether nucleic acids are single- or double-stranded but they are still limited to nanogram amounts and the staining is not restricted to newly transcribed RNA. In terms of sensitivity radioactive labelling of transcripts is the method of choice but requires specialized facilities with high standards of safety, which were not accessible during this project. Therefore, a different RNA labelling approach was chosen for this work.

In recent years, Click Chemistry has emerged as a collection of reactions for the joining of molecules, e.g. a biomolecule and a fluorescent dye (Agard et al, 2006). Click Chemistry comprises different reactions, among the most common ones are Copper(I)-catalyzed azide-alkyne cycloaddiction (CuAAC) and strain-promoted azide-alkyne cycloaddition (SPAAC). In both cases one of the molecules that are to be joined bears an azide group while the other one carries an (internal or terminal) alkyne. The azide and alkyne react in a cycloaddition to form a 1,2,3-triazole. Both the CuAAC and SPAAC reactions are variants of a 1,3-dipolar cycloaddition, the so-called Huisgen cycloaddition. The standard Huisgen cycloaddition, however, is not suitable for the use in biological systems because it usually requires high temperatures. However, the reaction can be greatly sped up by the presence of Cu(I) ions as catalysts, as is the case in CuAAC. In SPAAC, on the other hand, a cyclooctyne moiety is used as a reaction partner for the azide. The bond angles in this cyclooctyne are distorted which makes the molecule highly reactive. In both cases, the cycloaddition proceeds readily in physiological conditions. Importantly, both approaches share the advantage that neither azide nor alkyne groups appear in biological systems. A biomolecule bearing an azide or alkyne is introduced into the system and only this molecule will react with the reaction partner. Other biomolecules, and biological processes in general, will not be disturbed. Click Chemistry is therefore considered to be completely bioorthogonal.

For this work Click Chemistry was regarded as a suitable means of linking *in vitro* transcribed RNA to a fluorescent dye for simple visualization. The SPAAC method was chosen in particular. The general scheme and the important reactants can be seen in Fig. 2.18. RNA is produced during *in vitro* transcription from a plasmid that contains the gene of interest downstream of a T7 promoter. A T7 terminator sequence downstream of the gene of interest terminates transcription. All ribonucleoside triphosphates are provided for the reaction, and importantly, a mixture of natural UTP and 5-Azido-UTP is used. 5-Azido-UTP represents a UTP molecule which carries a C3 linker with an azide group at the $C^5$ atom of the uracil. The T7 RNA polymerase accepts both

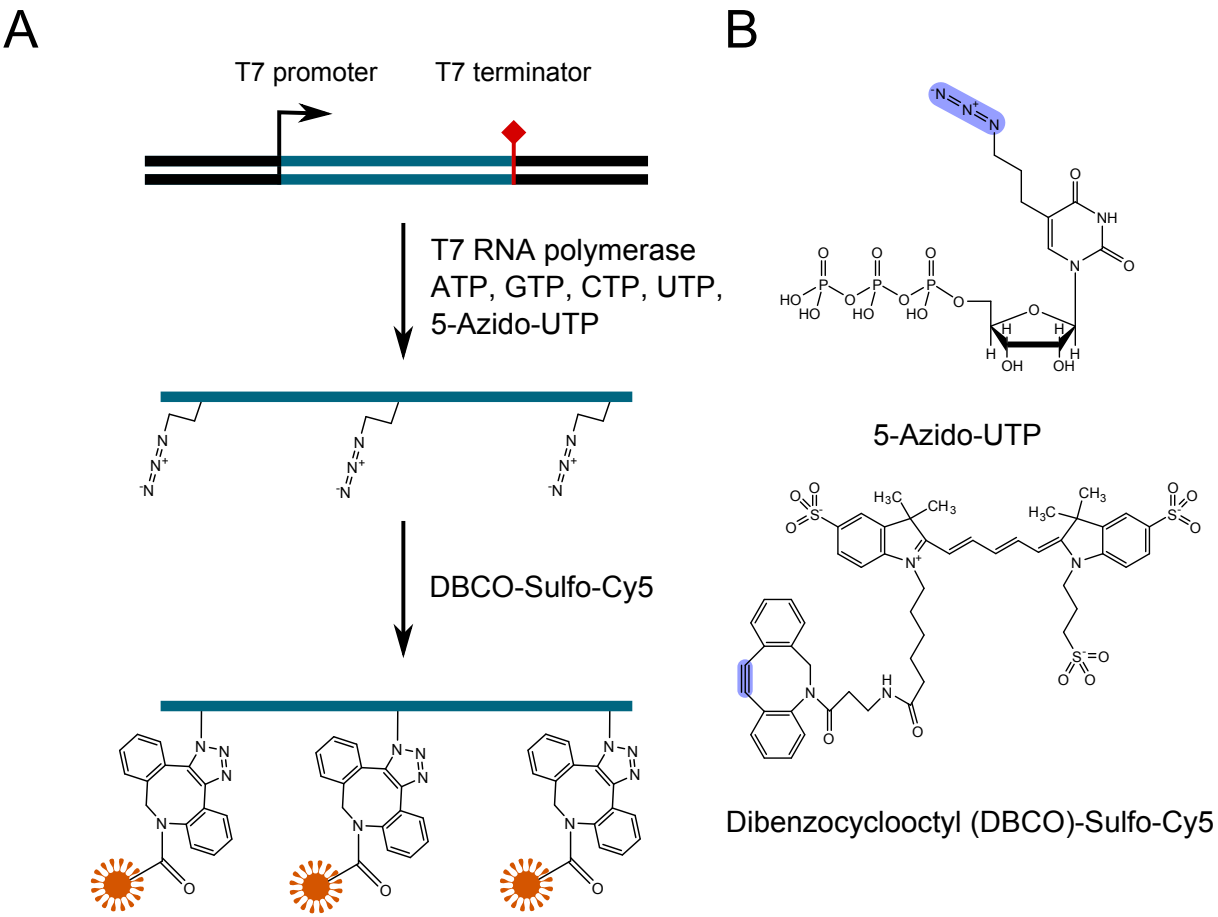


**Figure 2.18 – Fluorescent labelling of RNA transcripts. (A)** RNA transcripts are produced from a plasmid via T7 *in vitro* transcription. For the reaction ATP, GTP, CTP, UTP, and 5-Azido-UTP are provided in a 1:1:1:0.75:0.25 molar ratio. 5-Azido-UTP is randomly incorporated instead of UTP resulting in transcripts that contain on average two to three azide groups per 100 nt. The azide groups are then functionalized with DBCO-Sulfo-Cy5 via copper-free Click Chemistry. **(B)** Chemical structure of 5-Azido-UTP (top) and DBCO-Sulfo-Cy5 (bottom). The terminal azide and strained alkyne groups that are highlighted in blue form the 1,2,3-triazole during the Click reaction. ATP = adenosine triphosphate; GTP = guanosine triphosphate; CTP = cytidine triphosphate; (5-Azido-)UTP = (5-Azido-)uridine triphosphate; DBCO = Dibenzocyclooctyl

variants as substrates and incorporates them randomly into the growing RNA strand. This results in a mixture of RNA transcripts with identical sequences and randomly distributed azide groups that can be used for fluorescent labelling. On average, two to three azide groups per 100 nt can be expected. The RNA is purified via gel filtration to remove all non-incorporated nucleoside triphosphates. Afterwards, the addition of Dibenzocyclooctyl (DBCO)-Sulfo-Cy5 initiates the Click reaction which joins fluorescent Cy5 moieties to each 5-Azido-UTP in the RNA. The labelled RNA is purified again, separated via dPAGE, and then visualized by exciting the Cy5 moieties with light at $\lambda_{Ex} = 649\ nm$ and detecting fluorescence at $\lambda_{Em} = 666\ nm$. Since the Cy5 moieties are distributed randomly within the full-length RNA the fragments from DNAzyme-mediated cleavage are also labelled.

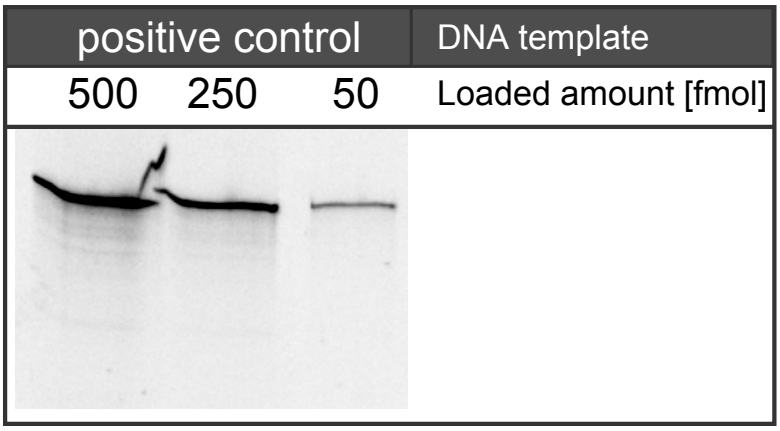


**Figure 2.19 – RNA can be fluorescently labeled via Click Chemistry.** A 1423 bp linear control template was *in vitro* transcribed in the presence of ATP, GTP, CTP, and UTP as well as 5-Azido-propyl-UTP in a 1:1:1:0.75:0.25 molar ratio to produce azide-labeled RNA transcripts. The transcripts were then incubated with a tenfold molar excess of DBCO-Sulfo-Cy5. Different amounts of the reaction products were separated via 5 % dPAGE. The procedure yielded Cy5-labeled RNA transcripts that were detectable even in low femtomolar amounts.

All necessary reaction components are commercially available in a single kit that is actually marketed as a simple method for the production of fluorescently labelled RNA probes for *in situ* hybridization and microarray analyses (Jena Bioscience GmbH, Jena, Germany). Its use is also convenient for the purposes of this work. The kit contains a linearized plasmid with a length of 1423 bp as a control template. Since the plasmid is linearized, the T7 RNA polymerase will fall off the end of the double-strand thus resulting in the production of so-called run-off transcripts of defined length without the need for a T7 terminator sequence. In an initial test, the control template was used for the *in vitro* transcription of a 1423 nt RNA molecule (Fig. 2.19). ATP, GTP, CTP, UTP, and 5-Azido-UTP were provided in a 1:1:1:0.75:0.25 molar ratio for an estimated labelling efficiency of 2 to 3 azide groups per 100 nt. Afterwards, the RNA was purified via gel filtration and its concentration was measured. Then the amount of azide modifications was calculated assuming an equal distribution of all four nucleotides and a 100 % substitution efficiency, i. e. a theoretical maximum of 25 azide groups per 100 nt of RNA. The RNA was incubated together with a tenfold molar excess of DBCO-Sulfo-Cy5 in regard to the amount of azide modifications for 1 h in the dark. During this time, the modified RNA is covalently linked to Cy5 moieties via Click Chemistry. The sample was then purified again and separated via 5 % dPAGE. When imaging the RNA via Cy5 fluorescence it becomes clear that even low femtomolar (50 fmol) amounts are easily detectable. As is evident from the results, a single RNA molecule of defined length was produced and successfully labelled.

Based on this initial test it can be considered feasible to produce PrP transcripts and label them in the same way. The procedure was employed with a plasmid as template that contains the human PrP23-230 coding sequence (CDS) flanked by a T7 promoter

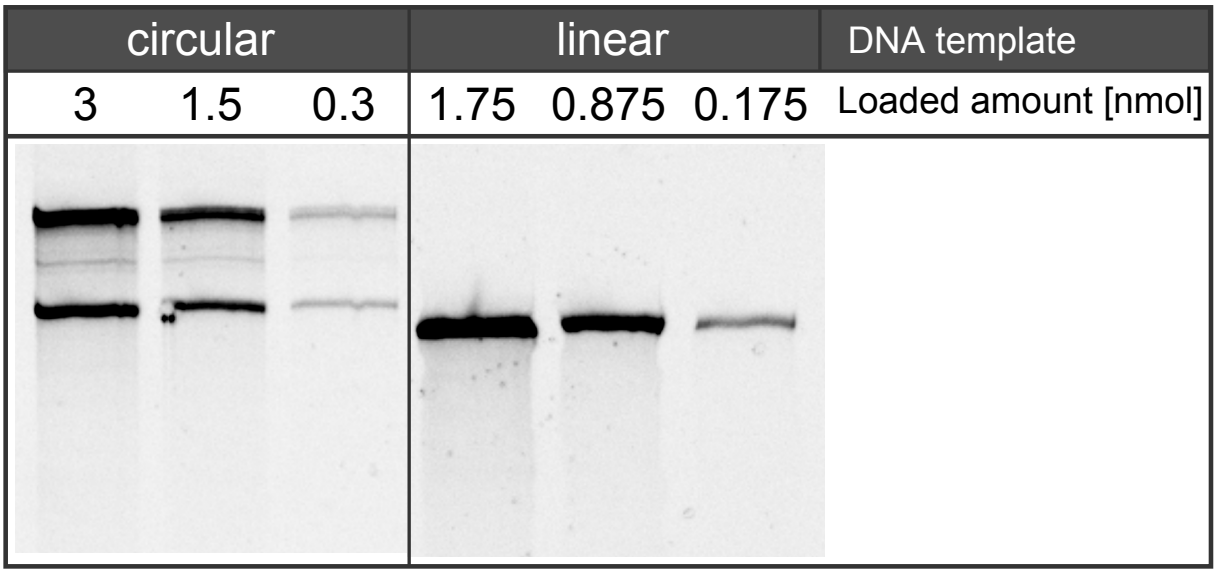


**Figure 2.20** – **Fluorescent labelling of human PrP transcripts.** Human PrP23-230 RNA transcripts were *in vitro* transcribed from a pET11a vector that contains the huPrP23-230 CDS insert flanked by a T7 promoter and a T7 terminator site. The template was either circular or linearized beforehand immediately downstream of the insert. Afterwards, the reaction products were fluorescently labelled via Click Chemistry and different amounts were separated via 5 % dPAGE. The different reaction products that arise during *in vitro* transcription from the circular plasmid show that the T7 terminator signal does not terminate transcription efficiently. When using a linear template, however, run-off transcripts of a defined length were produced.

and a T7 terminator site (Fig. 2.20). Transcription should result in RNA transcripts with an approximate length of 850 nt. The same molar ratio of nucleoside triphosphates as before was used during *in vitro* transcription. The azide-modified RNA was again purified and incubated with a tenfold molar excess of DBCO-Sulfo-Cy5 in regard to the calculated amount of azides. The products were purified, separated via 5 % dPAGE, and imaged. The results show that not a single defined transcript was produced when the circular plasmid was used as a template. Instead, two distinct bands of similar intensity are visible. A third band of lower intensity which migrates between the other two bands can also be seen. A possible explanation for these results is that the T7 terminator sequence does not terminate transcription effectively and the T7 RNA polymerase falls off the template at a later point. Indeed, run-off transcripts of a single defined length are produced when using a plasmid as a template that was linearized by endonuclease digestion immediately downstream of the PrP23-230 CDS insert. These RNA products migrate slightly faster than the smallest transcripts that were produced from the circular plasmid. The slight difference in length corresponds to a short stretch of approximately 60 bp between the insert and the T7 terminator sequence. Because of the restriction site that was chosen for linearization, the run-off transcripts do not contain this short stretch and are therefore expected to migrate slightly faster than the T7 terminated transcripts. These data point toward the conclusion that the shorter

products that result from *in vitro* transcription from the circular template represent the properly terminated transcripts. Apparently the T7 RNA polymerase continues transcription from the circular plasmid after the termination signal in up to 50 % of cases, leading to larger transcripts. However, it is not clear at this time why these longer products are so well-defined. If the T7 RNA polymerase transcribed the entire plasmid until it reaches the termination signal again a transcript length of approximately 7000 nt could be expected, i. e. nearly ten times larger than the properly terminated transcripts. A nucleic acid of this size would not easily migrate into a 5 % polyacrylamide gel. It is possible that the larger product size is just indicative of the natural processivity of the T7 RNA polymerase. At this point, no explanation can be offered for the medium-sized transcription product. However, it is clear that the use of a linear template resulted in transcripts with a single, well-defined length. These transcripts were efficiently labelled with fluorescent moieties and can be detected down to at least femtomole amounts. Clearly this protocol is suitable for the production of human PrP23-230 CDS transcripts that can be used in DNAzyme assays.

### 2.5.2 DNAzymes cleave *in vitro* transcripts

Since the production and labelling of human PrP23-230 CDS transcripts was successful the next task was to test whether these RNAs are efficiently cleaved by DNAzymes. Also, the predictions of the sequential folding algorithm on target site accessibility were evaluated. In a first experiment, the transcripts were produced during *in vitro* transcription in the absence of DNAzymes. After the first purification step, the transcripts were denatured and cooled down, enabling them to adopt a global folding. Separately denatured DNAzymes were added to the transcripts in the standard reaction conditions that were used in the activity assays before. After incubation for 3 h at 37 °C the reaction products were purified again. During gel filtration the DNAzymes are also discarded and only the (intact or cleaved) transcripts, together with the plasmid template, remain. Fluorescent labelling via Click Chemistry, a third purification step, and analysis were performed after that. When the products were separated by 5 % dPAGE and detected via fluorescence it is evident that the four DNAzymes Dz736, Dz839, Dz824, and Dz733 show different levels of cleavage activity (Fig. 2.21). Without the addition of DNAzymes, the PrP transcript remains intact during the incubation step. The DNAzymes Dz736, Dz839, and Dz733 are active which is apparent from the appearence of prominent bands for the cleavage products. But a large proportion of the transcripts are not cleaved. Dz824 shows no cleavage activity at all. These data do not fully agree with the accessibility that was predicted by the sequential folding calculations. According to the prediction DNAzymes Dz736 and Dz839 would perform best while medium performance for Dz824 and no performance at all for Dz733 were predicted. Yet, it is

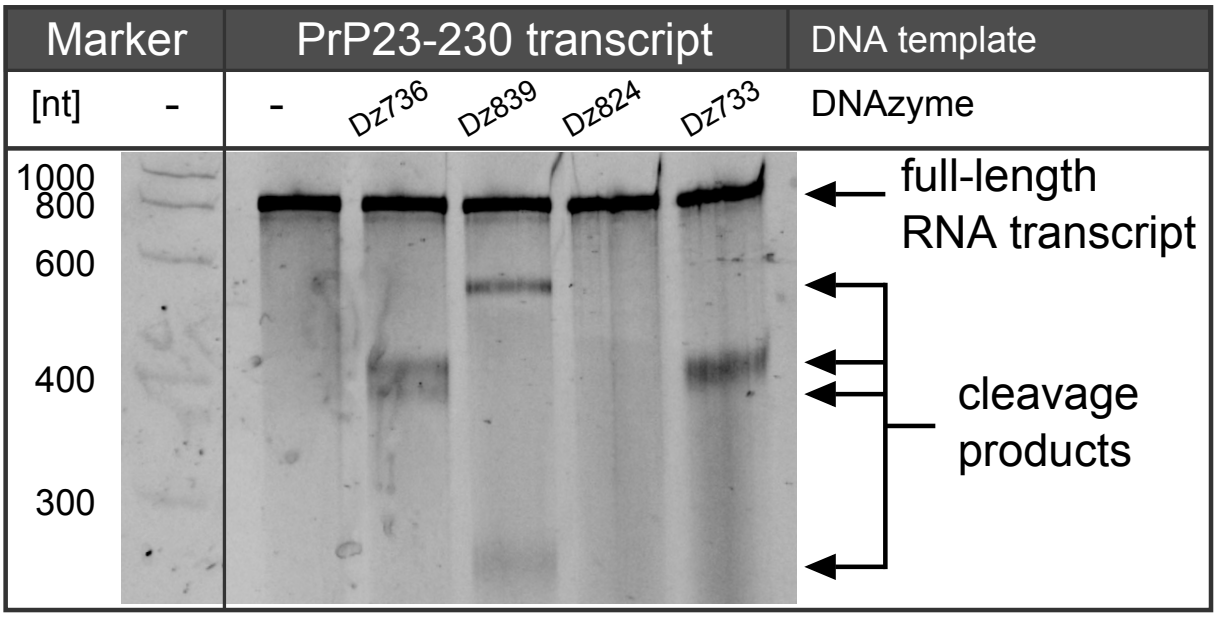


**Figure 2.21 – DNAzyme-mediated cleavage of RNA transcripts.** Human PrP23-230 RNA was produced via *in vitro* transcription. The RNA was denatured and cooled down, allowing it to adopt a global folding that is thermodynamically favoured. These *in vitro* transcripts were incubated together with the four DNAzymes Dz736, Dz839, Dz824, and Dz733 for 3 h at 37 °C, the reaction products were fluorescently labeled via Click Chemistry and separated via 5 % dPAGE. All DNAzymes cleaved the RNA transcripts to a certain extent with the exception of Dz824 which showed no detectable cleavage. Dz = 10-23 DNAzyme

important to note that the conditions in which the DNAzyme cleavage reactions were performed differ from the situation that is the basis for these calculations. In this experiment, the transcripts already formed secondary structures. The denaturation and cooling steps ensure that the thermodynamically favoured global folding is adopted. Only then are the DNAzymes added. The calculations, however, are based on local base-pairing probabilities with a maximal distance of 40 nt between two bases that are paired. This means that no long-range interactions are taken into account, yet those interactions often contribute to the formation of a thermodynamically favoured structure. In conclusion, the results demonstrate that the tested DNAzymes are indeed able to cleave long, structured RNA transcripts in standard conditions. The information that the data provide about target site accessibility, however, is limited and does not reflect the conditions in the cell. This cellular context is taken into consideration during the calculation of the target site accessibility.

To assess the validity of these calculations, several *in vitro* transcription reactions were set up as before but this time the different DNAzymes were added to each reaction before starting the transcription by adding the T7 RNA polymerase (Fig. 2.22). After 1 h at 37 °C the reaction was stopped, the products were purified, labelled, and analyzed via 5 % dPAGE. The results show that DNAzyme-mediated cleavage during *in vitro* transcription correlates well with the value of $u_{10}$, which expresses the accessibility of

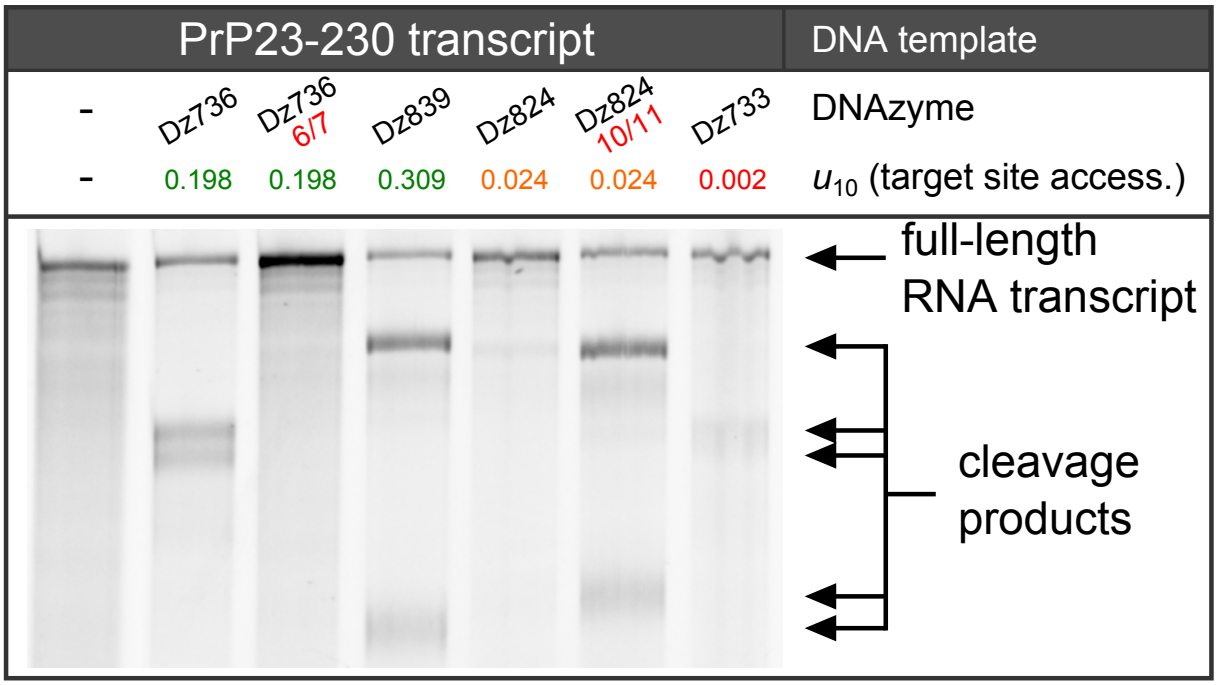


**Figure 2.22 – DNAzyme activity during transcription.** Human PrP23-230 RNA was produced via *in vitro* transcription in the presence of 10 mmol $l^{-1}$ of either Dz736, Dz736_6/7, Dz839, Dz824, Dz824_10/11, or Dz733. The reaction was carried out for 1 h at 37 °C. Afterwards, the products were purified, fluorescently labeled via Click Chemistry, and separated via 5 % dPAGE. The DNAzymes cleaved the RNA transcripts with observed efficacies that are consistent with the predicted target site accessibility. Dz = 10-23 DNAzyme; access. = accessibility. Colour coding for $u_{10}$ (target site accessibility): Green = highly accessible, orange = medium accessibility, red = inaccessible

the respective target site. DNAzymes Dz736 and Dz839, the target sites of which have the highest accessibility, cleave the *in vitro* transcribed RNA effectively. On the other hand, Dz824, with medium accessibility, and Dz733, where the target site is inaccessible, show almost no cleavage. Interestingly, the Dz736_6/7 variant did not cleave RNA transcripts substantially even though its single-turnover activity was previously shown to be comparable to that of Dz736_9/9 (Fig. 2.16 on page 36). One likely explanation is that the shortened variant lost the ability to compete with secondary structure formation.

The DNAzyme Dz824_10/11, on the other hand, was able to cleave RNA transcripts whereas its shorter counterpart showed no cleavage (Fig. 2.22). The observed activity of Dz824_10/11 was comparable to that reached by Dz736 and Dz839. It is clear that the Dz824_10/11 variant gained access to its cleavage site. This could be due to a higher capability to compete with secondary structure formation. However, as can be seen in Table 2.1 on page 35, the complex between DNAzyme Dz824_9/9 and its RNA target has a $T_m$ of 31 °C, which is lower than the incubation temperature of the experiment. Since the DNAzyme and the substrate were not incubated together in an initial renaturation phase, as was the case when using short substrates, it is likely

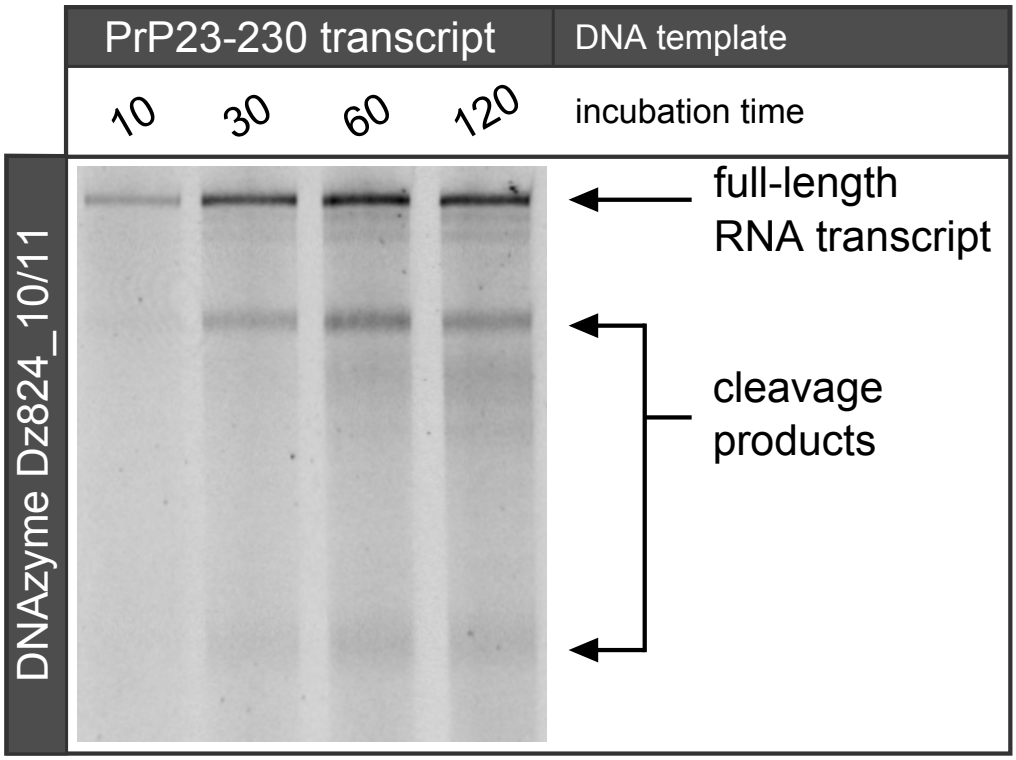


**Figure 2.23 – Kinetics of DNAzyme-mediated cleavage during transcription.** Human PrP23-230 RNA was produced via *in vitro* transcription. During the reaction 10 mmol $l^{-1}$ of Dz824_10/11 are present. The reaction was carried out for 2 h at 37 °C and samples were taken at the indicated time points. Then, the products were purified, fluorescently labeled, and separated via 5 % dPAGE. While Dz824_10/11 is able to cleave *in vitro* transcribed RNA, the T7 RNA polymerase produces new transcripts more quickly than cleavage can occur. Dz = 10-23 DNAzyme

that the Dz824_9/9 is unable to hybridize with the RNA transcripts in the first place. Dz824_10/11, on the other hand, forms a duplex with its complementary RNA with a $T_m$ of 42 °C. It is therefore feasible that the better performance of Dz824_10/11 in terms of transcript cleavage is actually not due to increased competition with secondary structure formation in the RNA transcripts but rather a product of a more stable hybridization between DNAzyme and substrate.

Lastly, the cleavage activities observed for Dz736 and Dz733 are markedly different. This is particularly interesting in light of the fact that the two cleavage sites for these DNAzymes are only 3 nt apart. While the effect of this small shift is striking it was correctly predicted by the sequential folding algorithm, which calculated a target site accessibility of $u_{10} = 0.198$ for cleavage site 736 and $u_{10} = 0.002$ for cleavage site 733.

While the data clearly show that several DNAzymes are able to cleave long, structured RNA transcripts, none of them cleaved their substrates to completion. Yet, it is important to note that during *in vitro* transcription the production of a single transcript is almost only limited by the concentration of nucleoside triphosphate precursors. Indeed, when looking at different time points during transcription, it is evident that Dz824_10/11

cannot compete with the rate of transcription of the T7 RNA polymerase (Fig. 2.23). The T7 polymerase transcribes RNA faster than the DNAzyme cleaves the transcripts. In cells, however, transcription is more tightly regulated to conserve energy and other resources. The copy number of an individual transcript can be much lower owing to the fact that polyribosomes can continuously translate a single mRNA into large amounts of protein. While a small decrease in mRNA levels is often buffered by high polyribosome activity, this also means that there are fewer transcripts to begin with. Taken together, these *in vitro* experiments are not necessarily indicative of the actual activity of DNAzymes in cells. They do, however, allow fundamental insights into the accessibility of cleavage sites for DNAzymes. Importantly, the performance of Dz733 was dependent on whether the RNA substrate was previously produced and allowed to adopt a global folding or if it was transcribed with the DNAzyme present (see Fig. 2.21 on page 44 and Fig. 2.22 on 46 for comparison). In the former case it cleaved a substantial part of the RNA transcripts while it completely failed to do so in the latter case. It cannot be concluded from these experiments whether global folding or sequential folding is superior at predicting the performance of DNAzymes in cells. The published data by Tafer et al (2008) clearly supports sequential folding. At any rate, Dz736 and Dz839 cleaved the RNA transcripts efficiently in both cases. Together with Dz824_10/11, which showed high activity during transcription, these DNAzymes are promising candidates for further tests in cell culture.

## 2.6 DNAzyme-mediated prion protein reduction in cells

The previous experiments demonstrate that it is possible to design DNAzymes that specifically cleave the prion protein mRNA. If properly adjusted, they do so in a catalytic fashion and they are able to bind their respective cleavage sites even in long, structured RNA transcripts. The next step is to apply them in living organisms. To this end the neuronal cell line WAC 2 was chosen as a model. WAC 2 are a line of immortalized neuroblastoma cells that derive from a subclone of the SH-SY5Y cell line, which is extensively used as a Parkinson's Disease model. Compared to the latter, however, WAC 2 express higher levels of $PrP^C$, making the detection limit of Western blotting less of an issue. Because of that, fewer cells and less DNAzyme material in general can be used per experiment. In order to assess the efficacy of DNAzymes in reducing $PrP^C$ expression WAC 2 cells were treated with varying dosages and for different durations. Initially, however, the issue of DNAzyme delivery into cells and their stability after uptake was addressed.

### 2.6.1 DNAzyme stability and uptake into cells

To test whether DNAzymes can be delivered effectively into cells a Dz839 variant was used that is tagged with a fluorescein molecule at its 5' end. This variant was named Dz839(FAM). In an *in vitro* assay Dz839(FAM) was incubated together with an equimolar amount of T839 for 3 h at 37 °C. The experiment shows that the 5' fluorescein modification does not prohibit DNAzyme activity to a major extent (Fig. 2.24). In the absence of kinetic data, however, it cannot be excluded that the fluorescent tag interferes with the DNAzyme to a limited degree. Femtomole amounts are detectable after dPAGE in a single band. Based on these results it can be expected that Dz839(FAM) will also be suitable for cell microscopy after the treatment of WAC 2 cells.

In a subsequent experiment the stability of Dz839 in WAC 2 cells was examined (Fig. 2.25). WAC 2 cells were treated with 100 nM Dz839(FAM) via two methods. The DNAzyme was either added directly to the media or the cells were transfected with Dz839(FAM) using the well-established transfection reagent Lipofectamine® 3000. After 24 h the cells were lysed and the nucleic acid contents were isolated via phenol-chloroform extraction. The nucleic acids were then separated via 18 % denaturing PAGE. Since Dz839(FAM) is fluorescently tagged it can be easily distinguished from other nucleic acids that migrate into the polyacrylamide gel. The same procedure was also performed for T839. This way, the stability of single-stranded DNA and RNA in WAC 2 cells can be compared directly. When using Lipofectamine® 3000 Dz839(FAM) remains almost completely intact. Only few degradation products are visible and their intensity is much smaller when compared to full-length Dz839(FAM). When directly ad-

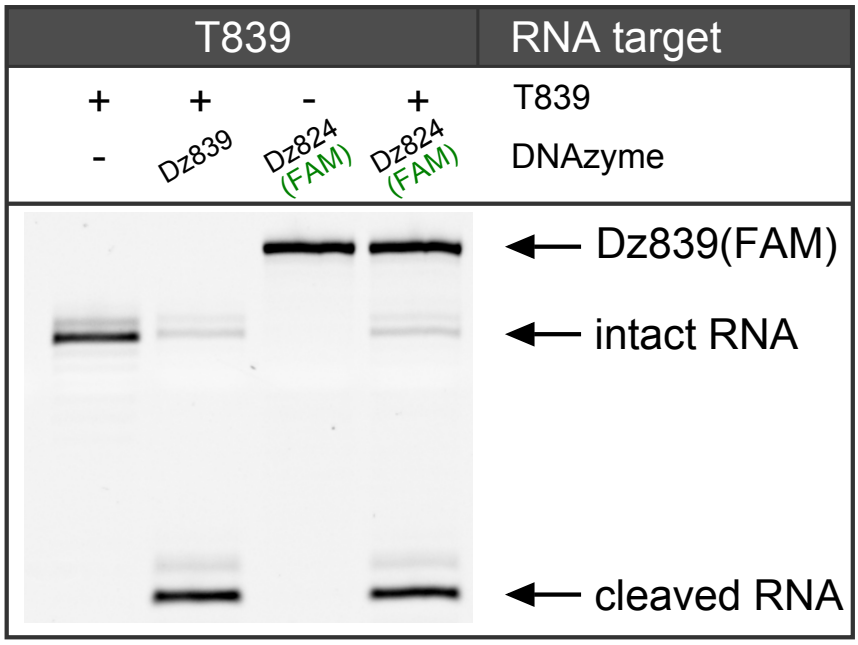


**Figure 2.24 – Fluorescently tagged DNAzyme retains cleavage activity.** T839 was incubated together with either Dz839 or the Dz839(FAM) variant which carries a fluorescein tag at its 5' end. The RNA and DNAzymes were incubated in a 1:1 molar enzyme-to-substrate ratio for 3 h at 37 °C in the presence of 10 mM $MgCl_2$. Afterwards, the samples were separated via 18 % dPAGE. Both Dz839 and Dz839(FAM) cleave T839 to completion. Furthermore, femtomole quantities of Dz839(FAM) are detectable as a distinct band (the amount of Dz839(FAM) that was loaded is 40 fmol). Dz = 10-23 DNAzyme; T = target (RNA); FAM = Fluorescein amidite

ded to the media, however, the intact DNAzyme is no longer detectable after 24 h. Instead a defined degradation product appears. Also the intensity of this product is lower than what was observed when the same amount of Dz839(FAM) was transfected via Lipofectamine® 3000. Either a large proportion of the DNAzyme was degraded completely or lower amounts of DNAzyme was taken up by the cells. In conclusion, Lipofectamine® 3000 seems to have a protective effect since large amounts of Dz839(FAM) remained completely intact after 24 h. A probable reason is that when in complex with Lipofectamine® 3000 Dz839(FAM) is less exposed to nucleases that are present in the serum-supplemented media. This protective effect is less prominent when WAC 2 cells were transfected with the RNA molecule T839. After 24 h the full-length RNA is not detectable. Instead three defined cleavage products appear. On the other hand, when T839 was added to the media no RNA was detected at all. This is in accordance with the low half-life of RNA in serum which is in the range of minutes. From the results of this experiment it can be concluded that DNAzymes can be administered to cells via different means. Dz839(FAM) could be isolated from WAC 2 cells both when using Lipofectamine® 3000 or when adding the DNAzyme directly to the media. When Lipofectamine® 3000 was used Dz839(FAM) remained intact. Therefore it is feasible that this protocol will allow the delivery of DNAzymes that display RNA cleavage activity. However, it is not possible to learn about the actual transfection efficiency from these

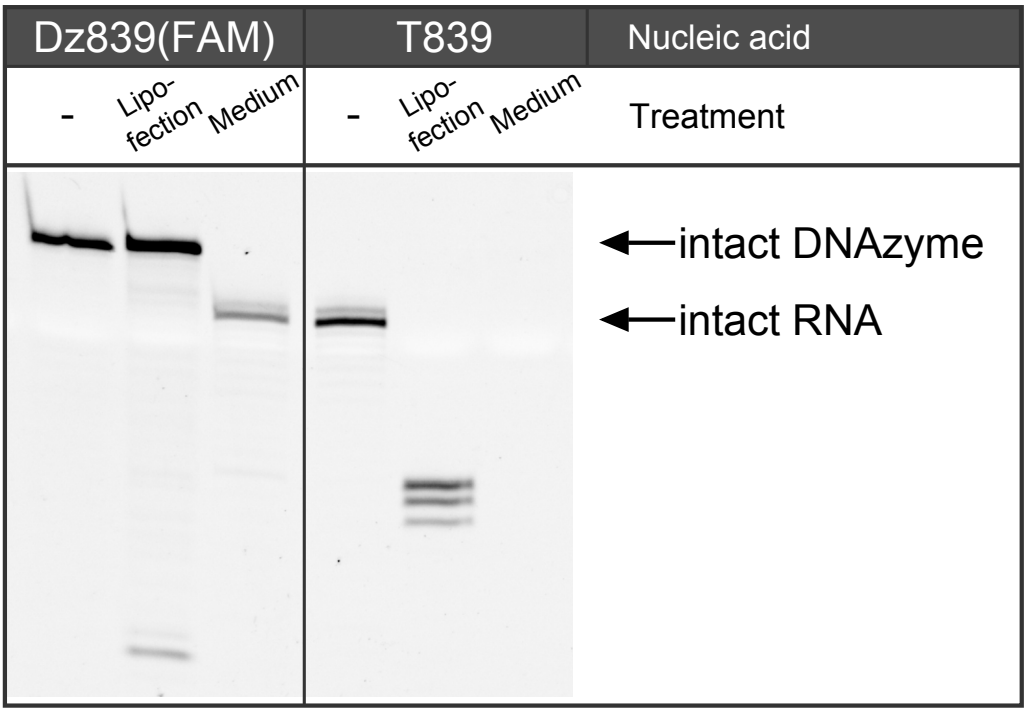


**Figure 2.25 – Stability of Dz839(FAM) in WAC 2 cells.** Human WAC 2 neuroblastoma cells were treated with 100 pmol of Dz839(FAM) or T839. The nucleic acids were either delivered using the transfection agent Lipofectamine® 3000 or added directly to the serum-containing media. After 24 h the cells were lysed, the nucleic acids were extracted via phenol-chloroform extraction, and the samples were separated by 18 % dPAGE together with samples from the Dz839(FAM) and T839 stocks as controls. When using Lipofectamine® 3000, the DNAzyme remains stable for 24 h whereas it is degraded to a shorter product when directly added to the media. The protective effect of Lipofectamine® 3000 is not sufficient for T839 to remain intact during the 24 h of incubation and products of degradation are clearly visible. However, no detectable amounts of T839 could be isolated from cells when it was directly added to the media. Dz = 10-23 DNAzyme; FAM = Fluorescein amidite

results. It is possible that only few cells are reached. If this were the case the effect of DNAzyme treatment on cellular protein levels would be obscured since the basal $PrP^C$ expression of cells that do not take up DNAzymes would to a certain degree even out the reduction that occurs in successfully transfected cells.

In order to assess the efficiency of Lipofectamine® 3000-mediated DNAzyme delivery WAC 2 cells were transfected with Dz839(FAM) for microscopical studies. The cells were seeded on glass cover slips 24 h prior to transfection. After transfection the cells were incubated for another 24 h before fixation in 4 % paraformaldehyde. The nuclei were stained with DAPI (4',6-diamidino-2-phenylindole), a blue dye that binds to the minor groove in DNA regions that are rich in A and T. The cover slips were mounted on miscroscope slides and the specimens were imaged via laser scanning microscopy (LSM). In an initial test approximately 400,000 cells were transfected with 75 pmol Dz839(FAM), which corresponds to a final concentration of 75 nM (Fig. 2.27). Microscopic pictures of these cells show clearly stained nuclei which make it possible

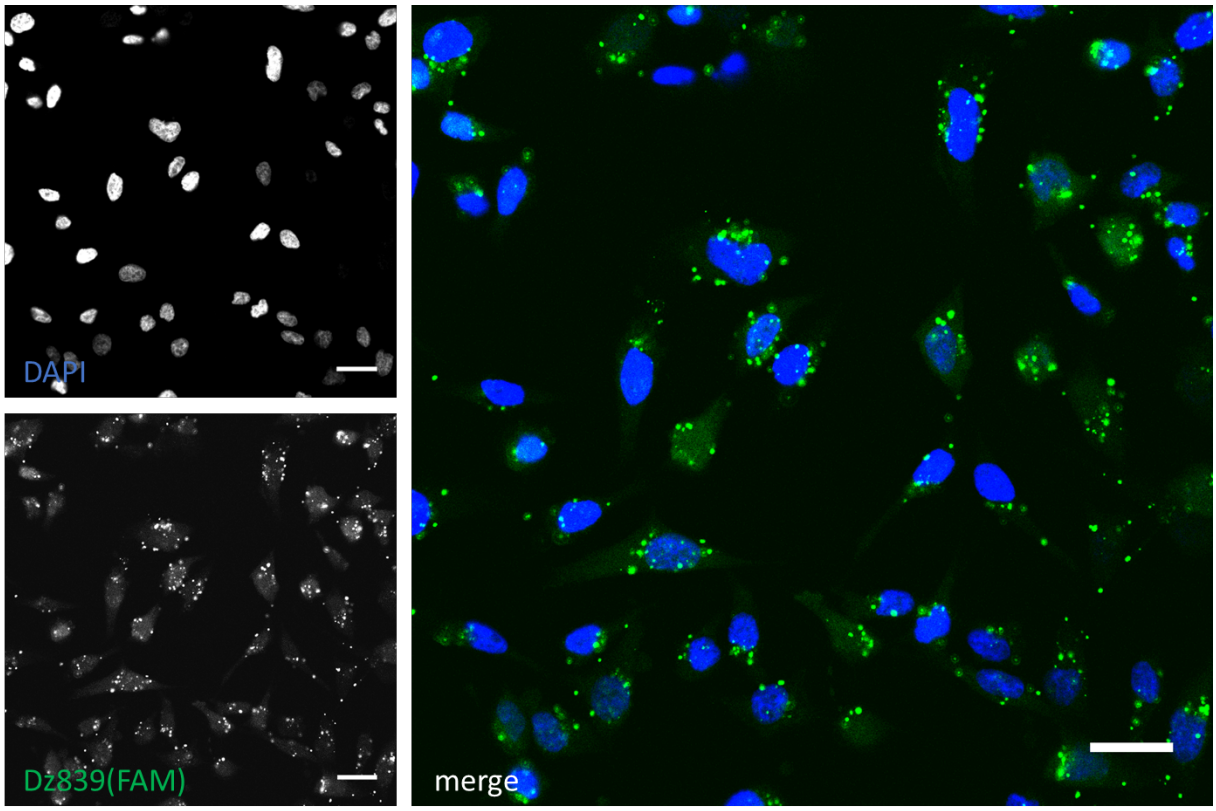


**Figure 2.26 – The DNAzyme Dz839(FAM) can be delivered to WAC 2 cells.** WAC 2 cells were transfected with 75 pmol of Dz839(FAM). 24 h after transfection the cells were fixed, the nuclei were stained with DAPI, and the specimens were mounted for microscopy. The nuclear staining allows a localization of the cells in microscope images (upper left). Dz839(FAM) (lower left) is concentrated in small clusters around the nuclei of the transfected cells. A less intense but highly dispersed signal for Dz839(FAM) is also visible throughout the cell bodies. Nearly all cells that were imaged showed these signs of DNAzyme uptake. Dz = 10-23 DNAzyme; DAPI = 4',6-diamidino-2-phenylindole; FAM = Fluorescein amidite

to generally locate the cells. When FAM fluorescence was imaged a dotted distribution of Dz839(FAM) can be seen. These clusters of labelled DNAzymes accumulate around the nuclei. In addition, a more dispersed distribution of Dz839(FAM) throughout the cell bodies is visible. The signal for these DNAzymes varies in intensity between cells but it is consistently less intense than the accumulations around the cell nuclei.

To see if the same protocol is also suitable for the delivery of higher DNAzyme doses into cells, the experiment was repeated with 500 pmol of Dz839(FAM) which amounts to a final concentration of 500 nM (Fig. 2.27). The microscopic data reveal that transfection of WAC 2 cells using Lipofectamine® 3000 was again successful in delivering Dz839(FAM) into cells. When compared to the previous experiment similar characteristic accumulations of DNAzymes around the cell nuclei are visible. This time, however, these clusters appear slightly smaller. The average amount of clusters per cell, on the other hand, is visibly increased. As before, it appears that all cells that were imaged also contain Dz839(FAM) and the amount of DNAzyme that was taken up is indeed

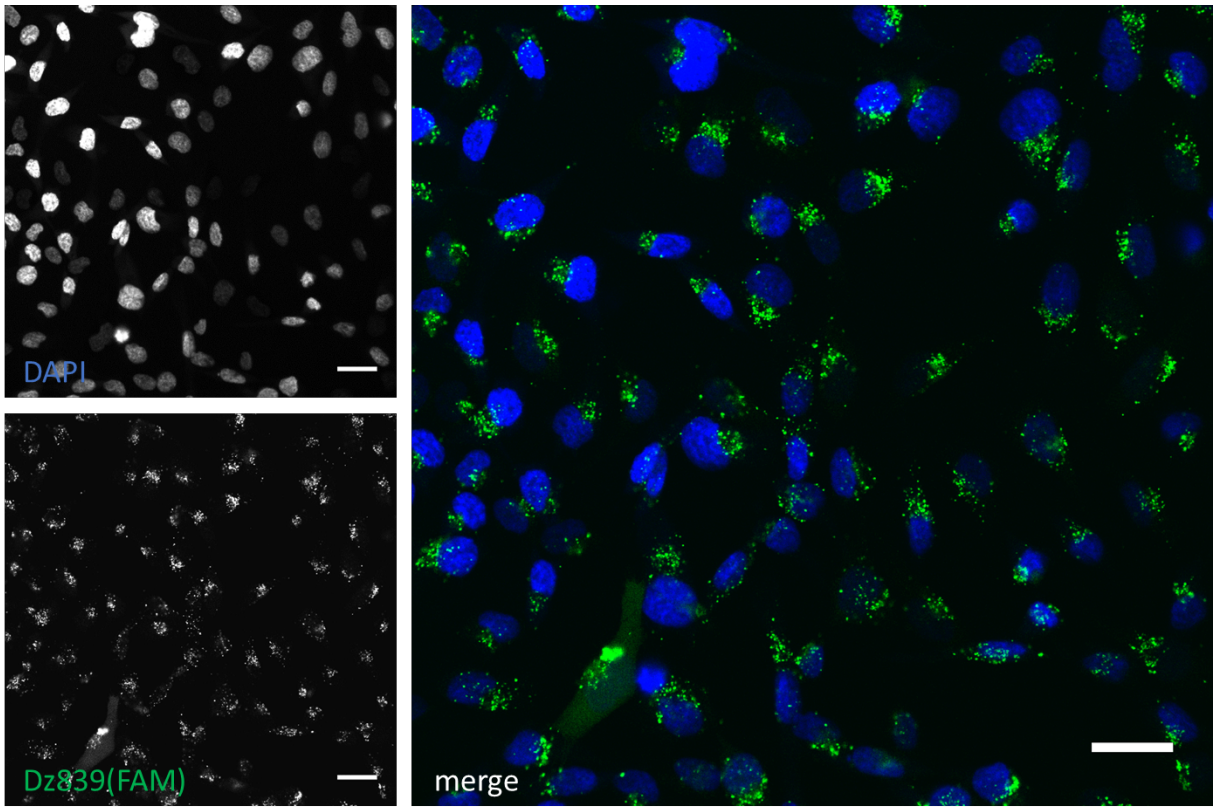


**Figure 2.27 – Lipofectamine® 3000 can be used to transfect cells with high amounts of DNAzymes.** Human WAC 2 neuroblastoma cells were transfected with 500 pmol of Dz839(FAM). After 24 h the cell nuclei were stained and the samples were prepared for microscopy. The images reflect the previous experiment in that uptake of the DNAzyme is evident in nearly all cells that were imaged. The DNAzyme accumulates in slightly smaller but more numerous clusters around the nuclei when compared to the images that were acquired for the treatment with 75 pmol of Dz839(FAM). Apparently higher amounts of DNAzymes are taken up when increasing the dose to 500 pmol. Dz = 10-23 DNAzyme; DAPI = 4',6-diamidino-2-phenylindole;FAM = Fluorescein amidite

higher when using 500 pmol of Dz839(FAM) instead of 75 pmol. Taken together, the experiments demonstrate that Lipofectamine® 3000 is a suitable agent for the transfection of WAC 2 cells with DNAzymes. The overall transfection efficiency seems to approach 100 % although great care should be exercised when data from microscopic images are interpreted quantitatively. Nevertheless it can be expected that a large proportion of cells takes up DNAzymes. Furthermore, the administered dose indeed results in different amounts of DNAzymes that are delivered into cells.

### 2.6.2 DNAzymes do not decrease protein levels in WAC 2 cells

The previous experiments demonstrated that different doses of DNAzymes can be delivered into WAC 2 cells with the use of the standard transfection reagent Lipofectamine® 3000. Judging from microscopic studies the transfection efficiency is nearly absolute. Also, when using Lipofectamine® 3000, the DNAzymes remain stable insi-

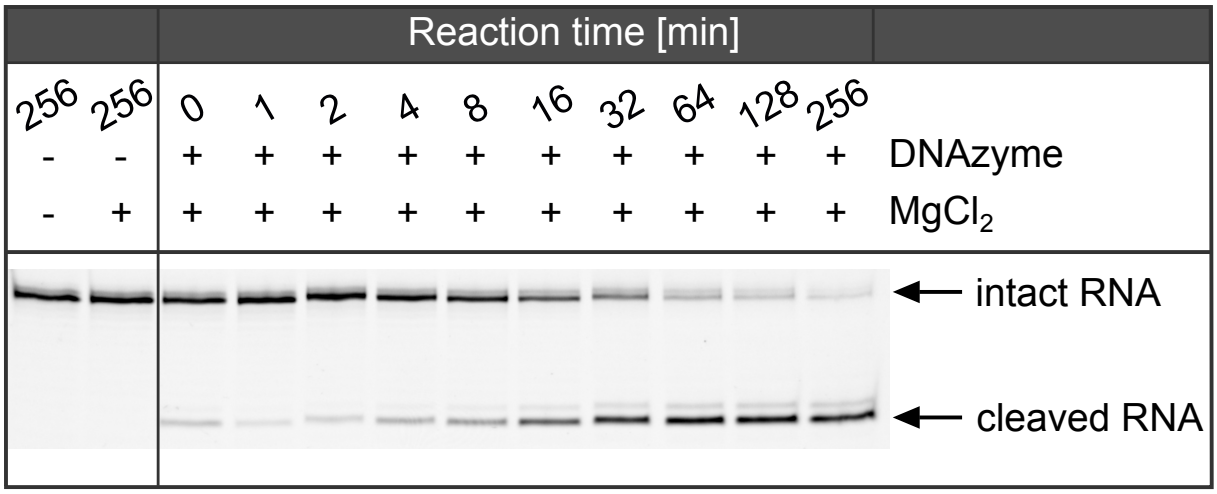


**Figure 2.28** – **Stabilizing modifications do not inhibit DNAzyme activity.** The RNA target was incubated together with the Dz839LL variant which is modified with two L-dT nucleotides at its 3' end for protection against 3' $\longrightarrow$ 5' exonuclease activity. The samples contain RNA and DNAzyme in a 0.1:1 molar enzyme-to-substrate ratio. Incubation was carried out at 37 °C and samples were taken at the indicated points in time. The samples were separated via 18 % dPAGE. The kinetics of cleavage are similar to the data that were previously obtained for Dz839, proving that the stabilizing L-dT modifications have no negative impact on DNAzyme activity.

de the cells for at least 24 h. Even so, two deoxythymidine nucleotides in L-configuration will be added to the 3' end of each DNAzyme in order to protect them from 3' $\longrightarrow$ 5' exonuclease activity, i. e. the most important degradation pathway for single-stranded DNA *in vivo* (Ortigão et al, 1992). Importantly, this modification to the DNAzymes has no impact on their activity, as is demonstrated by the multiple turnover kinetics of Dz824LL (a variant of Dz824_10/11 thus named because it carries two L-dT nucleotides) in Fig. 2.28. Dz824LL cleaves a tenfold molar amount of T824 within 64 min which is consistent with the kinetics that were observed for the unmodified Dz824_10/11 variant (see 2.17 on 37).

The *in vitro* data revealed that Dz824_10/11 is a promising candidate for the knockdown of prion protein expression in cells. Therefore, the first knockdown experiments in WAC 2 cells focus on this particular DNAzyme. For these studies, the four following oligodeoxynucleotides were used: (i) the DNAzyme Dz824_10/11, (ii) the modified Dz824LL variant which carries two dT nucleotides in L-configuration at its 3' end, (iii) an antisense deoxynucleotide (ASO824) which lacks the catalytic core of the DNAzyme but is completely complementary to the RNA target sequence of Dz824_10/11, including the otherwise unpaired guanosine of the GU cleavage site, (iv) a scrambled control which comprises the same number of each nucleotide as Dz824_10/11 in a shuffled order. The antisense deoxynucleotide ASO824 can be used to distinguish the reduction of protein expression which results from DNAzyme activity from that which is due to mere antisense effects. The scrambled control, on the other hand, has the same chemical composition as Dz824_10/11 but loses its sequence specificity for the

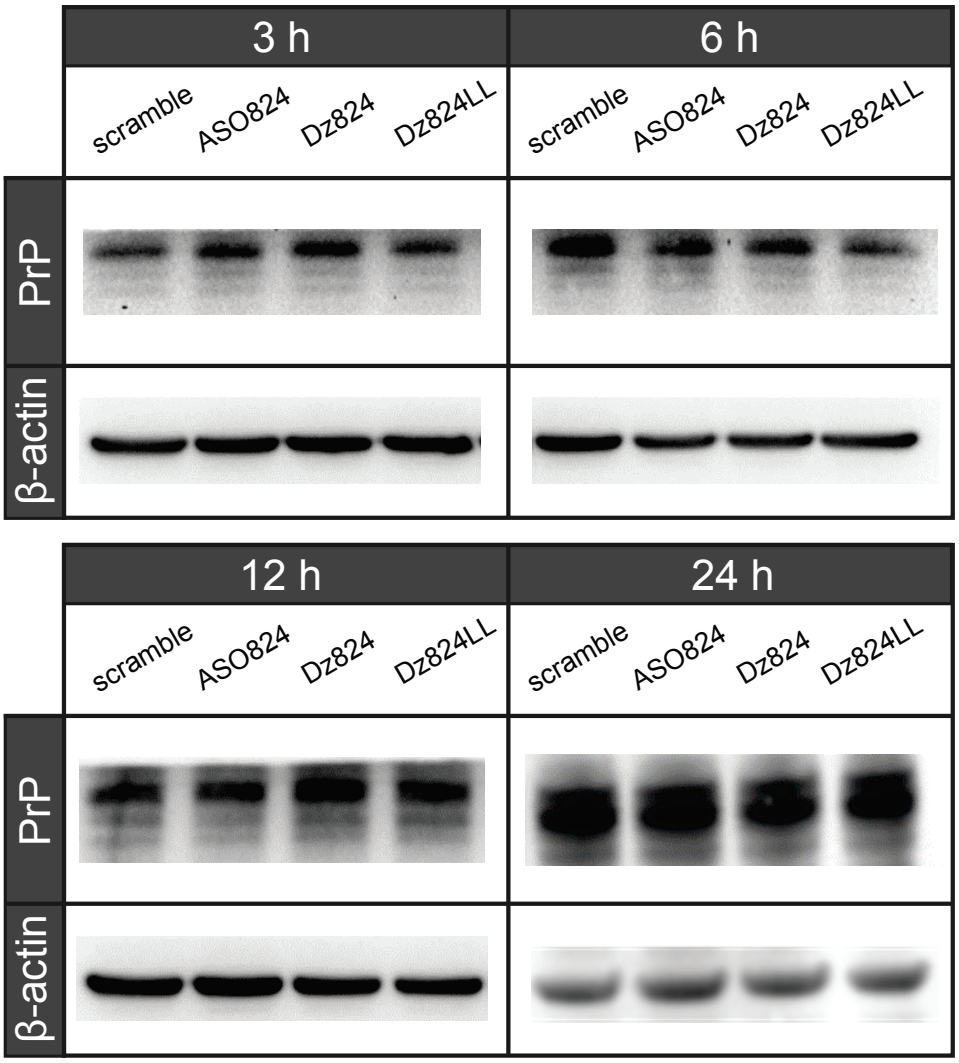


**Figure 2.29 – Kinetics of DNAzyme-mediated prion protein knockdown.** WAC 2 cells were transfected with 75 pmol of Dz824_10/11, Dz824LL, a scrambled control or the antisense oligodeoxynucleotide ASO824. The cells were incubated for 3, 6, 12, or 24 h before they were analysed via Western blotting. The prion protein was detected with the use of the Saf32 antibody. The levels of $\beta$-actin expression were measured for reference. No clear impact of DNAzyme treatment on $PrP^C$ levels could be observed. Dz = 10-23 DNAzyme

respective target site. Any effect of the scrambled control on protein levels can therefore be attributed solely to the experimental procedure or the chemical composition of the oligodeoxynucleotide and must be substracted from the reduction that results from catalytic cleavage or antisense effects.

WAC 2 cells were seeded 24 h prior to transfection. Then, the cells were transfected with 75 pmol of either the scramble, ASO824, Dz824_10/11, or Dz824LL (Fig. 2.29). The cells were incubated for another 3, 6, 12, or 24 h during which the DNAzymes can exert their cleavage activity. At these points in time, the cells were lysed, the samples were separated via 12 % SDS-PAGE, and transferred to a polyvinylidene fluoride (PVDF) membrane via Western blotting. The prion protein was detected with specific primary antibodies (Saf32). The protein $\beta$-actin was also detected for normalization.

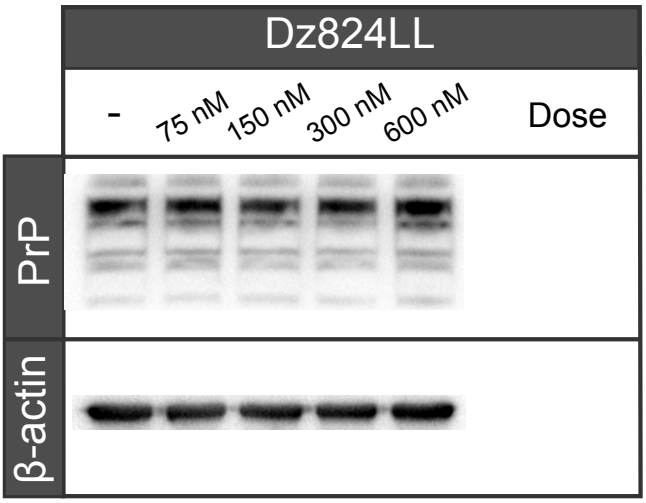


**Figure 2.30** – **Dose-response relationship of Dz824LL.** WAC 2 neuroblastoma cells were transfected with increasing doses of Dz824LL. After 24 h lysates were prepared and analysed via Western blotting. The 3F4 antibody was used to detect $PrP^C$ and $\beta$-actin was measured for reference. No clear dose-response relationship for Dz824LL could be observed. Overall, the effect on protein expression was minimal up to a dose of 600 nM. Dz = 10-23 DNAzyme

Contrary to what was expected, no distinct effect of any of the four oligodeoxynucleotides on $PrP^C$ levels was observed. The difference in protein levels between the cells that were treated with DNAzymes and those treated with the scrambled and ASO824 controls was minimal. This is true for every incubation period that was tested. Apparently, Dz824_10/11 and Dz824LL were unable to cleave the $PrP^C$ mRNA to an extent that led to an observable reduction on the protein level.

It is possible that a DNAzyme concentration of 75 nM is too low to cause noticeable effects on protein levels, even though this dose was sufficient for microscopic detection in cells. In a subsequent experiment this concentration was taken as a starting point for an increase in dose up to 600 nM (Fig. 2.30). The cells were treated with a respective dose of Dz824LL or left untreated. Cell lysis and analysis of the lysates was performed 24 h after transfection. Again, only minimal effects on $PrP^C$ expression following DNAzyme treatment could be observed. Indeed, even a Dz824LL concentration of 600 nM was insufficient to cause a noticeable reduction in protein levels although this dose is twentyfold higher than the standard dose that is recommended for siRNA treatment according to the reaction protocol that accompanies Lipofectamine® 3000. Since no clear dose-response relationship is evident from the data it can be assumed that the slight variations in protein levels that are observed are probably due to the variations that are inherent to the experimental procedure.

In conclusion the data show that even though DNAzymes can be delivered into WAC 2 cells efficiently and remain stable over the course of 24 h no marked reduction in prion protein levels occurs during this time. Increasing the dose stepwise to a maximum of 600 nM was not sufficient to induce an effective knockdown. A possible explanation

is that Dz824LL was not able to cleave the mRNA in a cellular environment. Another possibility is that the sequential folding algorithm and *in vitro* transcription, which were used to predict accessible cleavage sites in the prion protein mRNA, are not accurate models for the *in vivo* situation. However, at this point only one of the DNAzymes was tested in WAC 2 cells and it is feasible that one of the other candidates shows a higher performance in terms of knockdown efficiency.

### 2.6.3 Inefficiency of DNAzymes is not due to target site accessibility

The previous experiment showed no clear effect of DNAzyme treatment on $PrP^C$ expression levels in cells. Even high doses of Dz824LL are apparently unable to cleave the prion protein mRNA to a sufficient degree even though the DNAzyme performed well in *in vitro* studies when long, structured RNAs were used as substrates. In the following experiments the other DNAzymes that proved to be promising candidates in *in vitro* experiments will be tested in cells. Dz736 and Dz839 both cleaved PrP23-230 RNA during transcription (see Fig. 2.22 on page 45). WAC 2 cells were transfected with 75 pmol of Dz736 and Dz839 which amounts to a final concentration of 75 nM. Both DNAzymes were protected from nuclease activity by adding two dT nucleotides in L-configuration to their 3' end. The cells were lysed after 24 h and the samples were subjected to immunoblotting. In clear contrast to the *in vitro* data, but in accordance with the cellular data for Dz824_10/11, no clear reduction of $PrP^C$ levels was observed after treating cells with either Dz736 or Dz839 (Fig. 2.31). As positive controls, two siRNA molecules were designed that are specific to the same RNA region as the DNAzymes. While treatment with siR736 did not have an effect, transfection of WAC 2 cells with siRNA839 abolished prion protein expression nearly completely. It is evident from this reduction that the mRNA stretch that is the target for both Dz839 and siR839 is indeed accessible for hybridization. The siRNA molecule siR839 also needs to anneal to the mRNA in order to exert its function. This result also means that the lack of any effect after Dz839 treatment cannot be explained by an inaccessible cleavage site since siR839 and Dz839 hybridize to the identical part of the prion protein mRNA. As expected, a negative control siRNA without sequence specificity for any known mammalian mRNA had no effect on prion protein levels.

It is not clear from this experiment why siR736 did not reduce protein levels (Fig. 2.31). It is possible that the target site for siR736 and Dz736 in the human $PrP^C$ mRNA is not accessible for hybridization even though high accessibility was predicted *in silico* and determined experimentally during *in vitro* transcription. The *in silico* and *in vitro* models can only be approximations of the actual *in vivo* conditions. But besides the lack of accessibility other factors might be involved in the poor performance of siR736.

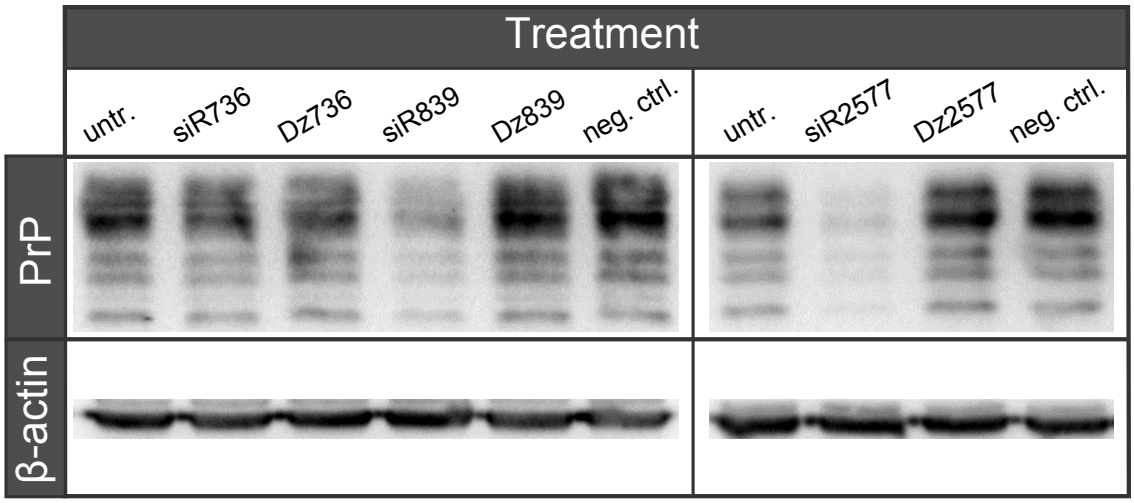


**Figure 2.31 – Treatment with siRNA reduces prion protein expression in cells.** WAC 2 cells were transfected with 75 pmol of DNAzymes and siRNAs that target identical stretches of the human PrP mRNA. The cells were lysed after 24 h and analysed via Western blotting with the use of the 3F4 $\alpha$-PrP antibody. Dz736 and siR736 had no effect on protein expression. While siR839 clearly reduced $PrP^C$ levels, Dz839 did not do so. Additionally, the highly ranked siR2577 duplex from QIAGEN was compared to a DNAzyme that is specific for the same part of the PrP mRNA. The siRNA nearly completely abolishes prion protein expression whereas Dz2577 exhibited no effect. As a negative control, an siRNA with no sequence specificity for any known mammalian mRNA was used. Dz = 10-23 DNAzyme; siR = small interfering RNA; neg. ctrl. = negative control siRNA; untr. = untreated

In contrast to the work of Tafer et al (2008), siRNA selection tools from commercial siRNA suppliers often predict siRNA performance based on other criteria. For example, QIAGEN offers gene-specific siRNA sequences based on calculations performed by the BIOPREDsi neural-network (Birmingham et al, 2007). The results are further refined by favouring siRNA with asymmetric stabilities, which helps the antisense strand in entering the RIS complex and generally produces highly functional siRNAs. A number of other criteria are taken into account in order to reduce off-target effects. Coincidentally, the target site of one of these highly ranked siRNAs for prion protein knockdown contains a GU dinucleotide that could serve as a cleavage site for a 10-23 DNAzyme. This siRNA was purchased and compared to the specifically designed DNAzyme Dz2577 which recognizes the same part of the prion protein mRNA (Fig. 2.31). However, while treatment with siR2577 inhibited $PrP^C$ expression by more than 90 %, transfection of WAC 2 cells with Dz2577 again had no effect on protein levels. In conclusion, none of the tested DNAzymes had a therapeutically relevant effect on prion protein expression. Not only different time points but also DNAzyme doses that are twentyfold higher than recommended concentrations for siRNA-mediated knockdown were tested without success. Importantly, specific siRNAs almost completely reduced $PrP^C$ levels under conditions were DNAzyme treatment failed. As mentioned above the siRNA molecules and

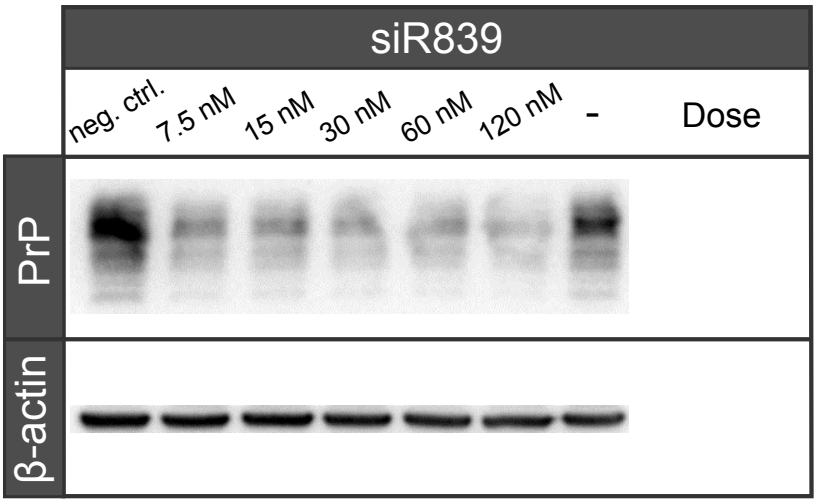


**Figure 2.32 – Dose-response relationship for siR839-mediated knockdown of prion protein expression.** WAC 2 neuroblastoma cells were transfected with varying concentrations of siR839. The cells were analysed after 24 h via Western blotting where the 3F4 antibody was used for the detection of $PrP^C$. Treatment with siR839 led to a nearly complete reduction of prion protein expression even at a concentration of 7.5 nM, i. e. four times lower than the standard recommended dose. neg. ctrl. = negative control siRNA

DNAzymes hybridize to identical parts of the prion protein mRNA. Therefore, it can be excluded that inaccessible target sites are the reason for poor DNAzyme performance.

Although the work up to this point did not produce DNAzymes that can be used for the therapeutic reduction of prion protein levels, the *in silico* studies still predicted an siRNA molecule with the capability to repress $PrP^C$ expression, namely siR839. Indeed, when probing the dose-response relationship of siR839-mediated prion protein reduction, it could be observed that siR839 almost completely abolishes $PrP^C$ expression even at concentrations that are fourfold lower than the standard recommended dose of 30 nM (Fig. 2.32). These results demonstrate that siR839 could potentially be used for therapeutic purposes, provided it can be delivered to its effector site.

One of the aims of this work was to establish JCV-based virus-like particles as a brain-specific vehicle for the delivery of 10-23 DNAzymes into cells. However, this method can in principle be adjusted to transport any cargo of choice, including siRNA. The use of 10-23 DNAzymes for therapeutic purposes will therefore be abandoned in favour of VLP-mediated delivery of siRNAs. Before these experiments will be discussed, however, the next section aims at elucidating the reason for the poor performance of DNAzymes in cells.

## 2.7 Low $Mg^{2+}$ concentrations inhibit DNAzyme activity

From the previous studies it is evident that the tested DNAzymes did not inhibit $PrP^C$ expression in cells considerably even though they showed favourable performance *in vitro*. In the same conditions the corresponding siRNA proved to be far superior at reducing protein levels. Therefore it can be assumed that the *in silico* and *in vitro* data accurately depict the accessibility of the respective target sites since otherwise no effect could have been observed for siRNA, either. This raises the question as to what other factors might negatively influence DNAzyme performance in cells.

In a recent publication Silverman (2016) commented that up to this point no clear evidence for DNAzyme-mediated RNA cleavage in cells existed. The author speculated that intracellular $Mg^{2+}$ concentrations might be too low to enable substantial DNAzyme activity. For the *in vitro* cleavage assays standard conditions were chosen that are similar to the conditions during which the 10-23 DNAzyme was initially selected. Santoro and Joyce (1997) used a Tris buffer with 10 mM $MgCl_2$ to elute catalytically active DNA sequences by cleavage of an RNA stretch linking the sequences to a solid support (see chapter 1.4 Deoxyribozymes and Fig. 1.2 – Selection of RNA-cleaving DNAzymes on page 7ff. for a more detailed description). While these conditions were suitable for the isolation of active DNAzymes they are different from what has been reported for $Mg^{2+}$ concentrations *in vivo*. Several reports place the total $Mg^{2+}$ concentration in most mammalian cell types between 17 and 20 mM. The majority of cytosolic $Mg^{2+}$, however, is bound to adenosine triphosphate and cytosolic proteins (Romani, 2011). This means that the concentration of free $Mg^{2+}$ in the cytosol is actually much lower. Estimates range from 0.5 to 1 mM, but concentrations as low as 0.2 mM have also been reported (Romani and Scarpa, 1992).

It has previously not been studied in detail whether the 10-23 DNAzyme retains activity at these low $Mg^{2+}$ concentrations. Breaker et al (2003) determined that the value of $k_{obs}$ changes considerably in response to variations in $Mg^{2+}$ concentration but no data for submillimolar concentrations have been reported. The rapid nature of the reaction makes it difficult to obtain reliable data about cleavage kinetics which are usually determined based on a mobility shift of the reaction products during gel electrophoresis. Generation of quantifiable kinetic data is very laborious and material-consuming since at least one sample for each time point of every condition needs to be prepared and analysed.

In order to overcome these difficulties an *in vitro* system was designed with which it is possible to monitor the DNAzyme-mediated cleavage of RNA in real time (Fig. 2.33). The RNA substrate T839FRET was used, which is labelled with a fluorophore (fluorescein) at its 5' end and a dark quencher (BHQ-1) at its 3' end. As described in figure legend 2.33 this setup allows measuring the real-time kinetics of DNAzyme-mediated

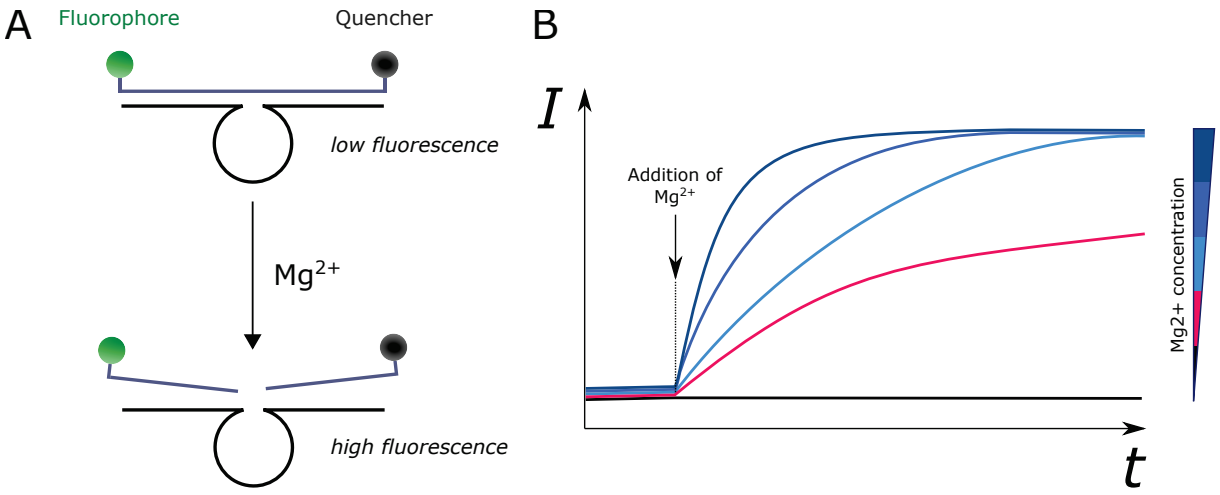


**Figure 2.33 – FRET-based real-time DNAzyme activity assay. (A)** Fluorescence-based cleavage assay. The RNA target T839FRET is dual-labelled with a fluorophore and a dark quencher at its 5' and 3' end, respectively. The close proximity of fluorophore and dark quencher allow for a transfer of energy between the two moieties following the principle of Förster resonance energy transfer (FRET). When the fluorophore is excited it transfers part of the excitation energy to the dark quencher where it dissipates as heat. Thereby, fluorescence emitted by the fluorophore is diminished. When hybridized to its specific DNAzyme (Dz839) and in the absence of $Mg^{2+}$ T839FRET remains intact and fluorophore and quencher are within close proximity. Upon addition of $Mg^{2+}$, however, T839FRET is cleaved, fluorophore and dark quencher are separated from each other, and fluorescence increases. **(B)** Simulated measurements of DNAzyme activity in dependence of the $Mg^{2+}$ concentration. After the addition of $Mg^{2+}$ cleavage of T839FRET results in increased fluorescence which can be monitored in real-time with a flurometer. Exemplary time courses are plotted as fluorescence intensity *I* over time *t*. With the use of a microplate reader several conditions, e. g. different concentrations of $Mg^{2+}$, can be tested in parallel. A mixing device would in principle allow a pulse-chase experimental setup where the reactions could be measured before, during, and immediately after $Mg^{2+}$ is added.

RNA cleavage in a single sample with high temporal resolution and minimal use of material. Furthermore, with the use of a microplate reader several reaction conditions can be monitored in parallel. Equipping the fluorometer with a mixing device would also make it possible to acquire data immediately before, during, and after addition of $Mg^{2+}$ but the current work was limited to manual addition which introduces a slight delay between initiation of the reaction and the start of the measurements. Nonetheless, with the use of this experimental design it was possible to systemically obtain quantifiable data on the kinetics of DNAzyme-mediated RNA cleavage in the presence of variable $Mg^{2+}$ concentrations in a time and material-efficient way.

### 2.7.1 The 10-23 DNAzyme binds several $Mg^{2+}$ ions cooperatively

The experimental setup that was described in the previous section was applied to study how DNAzyme activity changes in response to submillimolar concentrations of $Mg^{2+}$ ions. The RNA substrate T839FRET and the DNAzyme Dz839 were incubated together

in equimolar concentrations. It has already been shown in chapter 2.4.2 (page 32ff) that $k_{obs}$ only changes negligibly at molar excesses of DNAzyme. Based on this it is assumed that at a 1:1 molar RNA-to-DNAzyme ratio almost all RNA substrates are bound to a DNAzyme molecule. Therefore potentially rate-limiting steps of the catalytic process, such as association of the substrate and dissociation of the products, can be disregarded and $k_{obs}$ will be close to the speed of the actual chemical transformation. A simple two-state model was assumed as a description of the influence of $Mg^{2+}$ ions on the activity of the DNAzyme:

$$\text{DNAzyme}_{\text{inactive}} + n\text{Mg}^{2+} \rightleftharpoons \left(\text{DNAzyme} \cdot n\text{Mg}^{2+}\right)_{\text{active}} \tag{1}$$

In this model $Mg^{2+}$ ions are bound cooperatively. Otherwise it would have been necessary to assume several intermediate states which could not be elucidated with the experimental setup. The concentration of the active DNAzyme complex is proportional to $k_{cat}$. Based on equation (1) the binding constant $K$ for cooperative binding of $n\text{Mg}^{2+}$ follows equation (2).

$$K = \frac{[\text{D}_{\text{ac}}]}{[\text{D}_{\text{inac}}] \cdot [\text{Mg}^{2+}]^n} \tag{2}$$

where $\text{D}_{\text{ac}} = \left(\text{DNAzyme} \cdot n\text{Mg}^{2+}\right)_{\text{active}}$ and $\text{D}_{\text{inac}} = \text{DNAzyme}_{\text{inactive}}$ stand for cleavage-competent and inactive DNAzymes, respectively. Furthermore, it is assumed that $[\text{D}_{\text{total}}] = [\text{D}_{\text{inac}}] + [\text{D}_{\text{ac}}]$. Also, $[\text{Mg}^{2+}_{\text{total}}] = [\text{Mg}^{2+}]$ because $[\text{Mg}^{2+}_{\text{total}}] \gg [\text{D}_{\text{total}}]$, namely the concentrations of $Mg^{2+}$ that were used in the experiment are between three to four orders of magnitude higher than the concentration of DNAzyme. Taken together, from equation (2) the following equation (3) can be derived.

$$\log\left(\frac{[\text{D}_{\text{total}}]}{[\text{D}_{\text{ac}}]} - 1\right) = -\log K - n \cdot \log\left[\text{Mg}^{2+}\right] \tag{3}$$

Cleavage reactions were performed with different $Mg^{2+}$ concentrations and either with or without 0.1 M NaCl, which resembles *in vivo* conditions more closely. Importantly, 0.1 mM EDTA was added to each sample in order to correct for possible divalent ion contamination in the stock samples. The values for $k_{cat}$ were derived from the experimental data by fitting each FRET curve to a single exponential. Those values for $k_{cat}(s^{-1})$ are plotted against the $Mg^{2+}$ concentration and the curves were fitted according to equation (2) in Fig. 2.34 A. The curves were modelled with $n = 3$ and $K = (5.8 \cdot 10^3)^3 = 1.9 \cdot 10^{11}$ for the data without NaCl and with $n = 1$ and $K = 5.8 \cdot 10^3$ for the data in the presence of 0.1 M NaCl. The same data are displayed as Hill plots according to equation (3) in Fig. 2.34 B. From the data in the absence of NaCl the Hill

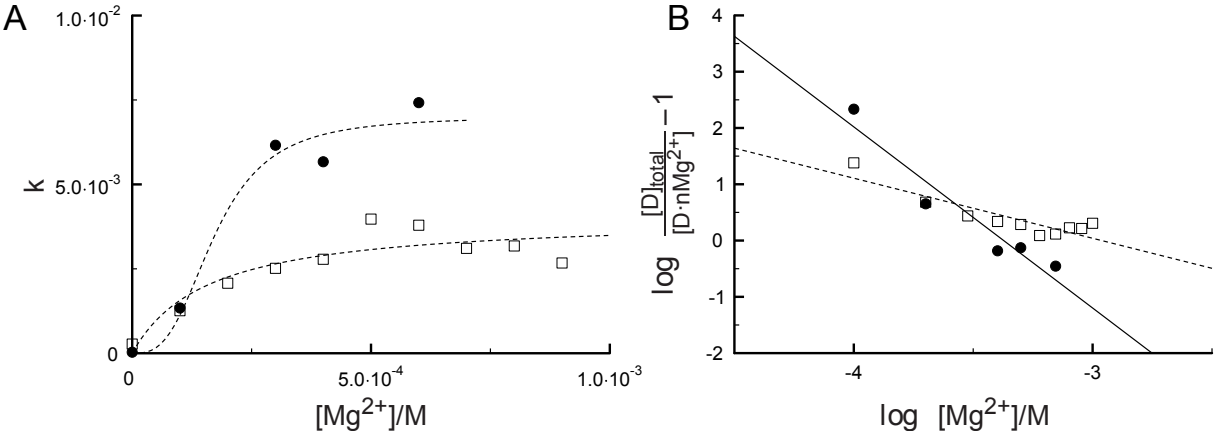


**Figure 2.34 – Binding of $Mg^{2+}$ to DNAzymes. (A) Binding curves.** Fluorescein/BHQ-1-labelled T839FRET was incubated together with an equimolar concentration of Dz839. Cleavage was observed based on the increase in fluorescence due to the separation of fluorophore and quencher. The activity of Dz839 was monitored in dependence on the $Mg^{2+}$ concentration with or without NaCl. The FRET curves were fitted with a single exponential to yield $k_{cat}$. For the values for $k_{cat}$ in the absence of NaCl the curve (•, - - -) according to equation (2) was modeled with $n = 3$ and $K = \left(5.8 \cdot 10^3\right)^3 = 1.9 \cdot 10^{11}$. The curve for the values of $k_{cat}$ with 0.1 M NaCl (□, - - -) were fitted according to equation (2) with $n = 1$ and $K = 5.8 \cdot 10^3$. **(B)** Hill plot. The same experimental data as in **(A)** were fitted according to equation (3). Based on the data the following Hill coefficients were obtained: $n = 3.2$ (•, —) for the data without NaCl, which is indicative of cooperative binding of at least three $Mg^{2+}$ ions, and $n = 1.1$ (□, ---) for the data with 0.1 M NaCl, which does not suggest cooperative binding. The author would like to thank Gerhard and Matthias Steger who fitted the data in Fig. A with the use of PYTHON. These results have been published in Victor et al (in press).

coefficient $n = 3.2$ can be obtained. This is indicative of cooperative binding of at least three $Mg^{2+}$ ions. For the data which was acquired in the presence of 0.1 M NaCl a Hill coefficient of $n = 1.1$ was obtained which does not indicate cooperative binding. It does not imply that the DNAzyme binds fewer $Mg^{2+}$ ions in the presence of NaCl, however. Rather, the ions might be bound in a stepwise manner. It is important that the number of $Mg^{2+}$ ions that are bound by the DNAzyme be considered rough estimates but it is clear from the data that several $Mg^{2+}$ ions need to be bound in order for the DNAzyme to exert its activity. It is also evident that DNAzyme activity is influenced dramatically by changes in $Mg^{2+}$ ion concentrations in the submillimolar range, i. e. the concentration of free $Mg^{2+}$ in most mammalian cell types. This circumstance might be one reason why the DNAzymes used in this work showed poor performance in cells.

## 2.7.2 ATP competes with DNAzymes for the binding of $Mg^{2+}$

While the concentration of free $Mg^{2+}$ ions might be too low for appreciable DNAzyme activity, a vast pool of total $Mg^{2+}$ ions is potentially available. As was described in the previous section a large proportion of all $Mg^{2+}$ ions inside the cell is bound to nucleoside triphosphates, especially ATP, and also to proteins. If the 10-23 DNAzyme

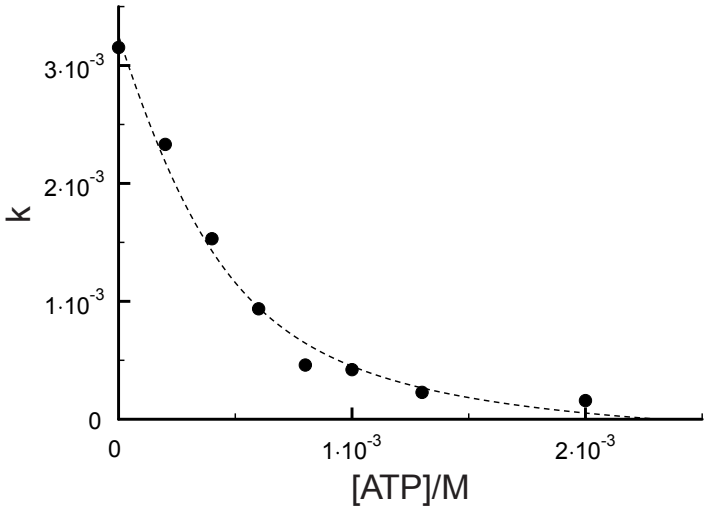


**Figure 2.35 – ATP competes with DNAzymes for $Mg^{2+}$ binding.** T839FRET was cleaved by Dz839 in the presence of 0.5 mM $Mg^{2+}$, 0.1 M NaCl, and increasing concentrations of ATP. The FRET curves were fitted with a single exponential to yield $k_{cat}$ (•). The curve was fitted to equation (2) with $K = 5.4 \cdot 10^3$ and $n = 1$. The data demonstrate that DNAzyme activity diminishes drastically in response to increasing amounts of ATP. About 70 % of its activity are lost when $Mg^{2+}$ and ATP are at equimolar concentrations. These results have been published in Victor et al (in press).

was not able compete with ATP for $Mg^{2+}$ binding, it could not acquire enough $Mg^{2+}$ ions for its own optimal activity.

In order to test whether or not the 10-23 DNAzyme can compete with ATP for $Mg^{2+}$ binding, cleavage experiments with T839FRET and Dz839 were designed. The concentration of $Mg^{2+}$ in the samples was kept constant at 0.5 mM. This concentration is within the range that was described for free $Mg^{2+}$ in cells. Also, at a 0.5 mM $Mg^{2+}$ concentration the DNAzyme is nearly fully active. Varying amounts of ATP were added to the samples. The reactions proceeded in the presence of 0.1 M NaCl to resemble physiological conditions more closely. As before the reaction was monitored by the increase in fluorescence that occurs due to the cleavage-dependent separation of fluorophore and dark quencher. Values of $k_{cat}$ were derived from the experimental data and plotted over the concentration of ATP (Fig. 2.35). The curve was fitted according to equation (2) with $K = 5.4 \cdot 10^3$ and $n = 1$. The data clearly demonstrate that increasing amounts of ATP potently inhibit DNAzyme activity. Importantly, this relationship is not linear. At an equimolar concentration of ATP and $Mg^{2+}$, i. e. 0.5 mM, the DNAzyme loses approximately 70 % of its activity. This relationship points toward the conclusion that ATP binds $Mg^{2+}$ with higher affinity and is therefore able to sequester $Mg^{2+}$ ions from binding to the 10-23 DNAzyme.

In summary, the effects that were analysed with the FRET setup likely explain the poor performance of DNAzymes in cells. In the concentration range of free $Mg^{2+}$ ions in cells DNAzyme activity is lowered drastically. The reason for that might be that the

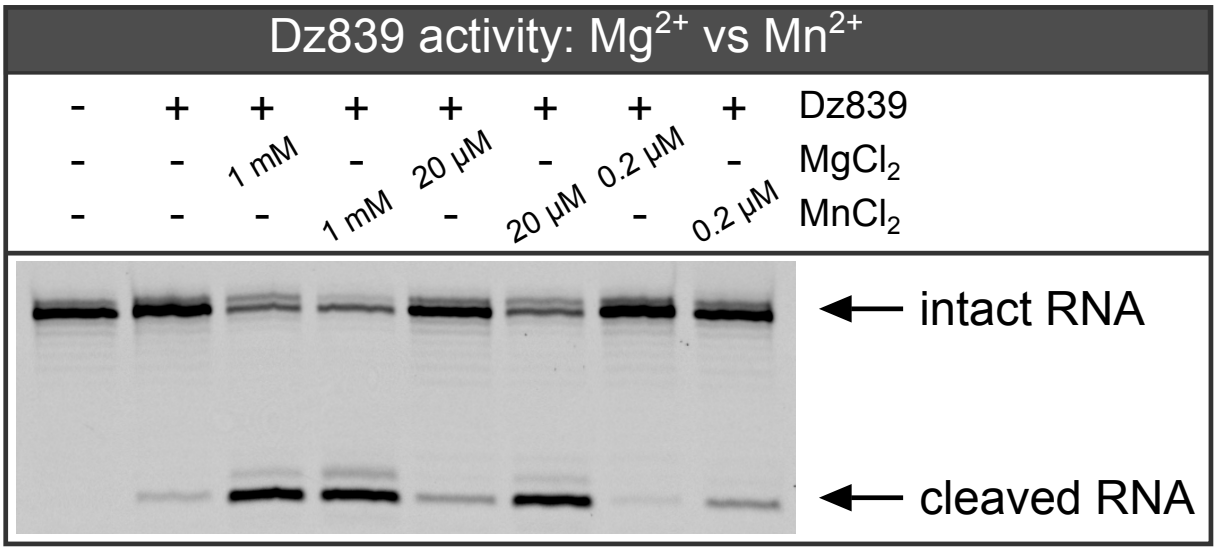


**Figure 2.36 – DNAzymes cleave more efficiently in the presence of manganese.** T839 was incubated together with a tenfold lower amount of Dz839 in the presence of different concentrations of $MgCl_2$ and $MnCl_2$. The samples were incubated for 3 h at 37 °C. While cleavage was efficient at a 1 mM concentration of either divalent metal ion, the DNAzyme was substantially more active at 20 µM $Mn^{2+}$ when compared to 20 µM $Mg^{2+}$. Residual cleavage activity was detected in the presence of 0.2 µM $Mn^{2+}$. Since divalent metal ion concentrations in the low micromolar to submicromolar range were used no EDTA was added to the samples, which results in some background activity due to metal ion contaminations. Dz = 10-23 DNAzyme

DNAzyme needs to bind at least three $Mg^{2+}$ ions in order to exert full activity. Furthermore, the data demonstrate that the DNAzyme cannot compete with ATP for $Mg^{2+}$ binding under simulated physiological conditions. It has been noted in the literature that the 10-23 DNAzyme is active at lower concentrations of $Mn^{2+}$ when compared to $Mg^{2+}$ (Santoro and Joyce, 1998). The same relationship could be observed in more detail in this work (Fig. 2.36). The DNAzyme efficiently cleaves a tenfold molar excess of RNA substrate in the presence of 1 mM of either $Mg^{2+}$ or $Mn^{2+}$ whereas $Mn^{2+}$ but not $Mg^{2+}$ concentrations as low as 20 µM resulted in sizeable activity. Residual RNA cleavage could even be observed with $Mn^{2+}$ concentrations as low as 0.2 µM. However, an initial experiment in which WAC 2 cells were cultivated in media supplemented with 20 µM $MnCl_2$ and treated with DNAzymes did not result in a rescue of intracellular DNAzyme activity (data not shown).

## 2.8 RNAi delivery via virus-like particles

Although the initial aim of using therapeutic DNAzymes in cells cannot be met due to their lacking performance *in vivo*, siRNA duplexes with high silencing efficiency were obtained instead. A fundamental advantage of nucleic acid therapeutics is that the pharmacophore can be functionally separated from the dianophore (Khvorova and Watts, 2017). The term pharmacophore describes the molecular features that determine activity and target specificity of a drug. The term dianophore summarizes the molecular features that are responsible for its uptake, distribution, and metabolism. This means that one delivery mechanism can be utilized for a wide range of different nucleic acid therapeutics if they are to be delivered to the same effector site. For this reason it is possible at this point in the project to focus on siRNA instead of DNAzymes and still use virus-like particles (VLPs) as a delivery platform. The final section of this work focusses on the knockdown of $PrP^C$ in WAC 2 cells by using specific siRNAs that are delivered via VLPs derived from the John Cunningham virus (JCV).

VLPs were loaded with siRNAs by cooperators from NEUWAY Pharma AG in Bonn, Germany. Packaging involves the disassembly of viral capsids into pentamers composed of the protein VP1 by dissociation in buffer with EGTA (ethylene glycol-bis($\beta$-aminoethyl ether)-N,N,N',N'-tetraacetic acid). EGTA binds $Ca^{2+}$ ions which are necessary for capsid formation. The resulting pentameric capsomers are then incubated together with their cargo in a buffer containing $Ca^{2+}$, leading to their reassembly. The siRNA molecules are encapsulated in the process. The loaded VLPs can then be added to the cells. Depending on the cell type, the VLPs will be taken up and disassemble to release their cargo into the cytosol. In the first experiments this method was tested for its ability to deliver fluorescently labelled cargo into WAC 2 cells.

### 2.8.1 Low amounts of cargo are delivered to WAC 2 cells via VLPs

To test whether WAC 2 cells can be transduced the DNAzyme Dz839(FAM) was packaged into VLPs which were subsequently added to the cells. Although it was already shown that no silencing effect could be expected with DNAzymes, the fluorescently labelled Dz839(FAM) is still useful as a means of visualizing uptake into cells. 24 h after addition of the particles the cells were fixed and the nuclei were stained with DAPI. Also, WGA (wheat germ agglutinin) conjugated to the fluorescent dye Alexa Fluor™ 647 was used to stain the cell membranes. When using 750 pmol of Dz839(FAM) packaged into VLPs it becomes clear that the amounts of DNAzyme that are delivered into WAC 2 cells are unexpectedly low (Fig. 2.37). The staining pattern for Dz839(FAM) is similar to that previously observed for Lipofectamine® 3000-mediated transfection (see Fig. 2.26 on page 51), with small clusters around the cell nuclei, but much less intense.

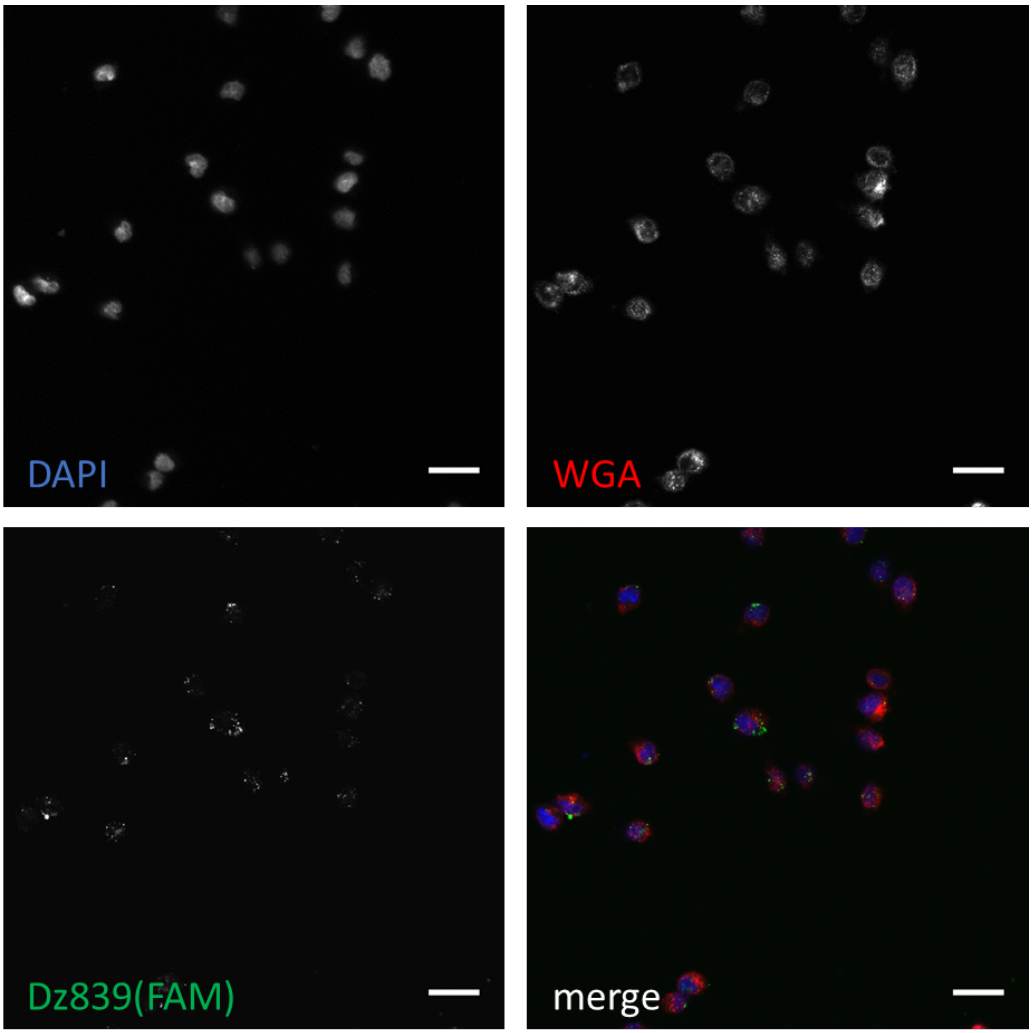


**Figure 2.37 – Virus-like particles deliver only low amounts of cargo to WAC 2 cells.** WAC 2 cells were treated with 750 pmol of Dz839(FAM) loaded into VLPs for 48 h and prepared for fluorescence microscopy. The nuclei were stained with DAPI while the membranes were stained with WGA-647. Only very low amounts of Dz839(FAM) were taken up by the cells. Dz = 10-23 DNAzyme; DAPI = 4',6-diamidino-2-phenylindole; WGA = wheat germ agglutinin

In comparison, transfection of WAC 2 cells with 750 pmol of Dz839(FAM) using Lipofectamine® 3000 results in the delivery of very high amounts of DNAzyme (Fig. 2.38). Judging from these microscopical studies alone it appears that VLP-mediated transduction of WAC 2 cells is several orders of magnitude less effective than Lipofectamine® 3000-mediated transfection. However, quantitative interpretation of microscopical data is only of limited accuracy. Furthermore, it is to be expected that delivery methods with cell type- or tissue-specificity gain this selectivity at the cost of general efficacy.

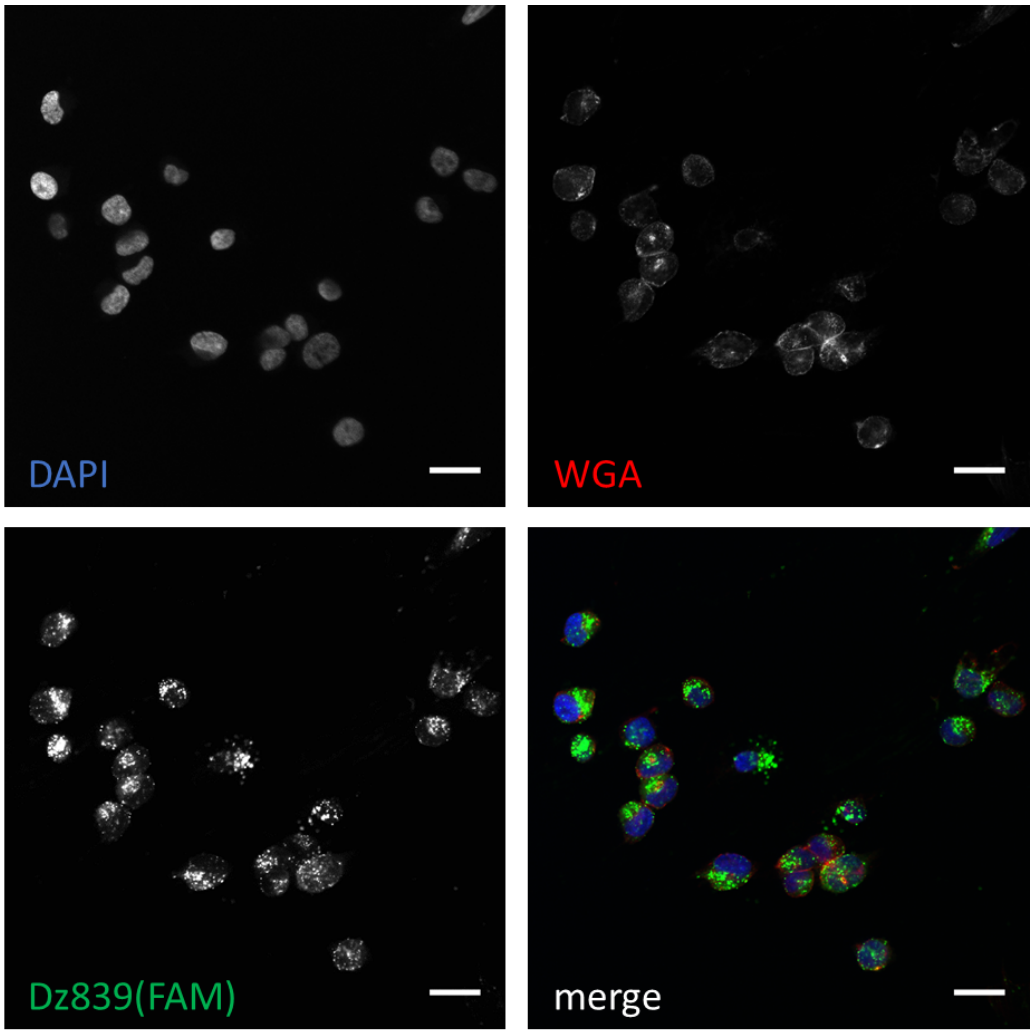


**Figure 2.38 – Lipofectamine® 3000 delivers high amounts of Dz839(FAM) to WAC 2 cells.** For comparison with VLP treatment, Lipofectamine® 3000 was used to deliver 750 pmol of Dz839(FAM) into WAC 2 cells. This protocol results in the uptake of large amounts of Dz839(FAM) in a pattern that has been observed experimentally in the previous work. The overall intensity is very high when compared to the results obtained after VLP treatment. Dz = 10-23 DNAzyme; DAPI = 4',6-diamidino-2-phenylindole; WGA = wheat germ agglutinin

### 2.8.2 RNAi delivery via VLPs does not reduce protein levels in cells

In the next step the previously tested siRNA duplexes siR839 and siR736 were packaged into virus-like particles. WAC 2 cells were treated with these VLPs and protein levels were assessed after 48 h (Fig. 2.39). The cells were also treated with a negative control RNA packaged into VLPs to see whether the VLP-treatment alone affects protein levels. As a positive control, the cells were transfected with siRNAs using Lipofectamine® 3000. While protein levels were slightly lower in cells treated with VLPs containing siR839 or siR736 when compared to untreated cells, the silencing effect did not exceed that of the VLPs that contained negative control siRNA. It must therefore

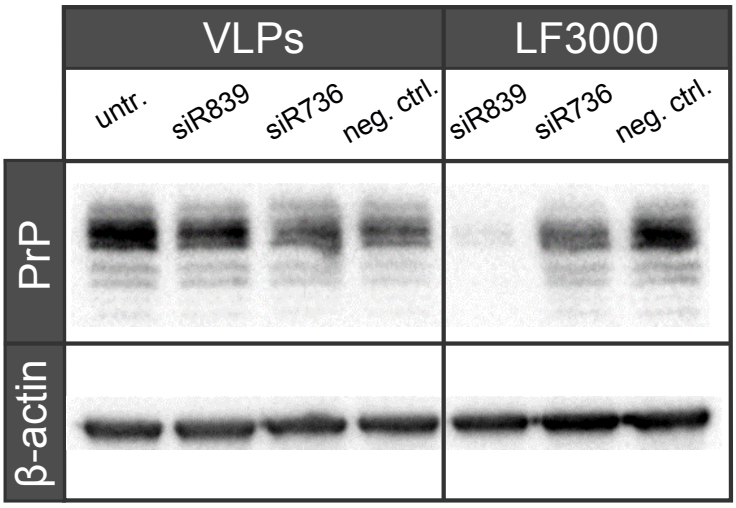


**Figure 2.39 – Virus-like particles do not effectively deliver siRNA into WAC 2 cells.** WAC 2 cells were treated with siR839 and siR736 packaged into VLPs. The levels of prion protein expression in these cells was not substantially lowered when compared to cells that were treated with VLPs containing a negative control siRNA. Both siR839 and siR736 lowered protein levels when delivered with the use of Lipofectamine® 3000. VLP = virus-like particle; LF3000 = Lipofectamine® 3000; neg. ctrl. = negative control siRNA; siR = siRNA

be assumed that the observed reduction is due to the VLPs alone and not specifically because of the delivered siR839 or siR736 duplexes. As expected, Lipofectamine® 3000-mediated transfection of WAC 2 cells with siR839 abolished $PrP^C$ expression completely while siR736 led to a modest reduction. The discrepancy between VLP- and Lipofectamine® 3000-mediated siRNA delivery in respect to their silencing efficiency is likely due to the fact that Lipofectamine® 3000 is a much more potent delivery agent. However, since siR839 was proven to be very effective at reducing $PrP^C$ expression even at low doses, it is surprising that no specific effect could be observed with VLP-delivered siR839 at all.

At the suggestion of NEUWAY Pharma AG several shRNA expression plasmids were produced to overcome the low transduction efficacy of VLPs. Since a single plasmid can serve as a template for continuous shRNA production the effective dose can in principle be lower than for siRNA. Therefore measurable effects on protein expression could be achieved even with a lower transduction efficiency. Several shRNAs specific for the prion protein mRNA sequence were designed using the Thermo Fisher Scientific shRNA designer tool and cloned into the pENTR™ U6 vector downstream of a U6 pol III type promoter. This promoter facilitates ubiquitous expression in most cell types. Two of these shRNA expression plasmids reduced $PrP^C$ expression in WAC 2 cells after transfection with Lipofectamine® 3000 when compared to cells that were transfected with an shRNA plasmid specific for lacZ as a negative control (Fig. 2.40). When treating cells with these plasmids for shR1042 and shR1416 expression packaged into VLPs, however, the effect on prion protein expression was only minimal. Taken together, VLP-

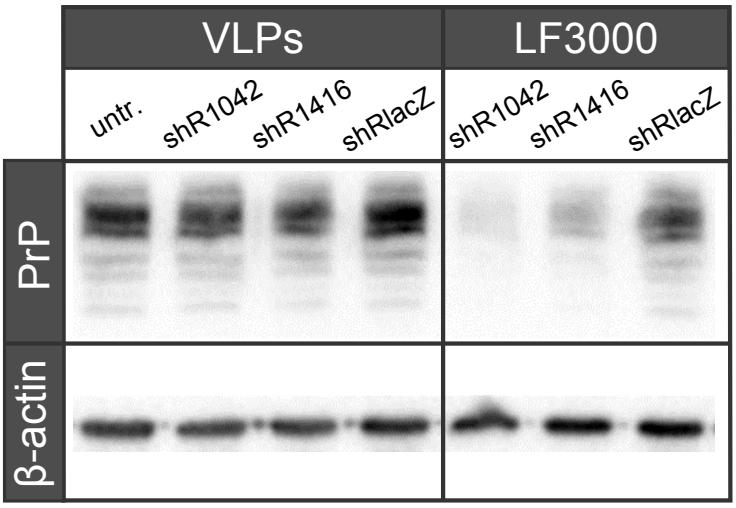


**Figure 2.40 – Expression plasmids for shRNAs are not delivered effectively into cells by VLPs.** WAC 2 cells were treated with VLPs containing expression plasmids for the shRNAs shR1042 and shR1416. Treatment resulted only in a minimal reduction of $PrP^C$ expression when compared to cells transduced with a negative control shRNA specific for lacZ. The transfection of WAC 2 cells with shR1042 or shR1416 with the use of Lipofectamine® 3000, however, nearly completely abolished $PrP^C$ expression. VLP = virus-like particle; LF3000 = Lipofectamine® 3000; shR = shRNA

mediated delivery of both siRNA or shRNA failed to lower the expression of $PrP^C$ in WAC 2 cells substantially. These results raise the question as to whether WAC 2 cells can be efficiently transduced with the use of VLPs at all.

### 2.8.3 Virus-like particles do not deliver expression plasmids into WAC 2 cells

In order to assess whether virus-like particles are able to deliver plasmids, such as the shRNA expression vectors, into WAC 2 cells, delivery of an expression plasmid for luciferase was used as a general transduction control. Luciferase is an enzyme that processes the luminogenic agent luciferin. Chemical transformation of the substrate generates luminescence which can be measured by means of a luminometer. The presence of few luciferase enzymes are sufficient for the detection of a luminescence signal. Therefore, this method can be used to identify and quantify even transduction that is very ineffective. WAC 2 cells were treated with the luciferase expression plasmid pGL4.51. The plasmid was either packaged into VLPs, added directly to the media, or delivered with the use of Lipofectamine® 3000. Luminescence was measured after 48 h. Treatment with 50 µg VLPs loaded with 25 µg pGL4.51 or 25 µg VLPs with 12.5 µg pGL4.51, respectively, did not result in higher luminescence than that measured in cells treated with buffer alone (Fig. 2.41). Also, adding the plasmids directly to the media had no effect on the luminescence signal. Transfecting the cells with 0.5 µg plasmid with the

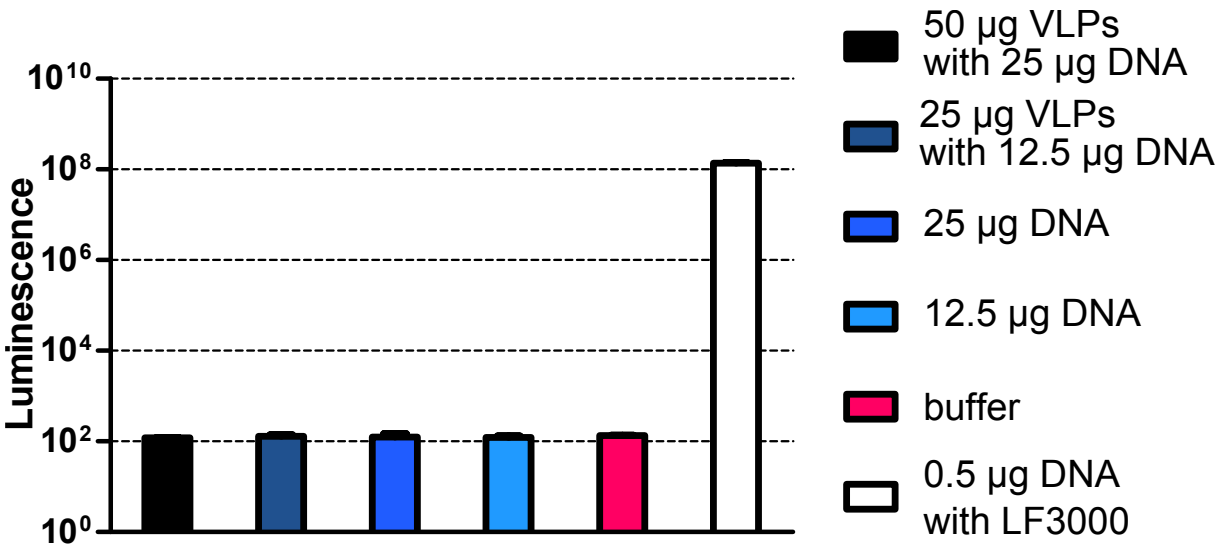


**Figure 2.41 – VLPs do not deliver expression plasmids into WAC 2 cells.** WAC 2 cells were treated with VLPs containing the luciferase expression plasmid pGL4.51. Luminescence in these cells after 48 h did not change when compared to cells where the DNA was directly added to the media or that were treated with buffer. Transfection of WAC 2 cells with 0.5 µg of plasmid DNA using Lipofectamine® 3000, however, results in a luminescence signal which is six orders of magnitude higher. Erros bars represent standard deviation of triplicate measurements of the same samples. LF3000 = Lipofectamine® 3000; VLP = virus-like particle

use of Lipofectamine® 3000, on the other hand, resulted in a luminescence signal six orders of magnitude higher than the negative buffer control. These results are clearly indicative of luciferase expression even when using only 0.5 µg DNA and Lipofectamine® 3000. The use of VLPs, however, failed at delivering the expression plasmid to WAC 2 cells. It must therefore be concluded that VLPs derived from the JC virus are not suitable for the delivery of either siRNA molecules or shRNA expression plasmids to WAC 2 cells under the protocol that was used. It is also evident from these data that minimal changes in $PrP^C$ expression in the previous experiments are to be expected because of experimental variation and an unspecific effect of the VLP treatment. It is possible that adjusting the experimental protocol will lead to effective transduction. It is also likely, however, that WAC 2 cannot be transduced with the use of JCV VLPs. This does not necessarily rule out that JCV VLPs can deliver the siRNA molecules or shRNA plasmids used in these studies to the brain. However, before employing the technique in a mammalian system, it is absolutely necessary to demonstrate the efficacy of the approach in an *in vitro* cell culture model first. To that end it might be reasonable to test the susceptibility of other cell lines that express $PrP^C$ for JCV VLP-mediated transduction. This line of work, however, could no be followed further during the course of these studies and will be the subject of future work.

# 3 Discussion

Prion disorders such as Creutzfeldt-Jakob disease are characterized by misfolding of soluble $PrP^{C}$ to insoluble $PrP^{Sc}$. The presence of $PrP^{Sc}$ accelerates the misfolding process in a positive feedback loop that culminates in the formation of pathogenic protein aggregates. Since this formation relies on constant production of $PrP^{C}$ reducing or abolishing $PrP^{C}$ biosynthesis could prolong or even halt disease progression. This work focussed on a targeted knockdown of prion protein expression for therapeutic purposes. The initial outline involved the use of the 10-23 DNAzyme, a single-stranded DNA molecule that is capable of cleaving RNA in a sequence-specific manner. DNAzymes which cleave the prion protein mRNA were to be employed for the reduction of $PrP^{C}$ levels in a cellular context. Furthermore, the work aimed at establishing virus-like particles as a delivery platform for DNAzymes to their effector site. While these goals could not be met with DNAzymes, siRNA molecules and shRNA expression plasmids with high silencing activity were developed that could serve as a basis for therapeutic approaches in the future. During the course of the project important insights into the behaviour and general properties of the 10-23 DNAzyme were also obtained. This chapter discusses and evaluates the data in context of the relevant scientific literature.

## 3.1 Design of DNAzymes specific for the prion protein mRNA

The 10-23 DNAzyme can be designed to recognize and cleave almost any RNA of interest with high sequence specificity. The prion protein mRNA contains 144 GU dinucleotides that could serve as favourable cleavage sites for DNAzymes. Since it is not feasible to test this many possible DNAzymes *in vitro* and *in vivo* the number of cleavage sites needs to be narrowed down. One possible approach is to randomly choose and test a few DNAzymes out of the collection of all possible DNAzymes. However, obtaining effective DNAzymes in these cases is a matter of chance. Ideally, DNAzymes would be picked based on criteria that determine the likelihood of effectiveness.

In this work a sequential folding algorithm was used to predict whether a cleavage site in the prion protein mRNA is accessible for DNAzyme hybridization or blocked due to secondary structure formation. This method has been used in the past to predict *in silico* the effectiveness of different siRNAs that target the same mRNA. Tafer et al (2008) employed an algorithm that calculates the local base pairing probability of regions in the mRNA while it is actively translated. During transcription RNA structure is formed locally in the newly synthesized segments and might be restructured later, i. e. after completion. During translation, mRNA secondary structures are broken up

by the helicase activity of the ribosome and reform locally with a probability that can be calculated. Tafer et al (2008) found that the silencing efficiency of siRNAs correlated better with the target site accessibility as determined by their sequential folding algorithm rather than global folding calculations or other criteria.

For initial studies highly accessible hammerhead ribozyme and 10-23 DNAzyme cleavage sites in the prion protein mRNA from the Syrian golden hamster were determined *in silico*. Short RNA molecules were designed that resemble stretches of the mRNA with the cleavage sites at their center. Those RNA targets were used to investigate the claim by Wyszko et al (2014) that hammerhead ribozymes and 10-23 DNAzymes in L-configuration, so-called Spiegelzymes, are able to cleave RNA of opposite chirality. If verified, Spiegelzymes would have favourable pharmacokinetic properties since they are much less susceptible to nuclease digestion than nucleic acids in D-configuration.

### 3.1.1 Spiegelzymes do not cleave RNA of opposite chirality

Contrary to the data by Wyszko et al (2014) the Spiegelzymes designed for this study did not show heterochiral activity. However, all Spiegelzymes that were tested were able to cleave their targets in L-configuration, i. e. in a homochiral setup. When the same samples were used that Wyszko et al (2014) utilized for their study the L-hammerhead ribozyme sample indeed displayed cleavage activity towards the D-RNA target. Intriguingly, the opposite setup, D-hammerhead ribozyme with L-RNA target, revealed no activity at all. Together with the fact that the heterochiral behaviour of DNAzymes could also not be shown the data raise doubts as to whether the results of Wyszko et al (2014) are valid. A possible explanation for their results is that the L-hammerhead ribozyme sample was at one point contaminated with ribozymes in D-configuration. Such a contamination could take place involuntarily when L-ribozymes are synthesized and purified using the same equipment that was previously used to produce the ribozyme in D-configuration. Even small amounts of residual D-hammerhead ribozymes would be sufficient for appreciable activity. For the present studies on PrP mRNA-specific Spiegelzymes the nucleic acid enzymes in L-configuration were obtained chronologically before those in D-configuration and L-RNA targets were chosen as positive controls. The nucleic acid enzymes in D-configuration that were used in the described experiments were ordered at a later point in time. Therefore cross-contamination of Spiegelzymes with DNAzymes and ribozymes in D-configuration during synthesis could be excluded.

In response to Wyszko et al (2014), Hoehlig et al (2015) come to the same conclusion. In their studies, contamination of L-ribozymes with as little as 0.01 % of D-hammerhead ribozyme was sufficient for the detection of false positive “heterochiral” activity. When these D-ribozyme contaminants were blocked with the use of comple-

mentary D-RNA antisense molecules the alleged “heterochiral” activity was completely abolished. Hoehlig et al (2015) also found no evidence for heterochiral hybridization that would be the basis for L-hammerhead ribozyme or L-DNAzyme-mediated cleavage of D-RNA. It should be noted that other studies have described stable heterochiral duplexes composed exclusively of homopurinic or homopyrimidinic sequences (Ashley, 1992). However, hybridization could not be observed for sequences containing all four nucleobases (Garbesi et al, 1993). In contrast to these data, Szabat et al (2016) recenctly described heterochiral D-RNA:L-RNA duplexes composed of all four nucleobases but their thermodynamic stability is dramatically lower than that of homochiral duplexes. In light of these data it is unlikely that L-DNA or L-RNA could be used as DNAzyme-, ribozyme- or antisense-based therapeutics. An interesting development in this regard is the recent *in vitro* selection of L-RNA-cleaving D-DNAzymes which shows that heterochiral activity is in principle possible (Tram et al, 2015). In this particular case, however, the interaction between substrate and DNAzyme still relies on homochiral duplex formation of DNA in D-configuration as the single L-ribonucleotide that is cleaved is embedded in an otherwise all-D-DNA substrate.

### 3.1.2 Properties of DNAzyme-mediated RNA cleavage

Because Spiegelzyme-mediated cleavage of D-RNA could not be achieved, a set of DNAzymes in D-configuration was used instead. These DNAzymes still have an advantage over ribozymes since they are instrinsically more stable against nucleases and are more cost-effective. Based on the principles laid out by Tafer et al (2008) DNAzymes were selected that are specific for variably accessible target sites in the human prion protein mRNA. When incubated together with short complementary RNAs the DNAzymes cleave their substrates rapidly and with high sequence specificity. These results are in accordance with other studies in which DNAzymes for different targets were designed. Santoro and Joyce (1998) described catalytic parameters for a HIV-1 *gag-pol* mRNA-specific DNAzyme. Depending on pH and $Mg^{2+}$ concentration, $k_{cat}$ values in the range of approximately 0.1 $min^{-1}$ for multiple turnover cleavage to a maximum of 10 $min^{-1}$ at alkaline pH and elevated levels of divalent ions were observed (Santoro and Joyce, 1997, 1998). It was also found that even single mismatch mutations in the RNA generally change the cleavage efficiency drastically although the presence of a single wobble pair is better tolerated. Depending on the position of the mismatch the reduction in cleavage efficiency can either be due to a decrease in $k_{cat}$, an increase in $K_M$, i. e. a lower substrate binding affinity of the DNAzyme, or a combination of both effects.

The interpretation of multiple turnover experiments is somewhat more involved. Only one of the DNAzymes, namely Dz839, displayed true catalytic capabilities. After a sin-

gle round of substrate cleavage the reactions involving the DNAzymes Dz736, Dz824, and Dz733 did not proceed further. One has to assume that unfavoured complex formation or insufficient product release prevent the respective DNAzymes from performing multiple turnover cleavage. Optimally, the $T_m$ value of the duplex formed between DNAzyme and full-length substrate should be higher than the incubation temperature (37 °C) while the $T_m$ value for the duplexes formed by the DNAzyme and the reaction products should be lower. Modification of the substrate binding arms based on the calculated $T_m$ values fully restored multiple turnover behaviour in the case of Dz824 and partially in the case of Dz736. Others have observed similar effects of hybridization arm length. In an early study, Wu et al (1999) noted that increasing the arm length of *bcr-abl* mRNA-specific DNAzymes generally improves their catalytic activity. However, only single turnover kinetics were considered while the impact on multiple turnover reactions was not taken into account. Later, a similar behaviour was noted by Kurreck et al (2002) for single and multiple-turnover kinetics of DNAzymes specific for the full-length mRNA of the vanilloid receptor subtype 1.

Schubert et al (2003) observed a close relationship between activity and the $T_m$ values of duplexes formed by RNA substrates and specific DNAzymes with locked nucleic acid (LNA) or 2′-*O*-methyl nucleotides in the binding arms. While these modifications protect DNA from nuclease activity, they also increase the melting temperature of duplexes which can lead to detrimental effects on multiple turnover catalysis. They found that the relationship between the reaction velocity and the melting temperatures of DNAzyme:RNA duplexes with different lengths resembles a Gaussian distribution with a maximum at the reaction temperature of 37 °C. Importantly, with increasing LNA/2′-*O*-methyl content, shortening of the hybridization arms resulted in favourable multiple turnover kinetics. However, shortening the sequence complementarity between a DNAzyme and its RNA target drastically decreases substrate specificity since shorter sequences have a higher probability to occur in more than one RNA transcript.

The data presented in this work generally agree with the mentioned literature in respect to the relationship between duplex stability and multiple turnover DNAzyme activity. However, deviating from the observations by Schubert et al (2003), it could be shown that Dz839 and Dz824_10/11 rapidly cleave a molar excess of their substrates even though they form duplexes with $T_m$ values well above 37 °C, namely 47 °C and 42 °C. The data lead to the conclusion that the melting temperature of the duplexes formed by the DNAzyme and the 5' and 3' reaction products are equally important and should be below 37 °C to enable efficient product release. While the use of DNAzymes with asymmetric hybridization arms was already tested in single turnover experiments by Cairns et al (2000), the adjustment of binding arm length in this work was carried out based on calculation and theoretical consideration rather than extensive experimentation with many DNAzyme variants. Overall, the work at hand shows that a fine tuning

of the hybridization arms based on calculated duplex stabilities enables the design of highly specific DNAzymes that display multiple turnover cleavage activity.

## 3.2 DNAzymes cleave structured RNA transcripts

After DNAzymes were obtained that cleave molar excesses of short RNA substrates it was tested whether these DNAzymes are able to cleave long, structured RNAs. Indeed, DNAzyme-mediated cleavage of pre-folded *in vitro* transcripts could be observed experimentally. The transcripts were also cleaved when the DNAzymes were added to the *in vitro* transcription reaction. Importantly, the DNAzyme Dz733 cleaved *in vitro* transcripts that were denatured and cooled down after transcription but was unable to cleave the transcripts during the actual transcription reaction. This behaviour illustrates the difference between an RNA that has adopted a thermodynamically favoured global folding with long-range contacts and one in which secondary structures form primarily due to local base pairing, as is the case during translation in the cell according to Tafer et al (2008). The experimental setup in which DNAzymes are present during *in vitro* transcription was chosen as a model for mRNA being translated *in vivo*.

The model has two key limitations. Firstly, after the *in vitro* transcribed RNA adopts secondary structures it will stay in that conformation. In the cell, secondary structures in the mRNA are repeatedly broken down after their reformation by multiple ribosomes passing in succession. Therefore, while cleavage sites within the mRNA may become accessible repeatedly, those same cleavage sites in the *in vitro* transcribed RNA may only be accessible for a limited amount of time. This is of course only the case if stable secondary structures form and block the respective cleavage site. The other important limitation is also due to the helicase activity of the ribosome. In the cell a DNAzyme hybridized to the mRNA may be displaced by a translating ribosome. The DNAzyme can therefore exert its cleavage activity only for a limited amount of time. This is not the case during *in vitro* transcription in which the potential DNAzyme:RNA complex remains undisturbed from any helicase activity.

These drawbacks notwithstanding, all tested DNAzymes behaved according to the predicted target site accessibilities during *in vitro* transcription. In regard to DNAzymes these experiments represent a novel approach for the detection of accessible cleavage sites in highly structured RNA. In contrast, many previous works have selected DNAzymes in a trial-and-error manner. In an attempt to determine accessible target sites in the Vanilloid Receptor Subtype 1 mRNA experimentally, Kurreck et al (2002) have used a messenger walk screen. In their work the mRNA was incubated together with antisense oligodeoxynucleotides (AS-ODNs) complementary to RNA stretches that contain a cleavage site. In case of successful hybridization, the AS-ODN:RNA duplex triggers

RNase H-mediated cleavage which is visualized via dPAGE. This method, however, requires extensive experimental work and only reveals accessible target sites in pre-folded RNA.

A different rationale was followed by Schubert et al (2003), Schubert et al (2004), and Vester et al (2006). In these studies locked nucleic acid and 2'-*O*-methyl ribonucleotides were incorporated into the binding arms of DNAzymes. Since these unnatural nucleotides increase duplex stability they also affect the ability of a DNAzyme to unfold higher-order RNA structures. In *in vitro* experiments, these DNAzymes indeed cleaved structured RNA more effectively as compared to constructs with only natural nucleotides. However, no data was presented that could show higher cleavage activity *in vivo*. While these modifications restored activity in DNAzymes that were previously unable to cleave structured RNA, it could be argued that an accessible, albeit shorter than usual, stretch of RNA would still be necessary to initiate DNAzyme binding and subsequent RNA unfolding.

The DNAzymes Dz736 and Dz839 performed RNA cleavage regardless of whether they were present during *in vitro* transcription or added to pre-folded transcripts. In these instances the advantage of choosing the Tafer et al (2008) approach over global folding calculations is not evident. On the other hand, Dz733 exclusively cleaved pre-folded RNA and the opposite case is conceivable for other hypothetical DNAzymes. Unfortunately, the usefulness of predicting the *in vivo* silencing efficiency of DNAzymes via this method remains in question since no DNAzyme-mediated knockdown of $PrP^C$ expression could be achieved during this work.

## 3.3 DNAzyme treatment fails in cell culture

Although several DNAzymes effectively cleaved highly structured RNA *in vitro* the effect on prion protein expression in WAC 2 cells was minimal at best. During the course of 24 h and over a large range of concentrations DNAzyme treatment did not reliably lower protein levels. However, siRNA molecules specific for the same target sites reduced prion protein levels almost completely. Even a dose four times lower than standard conditions abolished expression considerably. These experiments show that the cleavage sites in the prion protein mRNA are indeed accessible for hybridization of complementary siRNAs and DNAzymes since siRNA treatment would have been ineffective otherwise. Furthermore, it could be shown that the DNAzymes were internalized by WAC 2 cells with the use of a common transfection reagent and remained stable for at least 24 h. In light of these data it is evident that other factors must be responsible for the poor performance of DNAzymes in cells.

The results obtained in this work conflict with several studies in the literature that have described effects of DNAzyme treatment in cells. For example, Santiago et al (1999) showed a modest reduction of Egr-1 (Early growth response factor-1) mRNA and protein levels in smooth muscle cells (SMCs) treated with a specific DNAzyme. The DNAzyme also inhibited SMC proliferation and regrowth in an *ex vivo* rat carotid injury model. A DNAzyme that targets Vascular Endothelial Growth Factor Receptor 2 (VEGFR2) was shown to decrease mRNA levels and inhibit angiogenesis and tumor growth when injected into mouse tumors (Zhang et al, 2002). Furthermore, DNAzyme-mediated suppression of LMP1 expression and induction of apoptosis in CNE1-LMP1 cells was demonstrated (Lu et al, 2008).

Other published works have measured the effects of DNAzyme treatment without showing that protein levels are indeed affected. One example are the GATA3-specific DNAzymes that are currently studied for the therapy of $T_h2$-driven asthma (Krug et al, 2015). Those were tested in *in vitro* cleavage assays and for their effect on the cellular inflammatory response in mice but a reduction of GATA3 protein levels was not demonstrated (Sel et al, 2008). A DNAzyme specific for c-*myc* was tested for its ability to cleave RNA *in vitro* and its effects on smooth muscle cell proliferation without establishing that protein levels were diminished (Cairns et al, 1999). Fokina et al (2012) have made use of a reporter assay to measure the effects of DNAzyme treatment in cells but did not show a reduction in protein levels. Yen et al (1999) could show a reduction in Huntingtin levels in HEK-293 cells but the protein was transiently expressed from a plasmid that was cotransfected together with specific DNAzymes. Suppression of endogenous Huntingtin expression was not attempted by the authors.

In conclusion, an argument can be made that many studies that use DNAzymes have not demonstrated that treatment with DNAzymes indeed leads to a reduction of the respective protein levels. It is feasible that DNAzyme treatment affects cellular signaling in ways independent of protein reduction, leading to the observed phenotypes. Furthermore, in those studies that do show protein reduction it is not clear whether this is due to actual DNAzyme activity or an antisense effect. A recent review points out that compelling evidence for DNAzyme-mediated RNA cleavage *in vivo* is not available (Silverman, 2016). An important study that was cited in this regard is the work by Young et al (2010). They have used a DNAzyme with a photosensitive caging group, a chemical modification that renders the catalytic core inactive. Ultraviolet irradiation of the DNAzyme removes the modification and restores activity. The authors have found that the silencing efficiency of DNAzymes in cells was comparable between inactivated and active DNAzymes. These data lead to the conclusion that the majority of DNAzyme-mediated silencing effects depend on an antisense mechanism rather than an actual cleavage reaction. Taken together, these articles raise doubts about DNAzyme cleavage activity in cells. Silverman (2016) notes that intracellular $Mg^{2+}$ concentrations are

probably too low to sustain DNAzyme activity. This line of thought was investigated further during the course of this work. The results in this regard will be discussed in section 3.5.

The DNAzymes used in this work are not optimized as antisense agents which might be a reason for their poor performance in cells. Moreover, it is generally questionable to use DNAzymes if their function is primarily driven by antisense effects. If this is the case, then a key advantage of utilizing DNAzymes, i. e. their inherent cleavage ability, becomes obsolete. Under these circumstances it is reasonable to prefer optimized antisense oligodeoxynucleotides instead of adding a catalytic core that is probably inactive at physiological conditions. It was found that siRNA molecules against the prion protein mRNA displayed superior silencing properties under the same conditions that were used for DNAzymes. For this reason siRNA can be regarded a potential therapeutic for prion disease, provided that efficient delivery systems can be employed. Consequently, the initial aim of VLP-mediated DNAzyme delivery was adjusted to VLP-mediated siRNA delivery.

## 3.4 Virus-like particles as a delivery platform

Since effective siRNA molecules and shRNA plasmids for the knockdown of prion protein expression were obtained during this work it was tested whether these potential therapeutics could be delivered to WAC 2 cells with the use of JC virus-derived VLPs. This part of the project was planned in cooperation with Dr. Manninga (NEUWAY Pharma AG). However, transduction of these cells via VLPs was not successful. Previous studies have shown that VLPs are indeed viable delivery vehicles for plasmid DNA and siRNA (Chang et al, 2011; Chen et al, 2010; Hoffmann et al, 2016). The reason for the lacking performance in WAC 2 cells is currently not known.

The protocol that was used for preparing loaded VLPs might have produced particles with low potency. Indeed, analytical ultracentrifugation, which was performed by Luitgard Nagel-Steger, revealed that the used protocol did not produce a single well-defined species that could be expected for spherical capsids with a diameter of 40 nm (personal communication of unpublished data). Instead, an unresolvable mixture of particles with a wide range of sedimentation coefficients was observed that probably formed due to uncontrolled protein aggregation. Adjustments to the protocol and precise quality control could help in preparing a high yield of functional capsids.

Entry of the JC virus into cells requires sialic acid-containing cell surface glycoproteins, the serotonin receptor 5-hydroxytryptamine (5-HT) receptor 5-HT2AR as well as LSTc pentasaccharide-modified glycoproteins and glycolipids (Suzuki et al, 2001; Neu et al, 2010; Assetta et al, 2013; Sawa and Komagome, 2005). It is possible that WAC 2

cells do not sufficiently fulfil these requirements or that of other potential receptor molecules the involvement of which is currently unknown. The use of another cell line for transduction experiments could be a suitable alternative model system. Particularly promising in this regard are cell lines for which VLP-mediated transduction was already demonstrated, such as rat osteoblasts, HEK293A cells with exogenous 5-HT2AR expression, both of which are, however, not brain-derived, or the human SVG-A cell line which is of glial origin (Hoffmann et al, 2016; Assetta et al, 2013; Neu et al, 2010).

In addition, alternatives to JCV-derived VLPs should be explored. In recent years, advances in the field of targeted delivery have set the stage for nucleic acid-based therapies. The techniques that have been developed offer a lot of potential for siRNA and shRNA-mediated knockdown of prion protein expression in patients. Peptide vectors, such as the cell-penetrating rabies virus glycoprotein (RVG) and others, have been successfully used for nucleic acid delivery into cells and tissues (Wender et al, 2000; Kumar et al, 2007; Hoyer and Neundorf, 2012; Kordasiewicz et al, 2012). Other alternatives include lipids that are covalently linked to nucleic acids, stable nucleic acid lipid particles (SNALPs), and aptamer-mediated delivery (Raouane et al, 2012; Whitehead et al, 2009; Aaldering et al, 2015). In recent studies adeno-associated viruses (AAVs) have emerged as excellent delivery vectors for therapeutic plasmids and oligo(deoxy)nucleotides to tissues of the CNS, including the brain (Foust et al, 2009; Valori et al, 2010; Mendell et al, 2017). The advantages of AAVs include the fact that they usually do not integrate into the host genome and that they efficiently enter non-dividing cells, such as neurons. The method could also be suitable for the delivery of the shRNA plasmids developed in this work.

## 3.5 $Mg^{2+}$ concentration influences DNAzyme activity drastically

In order to investigate whether intracellular $Mg^{2+}$ concentrations are insufficient for DNAzyme activity an experimental setup was developed that allows the generation of quantifiable kinetic data. Detailed analysis revealed that DNAzyme activity is very sensitive to changes in $Mg^{2+}$ concentrations in the submillimolar range. Since the intracellular levels of free $Mg^{2+}$ vary greatly in this range (Romani and Scarpa, 1992; Romani, 2011) the data provide a possible explanation for the poor DNAzyme performance in cells. The data in this work support a model in which the DNAzyme binds three $Mg^{2+}$ ions in order to enable RNA cleavage. Because of the limited accuracy of the setup the number of bound ions has to be treated as a rough estimate. It is reasonable to assume that several $Mg^{2+}$ ions are needed for proper folding of the catalytic core of the

DNAzyme but it cannot be excluded that one ion also takes part in the actual cleavage reaction.

Santoro and Joyce (1998) explored the metal ion dependency of the 10-23 DNAzyme but they did not analyse submillimolar $Mg^{2+}$ concentrations. They did, however, already note that the DNAzyme cleaves more efficiently in the presence of $Mn^{2+}$. Cieslak et al (2003) investigated structural changes in the 10-23 DNAzyme in response to changes in the $Mg^{2+}$ concentration. According to their data DNAzyme folding proceeds in distinct stages: At a $Mg^{2+}$ concentration of 0.5 mM the previously extended DNAzyme adopts a more complex structure which binds RNA weakly and lacks catalytic activity. At 5 mM $Mg^{2+}$ the hybridization arms project at the right angles for RNA binding, and at 15 mM $Mg^{2+}$ additional structural changes in the catalytic core take place at which point the DNAzyme binds and cleaves RNA most effectively. While a folding model in which the DNAzyme undergoes distinct changes in response to different $Mg^{2+}$ concentrations is feasible, the values for $Mg^{2+}$ that Cieslak et al (2003) propose do not agree with the cleavage activity that was observed in this work and by others at submillimolar concentrations. It is important to note that Cieslak et al (2003) performed the spectroscopic measurements in their work at temperatures well below physiological conditions and only few of their experiments were carried out in the presence of NaCl.

It is intriguing that the 10-23 DNAzyme is probably not active under physiological conditions while natural ribozymes exist that cleave RNA in the cell. Indeed, the hammerhead ribozyme is catalytically active at free $Mg^{2+}$ ion concentrations as low as 0.1 mM (Khvorova et al, 2003). This disparity hints towards a fundamental difference between ribozymes and DNAzymes. Importantly, however, minimalist hammerhead ribozymes that contain only the minimal conserved HHRz motif show a similar behavior as DNAzymes. They also lack intracellular activity and exhibit poor cleavage *in vitro* at low $Mg^{2+}$ concentrations. Khvorova et al (2003) discovered that sequence elements outside the hammerhead ribozyme catalytic core stabilize the core in an active conformation, allowing the ribozyme to perform RNA cleavage at low $Mg^{2+}$ concentrations such as those present in the cell. An appealing rescue strategy was realized by Fedoruk-Wyszomirska et al (2009). They introduced a structural element into minimalist hammerhead ribozymes that stabilizes the catalytic core in its active conformation. Thereby, the ability of the ribozyme to cleave RNA at low $Mg^{2+}$ concentrations and even in the cell was restored.

It is a tempting speculation that the 10-23 DNAzyme could be modified in a similar way, either by the introduction of stabilizing DNA loops or functional groups or via chemical crosslinking. Fokina et al (2012) have shown that modifying the catalytic core of the 10-23 DNAzyme with 2′-*O*-methyl ribonucleotides in some cases increases cleavage activity, which is also retained at a 0.5 mM $Mg^{2+}$ concentration but whether these DNAzymes are active in cells was not clearly proven. Asanuma et al (2006) used

a covalently introduced intercalator that increased DNAzyme activity but whether this modification makes the DNAzyme less dependent on $Mg^{2+}$ remains an open question. Smuga et al (2010) modified the DNAzyme with a single amino acid-like functional group which enables it to operate without a metal ion cofactor but the catalytic rate is too low to use this DNAzyme for efficient gene silencing. The work of Khvorova et al (2003) and Fedoruk-Wyszomirska et al (2009) was based on a detailed structural understanding of the hammerhead ribozyme. A comparable level of knowledge about the 10-23 DNAzyme structure is currently lacking and would be mandatory before a similarly impactful adjustment of the DNAzyme could be accomplished.

## 3.6 Outlook

In this work DNAzymes specific for the prion protein mRNA were developed. The DNAzymes are functional *in vitro* but treatment of WAC 2 cells did not lead to substantial knockdown of prion protein expression. It could be shown that DNAzyme activity is sensitive to changes in $Mg^{2+}$ concentrations in the submillimolar range and that the DNAzyme needs to bind at least three $Mg^{2+}$ ions for proper activity. The use of siRNA and shRNA in the same conditions resulted in an appreciable silencing effect in cells but ultimately it had to be concluded that VLP-mediated delivery of siRNA and shRNA into WAC 2 cells could not serve as a model for this therapeutic strategy.

A feasible outline for future experiments include the use of JCV-derived VLPs in other cell lines, preferably those for which an efficient uptake was already demonstrated. These experiments notwithstanding, the reliable production of potent VLPs will require adjustments to the preparation protocols and a precise experimental quality control. Alternative delivery methods, such as the use of CPPs, aptamers, and AAVs, should also be considered.

The detailed kinetic data that was obtained for the DNAzyme in low $Mg^{2+}$ conditions will serve as a starting point for a more in-depth characterisation of the DNAzyme. A structural model of the 10-23 DNAzyme could lead to the development of certain rescue strategies that make the DNAzyme less reliant on high $Mg^{2+}$ concentrations. If achieved, these strategies can lead to a new generation of DNAzymes that display substantial cleavage activity in cells and could be used as potent silencing agents.

# 4 Material and Methods

## 4.1 Prediction of target site accessibility

Potential cleavage sites within the Syrian golden hamster and human prion protein mRNA sequences were ranked based on their accessibility according to the work of Tafer et al (2008). The SHa and human mRNA sequences were retrieved from GenBank, their accession numbers are K02234 and NM_000311, respectively.

The program RNAPLFOLD was used to compute local base pairing probabilities with a maximum base pair span $L = 40$ in a window $W$ of 80 nt length that is slid over the mRNA sequence. For each base pair the base pairing probabilities of all windows that contain the base pair are averaged. The mean probability $u_l$ describes the probability that regions of length $l = 10$ nt centered at a cleavage site are unpaired. The value of $u_{10}$ for each cleavage site defines its accessibility for intermolecular hybridization by single-stranded nucleic acids, such as DNAzymes. Target sites with $u_{10} < 0.01$ were defined as inaccessible, $u_{10} > 0.01$ was defined as medium accessible, and $u_{10} > 0.1$ as highly accessible. The output of the sequential folding algorithm was visualized with the use of GLE (Graphics Layout Engine).

## 4.2 Cleavage of short RNAs

Based on the calculations described above, short RNA molecules were designed that are identical to stretches of the SHa and human prion protein mRNA sequences with a cleavage site at the center. These RNA targets have a length of 14 nt in the case of SHa mRNA-derived sequences and 19 nt in the case of human mRNA-derived sequences. They are covalently linked to a fluorescein moiety at their 5' end. DNAzymes and Spiegelzymes, i. e. 10-23 DNAzymes and hammerhead ribozymes in L-configuration, were designed to be complementary to the RNA targets. All oligodeoxynucleotides and oligoribonucleotides that were used in this work were commercially acquired. The sequences for all DNAzymes, Spiegelzymes, siRNAs, and shRNAs can be found in section 4.7.3 on page 101.

### 4.2.1 Spiegelzyme-mediated RNA cleavage

The ability of DNAzymes to cleave short D-RNA substrates was tested *in vitro*. To this end 0.4 µM of each RNA target were prepared together with 4 µM or 40 µM of the respective DNAzyme in 50 mM Tris-HCl pH 7.5 in a total volume of 9 µl. As a negative control, samples were prepared that contain the RNA targets without any DNAzyme.

The samples were denatured at 73 °C for 2 min to break up possible secondary structures and allowed to cool down to room temperature for 15 min, giving the RNA and DNA time to hybridize and the catalytic centers of the DNAzymes to adopt their folding.

The cleavage reaction was initiated by adding 1 µl of 100 mM $MgCl_2$ to a final concentration of 10 mM. The samples were incubated at 37 °C for 3 h. The reaction was quenched by adding one volume of 2x RNA loading buffer (94 % formamide, 25 mM EDTA, 0.02 % bromophenol blue (w/v), and 0.02 % xylene cyanol (w/v)) and putting the samples on ice. The samples were denatured at 96 °C for 15 min, cooled down on ice, and briefly centrifuged at 16 000 rcf.

Afterwards, the samples were separated on 18 % polyacrylamide gels containing 7 M urea which were buffered with Tris-borate EDTA buffer (TBE). Gel electrophoresis proceeded for 1 h at 20 W for approximately 1 h. Images of the gels were acquired with the ChemiDoc™ MP System by detecting fluorescein fluorescence.

The activity of Spiegelzymes was tested according to the same protocol with a tenfold molar excess of Spiegelzyme over RNA target. The Spiegelzymes were tested in homochiral and heterochiral setup by using L-RNA and D-RNA, respectively. GFP-specific Spiegelzymes, hammerhead ribozymes, and DNAzymes were tested with samples provided by Eliza Wyszko and Volker A. Erdmann.

### 4.2.2 DNAzyme-mediated RNA cleavage

DNAzymes specific for the human prion protein mRNA sequence were tested as described in the previous section. A tenfold molar excess of DNAzyme over RNA target was used. After the reaction the reaction products were separated via 18 % denaturing polyacrylamide gel electrophoresis (dPAGE) for 1 h at 20 W and the full-length RNA as well as the 5' cleavage fragments were identified using fluorescein fluorescence.

### 4.2.3 Sequence specificity of DNAzymes

The sequence specificity of the DNAzymes was tested by incubating each DNAzyme together with each target RNA separately. For example, Dz736 was incubated together with T736, T839, T824, and T733 to assess which of the RNAs is cleaved by Dz736. In addition, T839 was incubated with Dz839, T824 with Dz824, and T733 with Dz733 during the same experiment to serve as positive controls. This experimental setup was adjusted for each of the DNAzymes. Specificity experiments were carried out with the DNAzymes in tenfold molar excess over the RNA targets. RNA and DNA were denatured in the absence of $Mg^{2+}$ as described before and the reaction was initiated by adding $MgCl_2$. After incubation for 3 h at 37 °C the reaction was stopped and the

products were denatured and separated by 18 % dPAGE. The RNA was visualized via fluorescence of the fluorescein label.

### 4.2.4 Multiple turnover RNA cleavage

To test whether the DNAzymes are capable of multiple turnover RNA cleavage, 0.4 µM of each RNA target was incubated together with 0.04 µM of the respective DNAzyme, i. e. a tenfold molar excess of RNA over DNA. The samples were prepared in 50 mM Tris-HCl pH 7.5. The samples were denatured at 73 °C for 2 min and allowed to cool down at room temperature for an additional 15 min. Cleavage was initiated by adding $MgCl_2$ to a final concentration of 10 mM. The reaction was allowed to proceed for 3 h at 37 °C and stopped by adding one volume of 2x RNA loading buffer. The samples were denatured and separated via 18 % dPAGE. Fluorescein-tagged RNA fragments were visualized by detecting fluorescence.

### 4.2.5 Kinetics of DNAzyme-mediated RNA cleavage

For the measurements of DNAzyme-mediated cleavage kinetics a sample for each point in time was prepared. Each sample contained 0.4 µM RNA substrate and 4 µM, 0.4 µM, or 0.04 µM DNAzyme, depending on the experiment, for enzyme-to-substrate ratios of 10:1, 1:1, and 0.1:1, respectively. The samples were prepared in 50 mM Tris-HCl at pH 7.5. Each sample was denatured at 73 °C for 2 min and allowed to cool down to room temperature for 15 min. Afterwards, the reaction was started by adding $MgCl_2$ for a final concentration of 10 mM to each sample separately. To avoid time delays that would be introduced because of the numerous pipetting steps, the $MgCl_2$ solution was added in such a way that it adheres as a single droplet to the wall of each 1.5 ml reaction tube without mixing with the reaction mix. Thereby all reactions could be started at the same time by simultaneous centrifugation of the reaction tubes. Three negative control samples were prepared. One of these contained the RNA without DNAzyme and without $MgCl_2$. The second control sample contained RNA alone in the presence of 10 mM $MgCl_2$ and the third sample contained RNA and the respective DNAzyme without addition of $MgCl_2$. Those samples were incubated for the same duration as the last time point of the reaction kinetics measurements.

After each of the respective reaction times one of the reactions was quenched by addition of 2x RNA loading buffer and incubating the sample on ice. All samples were denatured and separated via 18 % dPAGE. Visualization of the RNA fragments was carried out by fluorescence detection.

### 4.2.6 Detection of divalent metal ion impurities in nucleic acid samples

To test if divalent metal ion impurities were responsible for DNAzyme activity in samples were no $MgCl_2$ was added, reactions with the chelating agent EDTA were prepared. The reactions were carried out with 0.4 µM RNA and 4 µM DNAzyme in 50 mM Tris-HCl at pH 7.5. While one sample contained no EDTA, three samples were prepared with a final EDTA concentration of 10 mM, 1 mM, or 0.1 mM, respectively. Also, one sample without DNAzyme served as a negative control. The samples were denatured and cooled down as described before but no $MgCl_2$ was added. The samples were incubated at 37 °C for 3 h before one volume of 2x RNA loading buffer was added. All samples were denatured at 96 °C for 15 min and separated via 18 % dPAGE after which the labelled RNA fragments were visualized via fluorescein fluorescence.

### 4.2.7 Thermal stability of DNA:RNA duplexes

The Poland (1974) algorithm in the implementation described by Steger (1994) was used to calculate the thermal stability of the duplexes formed by the DNAzymes and their RNA substrates or the respective cleavage products. Thermodynamic values for DNA:RNA duplexes at 1 M NaCl according to Sugimoto et al (1995) were used. The respective service can be accessed via the web page of the Institut für Physikalische Biologie of the Heinrich Heine University Düsseldorf. For the duplexes formed by the DNAzymes and their full-length RNA substrates a single mismatch was assumed for the unpaired purine nucleotide of the target RNA.

According to these data, the DNAzyme variants Dz736_6/7 and Dz824_10/11 were designed. In order to test whether these DNAzymes are capable of multiple turnover RNA cleavage, respective reactions were prepared as described before. The RNA substrate T736 was incubated together with Dz736_9/9, i. e. the standard variant, or the shortened Dz736_6/7 in either a 10:1 or a 0.1:1 molar enzyme-to-substrate ratio. The RNA substrate T824 was incubated together with Dz824_9/9 or Dz824_10/11 in the same manner. The samples were incubated at 37 °C for 3 h before stopping the reaction and analysing the products via 18 % dPAGE.

## 4.3 Cleavage and labelling of *in vitro* transcripts

### 4.3.1 Plasmid linearization

For *in vitro* transcription a pET11a plasmid that contains the human PrP coding sequence for amino acids 23-230 under the T7 promoter was used as a template. The

plasmid was linearized before use. Five separate reactions with a volume of 20 µl were prepared that contain 1 µg of DNA, 2 µl 10x Fast Digest buffer, and 0.5 U $\mu l^{-1}$ BamHI Fast Digest (both from Fermentas, Waltham, Massachusetts, USA). The digestion was carried out at 37 °C for 15 min followed by heat inactivation of the enzyme at 80 °C for 5 min.

The digested samples were pooled and purified by phenol-chloroform-chloroform extraction. One volume of phenol-chloroform in a 1:1 mixture was added to the sample followed by vigorous mixing and centrifugation at 16 000 rcf for 10 min. The aqueous phase was recovered and the process was repeated with one volume of chloroform. The aqueous phase was again recovered. Sodium acetate was added to a final concentration of 0.3 mM. The samples were mixed with three volumes of ethanol and incubated on ice for 1 h. Afterwards, the samples were centrifuged for 1 h at 16 000 rcf and 4 °C in order to pellet the precipitated DNA. The supernatant was discarded and the precipitate was washed with 200 µl of 70 % ethanol. The samples were centrifuged for 10 min at 16 000 rcf and 4 °C. The supernatant was discarded and the pellet was air-dried for 10 min. Afterwards, the precipitate was resolubilized in 11 µl of $H_2O$ and the DNA concentration was measured spectrophotometrically.

### 4.3.2 Production of RNA transcripts

RNA transcripts were prepared by *in vitro* transcription and subsequent covalent attachment of Cy5 moieties to the transcripts via copper-free Click Chemistry. For these experiments the Cy5 RNA T7 Transcription Kit (Jena Bioscience, Jena, Germany) was used. The *in vitro* transcription reaction was carried out in 40 mM Tris-HCl pH 7.9 with 10 mM DTT, 10 mM NaCl, 6 mM $MgCl_2$, 2 mM spermidine, and 1 U $\mu l^{-1}$ RNase inhibitor. As a template a pET11a plasmid was used that contains the huPrP23-230 coding sequence under the T7 promoter. If not otherwise specified, the plasmid was linearized beforehand by digestion with BamHI (see section 4.3.1). For initial tests, the 1423 bp linear control template was used that is provided with the kit. The template was added to the reaction at a final concentration of 20 ng $l^{-1}$. Furthermore, 1 mM each of ATP, GTP, and CTP as well as 0.75 mM UTP and 0.25 mM 5-Azido-UTP were provided for the reaction, which was initiated by adding T7 RNA polymerase at a final concentration of 15 U $\mu l^{-1}$ in a final volume of 40 µl. The *in vitro* transcription reaction mix was incubated for 1 h at 37 °C. Afterwards, the samples were purified via gel filtration columns (illustra MicroSpin G-210 25 Columns, GE Healthcare Europe GmbH, Freiburg, Germany) according to the manufacturer's protocol to remove non-incorporated nucleoside triphosphates.

### 4.3.3 DNAzyme-mediated cleavage and fluorescent labelling of RNA transcripts

Activity assays for DNAzyme-mediated cleavage of transcripts were carried out *in vitro*. For these assays, 700 fmol of *in vitro* transcripts were denatured at 73 °C for 5 min in 50 mM Tris-HCl pH 7.5 and allowed to cool down for 1 h. Denaturation of 4 pmol of each respective DNAzyme was performed separately. The DNAzymes were added to the transcripts and $MgCl_2$ was added to a final concentration of 10 mM and a final volume of 10 µl. The samples were incubated at 37 °C for 3 h. The cleavage reaction was terminated by adding EDTA to a final concentration of 10 mM.

For labelling, 1.2 nmol of DBCO-Sulfo-Cy5 were added followed by an 1 h incubation step in the dark at 37 °C with shaking at 300 rpm. This ensures a tenfold molar excess of DBCO-Sulfo-Cy5 over the theoretical maximum amount of azide modifications in the transcripts when assuming an equal distribution of the four nucleotides and a 100 % substitution of uridine by 5-Azido-uridine. After the labelling a second purification step is unnecessary since the excess DBCO-Sulfo-Cy5 molecules are separated from the labelled transcripts during gel electrophoresis. One volume of 2x RNA loading buffer was added to each sample. The samples were denatured at 96 °C for 15 min. Then, the samples were separated via 5 % dPAGE with 7 M urea. The labelled full-length transcripts and cleavage products were visualized via Cy5 fluorescence.

Transcript labelling and analysis was performed according to the same protocol also for experiments were no DNAzyme was added. In each case, the amount of DBCO-Sulfo-Cy5 was adjusted to ensure a tenfold molar excess over the theoretical maximum amount of azide modifications in the sample.

### 4.3.4 Transcription in the presence of DNAzymes

For activity assays of DNAzymes during transcription samples were prepared in 40 mM Tris-HCl pH 7.9 with 10 mM DTT, 10 mM NaCl, 6 mM $MgCl_2$, 2 mM spermidine, 1 U $\mu l^{-1}$ RNase inhibitor, 20 ng $l^{-1}$ plasmid DNA (linearized huPrP23-230 in pET11a), 1 mM each of ATP, GTP, and CTP as well as 0.75 mM UTP and 0.25 mM 5-Azido-UTP, 10 µM of priorly denatured DNAzyme, and 15 U $\mu l^{-1}$ T7 RNA polymerase. The final reaction volume in these experiments was 10 µl. For purification with gel filtration columns the samples had to be adjusted to a volume of 25 µl by adding $H_2O$.

Labelling was carried out by adding 1 nmol of DBCO-Sulfo-Cy5 to ensure at least a tenfold molar excess over the theoretical maximum amount of azide modifications that could be expected based on previous experiments. The labelling reaction was incubated for 1 h at 37 °C and shaking at 300 rpm. Afterwards, one volume of 2x RNA loading

buffer was added to each sample followed by denaturation at 96 °C for 15 min. The samples were separated via 5 % dPAGE and analysed by detecting Cy5 fluorescence.

For time-course analysis of Dz824_10/11-mediated RNA cleavage during transcription the sample was prepared according to the same protocol. After 10, 30, 60, and 120 min 2 µl aliquots were taken from the sample. To stop the reaction, EDTA was added immediately to a final concentration of 10 mM and the aliquots were placed on ice. The aliquot volumes were adjusted to 25 µl with $H_2O$ prior to gel filtration. For labelling 1 nmol of DBCO-Sulfo-Cy5 was added to each aliquot. The samples were analysed as described before.

## 4.4 Treatment of WAC 2 cells

### 4.4.1 Culturing conditions for WAC 2 cells

The WAC II cells used in this work were cultivated in RPMI 1640 medium with GlutaMAX™ (Thermo Fisher Scientific, Waltham, Massachusetts, USA) at 37 °C in a 5 % $CO_2$ environment. The medium was supplemented with 10 % Fetal Bovine Serum and 50 U $ml^{-1}$Penicillin, 50 µg $ml^{-1}$ Streptomycin. The cells were kindly provided by Prof. Dr. Carsten Korth.

### 4.4.2 Stability of DNAzymes in cells

In order to test the intracellular stability of DNAzymes WAC 2 cells were transfected with fluorescently labelled Dz839(FAM). The cells were seeded in a 6-well format at a cell density of 200 000 cells /well. After 24 h the cells were transfected with 100 pmol of Dz839(FAM) with the use of Lipofectamine® 3000 (Thermo Fisher Scientific, Waltham, Massachusetts, USA) according to the manufacturer's protocol. In addition, the DNAzyme was added directly to the medium. Identical experiments were carried out with the fluorescently tagged RNA molecule T839 in parallel. After an additional 24 h the cells were lysed by adding 30 µl of RIPA buffer and scraping with the use of a cell scraper. The lysates were transferred to 1.5 ml reaction tubes and incubated on ice for 30 min with vigorous vortexing every 5 min. Cell debris was pelleted by centrifugation at 16 000 rcf and 4 °C for 30 min. The supernatant was transferred to a fresh reaction tube.

The nucleic acids were extracted via phenol-chloroform-chloroform extraction which removes proteins which are solubilized in the organic phase and genomic DNA which collects at the interphase between the organic and aqueous solvents. The samples were adjusted to a total volume of 200 µl with $H_2O$. The samples were mixed with one volume of phenol-chloroform, followed by centrifugation at 16 000 rcf for 10 min. After

recovering the aqueous phase the process was repeated with one volume of chloroform. The aqueous phase was recovered and the nucleic acids were precipitated by adding sodium acetate to a final concentration of 0.3 mM and three volumes of ethanol. The samples were incubated on ice for 1 h and then centrifuged for 1 h at 16 000 rcf and 4 °C. The supernatant was discarded and the nucleic acid pellet was washed with 200 µl of 70 % ethanol. After centrifugation at 16 000 rcf and 4 °C for 10 min the supernatant was discarded and the pellet was air-dried for 10 min. The pellet was then resolubilized in 10 µl of $H_2O$. One volume of 2x RNA loading buffer was added, the samples were denatured at 96 °C for 15 min and separated via 18 % dPAGE. Visualization of Dz839(FAM) and T839 was performed by detecting fluorescein fluorescence with the ChemiDoc™ MP System.

### 4.4.3 Fluorescence microscopy

In order to monitor the uptake of DNAzymes by WAC 2 cells fluorescence microscopy was utilized. The cells were seeded on glass cover slips in a 6-well format at a cell density of 200 000 cells/well. After 24 h the cells were transfected with 75 pmol of the fluorescently labelled DNAzyme Dz839(FAM). Lipofectamine® 3000 was used as a transfection agent according to the manufacturer's recommendations. 24 h after transfection the cells were washed with 1 ml of phosphate-buffered saline (PBS). Fixation of the cells was carried out with 4 % formaldehyde solution in PBS for 10 min on ice. Afterwards, the cells were washed three times with PBS for 5 min. The specimens were mounted in Mowiol 4-88 with 25 mg $ml^{-1}$ DABCO (1,4-diazabicyclo-(2,2,2)octan) and 1 µg $ml^{-1}$ DAPI (4',6-diamidino-2-phenylindole). The specimens were sealed with nail polish after 24 h.

Microscopic images were acquired on the Leica TCS SP5 microscope (Leica Microsystems, Wetzlar, Germany) using a HCX PL APO CS 63.0x1.20 water immersion objective with the LAS AF imaging software. Fluorescein was excited at $\lambda_{ex} = 488$ nm and emission was detected in a range from 498-560 nm. 4',6-diamidino-2-phenylindole (DAPI) was excited at $\lambda_{ex} = 405$ nm and emission was detected in a range from 413-477 nm. Wheat Germ Agglutinin Alexa Fluor™ 647 was excited at $\lambda_{ex} = 633$ nm and fluorescence was detected in a range from 645-739 nm. The images were processed with the public domain software ImageJ (build number 1.48v, Wayne Rasband, National Institutes of Health, Bethesda, Maryland, USA) which can be accessed via the web page of the NIH.

### 4.4.4 DNAzyme and siRNA treatment

For the assessment of DNAzyme- and RNAi-mediated knockdown efficiencies WAC 2 cells were transfected with DNAzymes, siRNA molecules, or shRNA expression plasmids.

DNAzyme-mediated silencing kinetics were determined by treating WAC 2 cells for the indicated durations. The cells were seeded in a 12-well format at a cell density of 100 000 cells/well. After 24 h the cells were transfected with 75 pmol of either Dz824_10/11, Dz824LL, a negative control variant of Dz824_10/11 (scramble) where the sequences of the hybridization arms were scrambled, or the antisense deoxynucleotide ASO824 with the use of Lipofectamine® 3000 according to the manufacturer's protocol. The cells were lysed after 3, 6, 12, or 24 h in 25 µl RIPA buffer and scraped off the substrate with the use of a cell scraper. The lysates were transferred to 1.5 ml reaction tubes and incubated on ice for 30 min during which they were vortexed every 5 min. The cell debris were pelleted by centrifugation for 30 min at 16 000 rcf and 4 °C and the supernatant was transferred to a fresh 1.5 ml reaction tube for Western blot analysis.

In order to compare siRNA- and DNAzyme-mediated silencing of prion protein expression 100 000 cells/well were seeded in a 12-well format. After 24 h, the cells were transfected with 75 pmol of siR736, Dz736, siR839, Dz839, siR2577, Dz2577, or with the AllStars Negative Control siRNA. The DNAzymes for these experiments were stabilized against 3' $\longrightarrow$ 5' exonuclease activity by adding two L-dT nucleotides to their 3' ends. In addition, one experiment was carried out in which the cells were left untreated. After 24 h the cells were lysed as described before and processed for Western blotting.

The dose-response relationship for DNAzyme-mediated knockdown of prion protein expression was performed similarly. For this experiment, the cells were transfected with 75, 150, 300, or 600 pmol of Dz824LL using Lipofectamine® 3000 or left untreated. Cell lysates were prepared after 24 h and processed as described before. For the dose-response relationship of siRNA-mediated knockdown, the cells were instead transfected with 7.5, 15, 30, 60, or 120 pmol siR839. As a negative control the cells were transfected with 120 pmol AllStars Negative Control siRNA. The cell lysates for Western blotting were prepared after 24 h as described in the previous section.

### 4.4.5 Western blotting

For the detection of protein levels in treated cell lysates 5 µl of each processed cell lysate were mixed with 1 µl of 6x SDS reducing sample buffer. These samples were denatured at 96 °C for 30 min, briefly put on ice, and centrifuged at 16 000 rcf and 4 °C

for 1 min. The samples were separated via 12 % discontinuous SDS-PAGE buffered with Tris-Glycine SDS buffer (TGS).

The separated samples were transferred to a PVDF (polyvinylidene difluoride) membrane via Western blotting for 2 h with constant 350 mA in a wet electroblotting system. The membrane was incubated in a 5 % non-fat milk in TBS-T solution (Tris-buffered saline with 0.05 % Tween® 20) for 30 min at room temperature. Afterwards, the membrane was incubated in Saf32 $\alpha$-PrP primary antibody or in 3F4 $\alpha$-PrP primary antibody (both diluted 1:10,000 in TBS-T) overnight at 4 °C. All subsequent steps were performed at room temperature. The membrane was washed three times with TBS-T for 5 min. Then, the membrane was incubated in peroxidase-labelled goat $\alpha$-mouse secondary antibody (stored 1:1 in glycerol and diluted 1:5,000 in TBS-T) for 1 h. The membrane was washed again three times in TBS-T for 5 min. The blot was developed with Enhanced Chemoluminescence (ECL) substrate and the signal was detected in a ChemiDoc™ MP System. The blot was then probed with peroxidase-labelled anti-$\beta$-actin antibody (1:30,000 in TBS-T) for 1 h, washed three times in TBS-T for 5 min, and developed.

## 4.5 Time-course measurements

### 4.5.1 Design of the FRET probe

A Förster resonance energy transfer (FRET) probe was designed in order to analyse DNAzyme cleavage kinetics under conditions of submillimolar $Mg^{2+}$ concentrations. The FRET probe T839FRET is identical in sequence to T839. It is labelled with a fluorescein molecule at its 5' end and a Black Hole Quencher-1 (BHQ-1) molecule at its 3' end, respectively. When the fluorophore is excited part of the excitation energy is transferred to the BHQ-1 molecule where it dissipates as heat. Thereby, fluorescence of the donor (fluorescein) is reduced as a function of its distance to the acceptor (BHQ-1). When the two labels are separated due to DNAzyme-mediated RNA cleavage the donor fluorescence increases.

### 4.5.2 Real-time measurements of DNAzyme-mediated RNA cleavage

For real-time measurements of DNAzyme cleavage kinetics 0.8 µM of both T839FRET and Dz839 were incubated together in 50 mM Tris-HCl pH 7.5 with 0.8 mM EDTA and optionally with 0.8 M NaCl. The samples were danatured at 96 °C for 10 min and allowed to cool down to room temperature for 15 min. The use of an initial nucleic acid concentration of 0.8 µM guarantees a nearly complete RNA:DNAzyme complex formation as was determined by electrophoretic mobility shift assays using 4 % agarose gel

electrophoresis (data not shown). Afterwards the sample was diluted 1:4 with 50 mM Tris-HCl pH 7.5. For every reaction 20 µl of the diluted sample were transferred to one well of a 384-well plate and equilibrated at 37 °C for 30 min. In parallel $MgCl_2$ solutions in 50 mM Tris-HCl pH 7.5 were equilibrated at 37 °C in a 96-well plate. With the use of a multichannel pipettor one volume of the respective $MgCl_2$ solution was added to each nucleic acid sample, bringing the final concentration to 0.1 µM RNA:DNAzyme complex, 0.1 mM EDTA and 0.1 to 1 mM $MgCl_2$ in 0.1 mM increments. The presence of 0.1 mM EDTA ensures that potential divalent metal ion contaminations in the samples were sequestered. For each $MgCl_2$ concentration reaction samples with or without 0.1 M NaCl were prepared. All samples were prepared and measured in triplicates. The addition of $MgCl_2$ initiates the reaction, therefore the fluorescence signal was immediately measured in a time-course experiment.

The increase in fluorescence that results from RNA cleavage was monitored with the use of the Tecan Spark 10M microplate reader. The fluorophore was excited at $\lambda_{ex} = 485$ nm and emission was detected at $\lambda_{em} = 530$ nm. Measurements were performed for 10 800 s during which data points were acquired every 30 s.

The data were corrected for a linear decrease in fluorescence intensity with time. This decrease is probably due to a photobleaching effect. The experimental curves were fitted with $F = f_{max}(1 - \exp(-k \cdot t)) + f_{min}$ (where $F$ are the relative fluorescence values, $f_{min}$ and $f_{max}$ are the minimum and maximum values of the experimental curves, $k$ is the apparent rate constant, and $t$ denotes time) using GLE.

### 4.5.3 ATP competition assays

For ATP competition assays the samples were prepared as described in the previous section. The $MgCl_2$ concentration in each sample was set to a constant 0.5 mM. The samples contained a final concentration of 0, 0.2, 0.4, 0.6, 0.8, 1, 1.3 or 2 mM of ATP. The data were acquired with the Tecan Spark 10M microplate reader. Data processing was performed as described in section 4.5.2.

## 4.6 Delivery via virus-like particles

### 4.6.1 Loading of virus-like particles

Virus-like particles were loaded with Dz839(FAM) for microscopic studies and with siRNA or shRNA expression plasmids for knockdown experiments. 50 µg of VP1 capsomers were incubated together with 750 pmol of Dz839(FAM) or 300 pmol siRNA, respectively, or with 5 µg of plasmid DNA in 10 mM Tris-HCl pH 7.5. The samples were dialysed against 10 mM Tris-HCl pH 7.5 with 150 mM NaCl and 2 mM $CaCl_2$ over night

at 4 °C in Slide-A-Lyzer™ MINI Dialysis Devices (ThermoFisher Scientific, Waltham, Massachusetts, USA) with a 14 kDa molecular weight cutoff while constantly stirring at approximately 130 rpm. During this step the capsomers assemble to capsids, encapsulating the respective cargo inside the particles. Those samples were directly used for the treatment of WAC 2 cells. The preparation was carried out by NEUWAY Pharma AG.

### 4.6.2 VLP-mediated delivery of Dz839(FAM) into WAC 2 cells

Virus-like particles were loaded with 750 pmol of the fluorescently labelled DNAzyme Dz839(FAM) as described in the previous section. 100 000 cells/well were seeded on glass cover slips in a 12-well format. After 24 h the WAC 2 cells were treated with the loaded VLPs by adjusting the total volume of the samples to 0.5 ml with OptiMEM medium and adding the mixture directly to the cells. In parallel, cells were transfected with 750 pmol of Dz839(FAM) by using Lipofectamine® 3000. After an additional 24 h the cells were incubated in Wheat Germ Agglutinin Alexa Fluor™ 647 Conjugate (WGA-647) at a working concentration of 5 µg $ml^{-1}$ in PBS for 10 min at 37 °C. Afterwards, the specimens were prepared for microscopy and imaged as described in section 4.4.3.

### 4.6.3 VLP-mediated delivery of siRNA and shRNA expression plasmids into WAC 2 cells

VLPs were loaded with 300 pmol of siRNA or with 5 µg of shRNA expression plasmid as described in section 4.6.1. WAC 2 cells were seeded in a 12-well format at a cell density of 100 000 cells/well. 24 h after seeding the cells were treated with the loaded VLPs. The VLP solution was adjusted to a total volume of 0.5 ml with OptiMEM medium and then added directly to the cells. In parallel, the cells were transfected with 75 pmol of siRNA or 0.5 µg of shRNA expression plasmid by using Lipofectamine® 3000 according to the manufacturer's instructions. 24 h post-transduction cell lysates were prepared as described in section 4.4.4 and the samples were subjected to Western blotting as described in section 4.4.5.

### 4.6.4 Luciferase assay

As a general transduction control, VLP-mediated delivery of a luciferase expression plasmid was carried out. The expression plasmid pGL4.51[*luc2*/CMV/Neo] was used for these experiments. It contains the luciferase reporter gene luc2 from *Photinus pyralis* the expression of which is driven by the cytomegalovirus (CMV) promoter. The plasmid also contains a neomycin resistance cassette which was not relevant for this

work. For the luciferase assay, the Luciferase Assay System kit from Promega (Madison, Wisconsin, USA) was utilized, which contains the luciferase expression plasmid, the substrate, and all buffers.

Loaded VLPs were prepared with 50 µg VP1 pentamers and 25 µg pDNA or with 25 µg VP1 pentamers and 12.5 µg pDNA, respectively, as described in section 4.6.1. WAC 2 cells were seeded at a density of 50 000 cells/well in a 24-well format 24 h before transduction. The cells were transduced by adding the VLP solution directly to the cells after adjusting the total volume to 0.5 ml with OptiMEM medium. As negative controls, 25 µg and 12.5 µg of pDNA were added directly to the media. The cells in one well were also treated with the VLP assembly buffer alone (10 mM Tris-HCl pH 7.5, 150 mM NaCl, and 2 mM $CaCl_2$). As a positive control, the cells in one well were transfected with 0.5 µg of pGL4.51[*luc2*/CMV/Neo] with the use of Lipofectamine® 3000.

After 48 h the cells were washed with 1 ml of PBS and then lysed by adding 200 µl of 1x Lysis buffer (from the Luciferase Assay System kit). The 24-well plate was incubated for 15 min at room temperature with constant agitation at 450 rpm. During this time the luciferase substrate solution was prepared by dissolving the lyophilized Luciferase Assay Substrate (luciferin) in 10 ml of Luciferase Assay Buffer and adding 500 µl of a 1 mM ATP solution. The cell lysates were transferred to 1.5 ml reaction tubes. The samples were vortexed for 5 s and centrifuged for 1 min at 12 000 rcf. Each sample was measured in triplicates: For each triplicate 20 µl of the supernatant were pipetted into one well of a 96-well plate. Afterwards, 100 µl of the substrate solution were added to each well. Bioluminescence was measured in a Tecan Spark 10M microplate reader.

# 4.7 Materials

## 4.7.1 Buffers and solutions

All buffers were prepared with ultrapure water.

| | | |
|---|---|---|
| 10x Tris borate EDTA buffer (TBE) | 890 mM | Tris |
| | 890 mM | Boric acid |
| | 20 mM | EDTA pH 8.0 |
| Tris-Glycine SDS buffer (TGS) | 25 mM | Tris |
| | 192 mM | Glycine |
| | 0.1 % | SDS (w/v) |
| | | pH 8.3 |

| | | |
|---|---|---|
| Towbin buffer for Western blots | 25 mM | Tris |
| | 192 mM | Glycine |
| | 20 % | Methanol (v/v) |
| | | pH 8.3 |
| RIPA buffer | 25 mM | Tris buffer pH 7.5 |
| | 150 mM | NaCl |
| | 0.1 % | SDS (w/v) |
| | 0.5 % | Sodium deoxycholate |
| | 1x | cOmplete Protease |
| | | Inhibitor Cocktail |
| 2x RNA loading buffer | 94 % | Formamide |
| | 25 mM | EDTA pH 8.0 |
| | 0.02 % | Bromophenol blue (w/v) |
| | 0.02 % | Xylene cyanol (w/v) |
| 6x SDS reducing sample buffer | 200 mM | Tris-HCl pH 6.8 |
| | 10 % | SDS (w/v) |
| | 20 % | Glycerol (v/v) |
| | 10 mM | $\beta$-mercaptoethanol |
| | 0.05 % | Bromophenol blue (w/v) |
| *in vitro* transcription buffer | 40 mM | Tris-HCl pH 7.9 |
| | 10 mM | DTT |
| | 10 mM | NaCl |
| | 6 mM | $MgCl_2$ |
| | 2 mM | Spermidine |
| | 1 U $\mu l^{-1}$ | RNase inhibitor |
| Phosphate-buffered saline (PBS) | 137 mM | NaCl |
| | 2.7 mM | KCl |
| | 10 mM | $Na_2HPO_4$ |
| | 1.8 mM | $KH_2PO_4$ |
| | | pH 7.4 |

| | | |
|---|---|---|
| Tris-buffered saline with Tween (TBS-T) | 50 mM | Tris |
| | 150 mM | NaCl |
| | 0.05 % | Tween® 20 |
| | | pH 7.6 |
| VLP assembly buffer | 10 mM | Tris-HCl pH 7.5 |
| | 150 mM | NaCl |
| | 2 mM | $CaCl_2$ |
| Polyacrylamide gel solution (RNA) | 1x | TBE buffer |
| | 7 M | Urea |
| | 5-18 % | Acrylamide/Bisacrylamide stock solution (19:1) (v/v) |
| | 0.1 % | TEMED (v/v) |
| | 1 % | APS (w/v) |
| Polyacrylamide gel solution (protein) | | |
| Stacking gel | 125 mM | Tris-HCl pH 6.8 |
| | 4 % | Acrylamide/Bisacrylamide stock solution (37.5:1) (v/v) |
| | 0.1 % | SDS (w/v) |
| | 1 % | TEMED (v/v) |
| | 0.05 % | APS (w/v) |
| Separating gel | 375 mM | Tris-HCl pH 8.8 |
| | 12 % | Acrylamide/Bisacrylamide stock solution (37.5:1) (v/v) |
| | 0.1 % | SDS (w/v) |
| | 0.5 % | TEMED (v/v) |
| | 0.05 % | APS (w/v) |

### 4.7.2 Chemicals

| | |
|---|---|
| Trizma® (TRIS base) p.a. | Sigma-Aldrich (St. Louis, Missouri, USA) |
| Boric acid, p.a. | AppliChem GmbH (Darmstadt, Germany) |
| EDTA disodium salt | AppliChem GmbH (Darmstadt, Germany) |

| | |
|---|---|
| Tris/Glycine/SDS buffer | Bio-Rad Laboratories (Hercules, California, USA) |
| Tris/Glycine buffer | Bio-Rad Laboratories (Hercules, California, USA) |
| Sodium dodecyl sulfate, granulated, pure | AppliChem GmbH (Darmstadt, Germany) |
| NaCl, p.a. | ThermoFisher Scientific (Waltham, Massachusetts, USA) |
| Sodium deoxycholate | Sigma-Aldrich (St. Louis, Missouri, USA) |
| cOmplete™ Protease Inhibitor Cocktail | Sigma-Aldrich (St. Louis, Missouri, USA) |
| Formamide, p.a. | Honeywell Riedel-de Haën (Seelze, Germany) |
| Bromophenol blue | Janssen Chimica (Beerse, Belgium) |
| Xylene cyanol FF | SERVA Electrophoresis GmbH (Heidelberg, Germany) |
| Glycerol | VWR International GmbH (Langenfeld, Germany) |
| 2-Mercaptoethanol | Carl Roth GmbH + Co. KG (Karlsruhe, Germany) |
| Azide Cy5 RNA T7 Transcription Kit | Jena Bioscience (Jena, Germany) |
| KCl, p.a. | Carl Roth GmbH + Co. KG (Karlsruhe, Germany) |
| Dulbecco's Phosphate-Buffered Saline | Biowest LLC (Riverside, Missouri, USA) |
| Tween® 20 | Sigma-Aldrich (St. Louis, Missouri, USA) |

| | |
|---|---|
| Urea, molecular biology grade | AppliChem GmbH (Darmstadt, Germany) |
| Acrylamide/Bis-acrylamide 40 % solution (Rotiphorese® Gel 40 (19:1)) | Carl Roth GmbH + Co. KG (Karlsruhe, Germany) |
| Acrylamide/Bis-acrylamide 30 % solution (Rotiphorese® Gel 30 (37,5:1)) | Carl Roth GmbH + Co. KG (Karlsruhe, Germany) |
| TEMED, p.a. | Carl Roth GmbH + Co. KG (Karlsruhe, Germany) |
| Ammonium persulfate, p.a. | Carl Roth GmbH + Co. KG (Karlsruhe, Germany) |
| Gibco™ RPMI 1640 Medium | ThermoFisher Scientific (Waltham, Massachusetts, USA) |
| Fetal bovine serum | Sigma-Aldrich (St. Louis, Missouri, USA) |
| Gibco™ Penicillin-Streptomycin (5000 U $ml^{-1}$) | ThermoFisher Scientific (Waltham, Massachusetts, USA) |
| Trypsin-EDTA (0.05 %), phenol red | ThermoFisher Scientific (Waltham, Massachusetts, USA) |
| Triton™ X-100 for molecular biology | Sigma-Aldrich (St. Louis, Missouri, USA) |
| Methanol, p.a. | ThermoFisher Scientific (Waltham, Massachusetts, USA) |
| Roti®-Phenol | Carl Roth GmbH + Co. KG (Karlsruhe, Germany) |
| Chloroform $\geq$ 99 % | Sigma-Aldrich (St. Louis, Missouri, USA) |
| Ethanol, p.a. | Sigma-Aldrich (St. Louis, Missouri, USA) |

| | |
|---|---|
| Saf32 $\alpha$-PrP antibody | IBL international GmbH (Hamburg, Germany) |
| 3F4 $\alpha$-PrP antibody | Merck Millipore (Billerica, Massachusetts, USA) |
| anti-$\beta$-actin antibody, peroxidase-labelled | Sigma-Aldrich (St. Louis, Missouri, USA) |

### 4.7.3 Sequences

**Spiegelzyme and DNAzyme sequences:**

The DNA and RNA oligonucleotides that were used in this work were acquired from Ella Biotech GmbH (Martinsried, Germany) and biomers.net GmbH (Ulm, Germany). The Spiegelzymes and Spiegelzyme substrates were acquired from IBA Lifesciences (Göttingen, Germany). The sequences of the different DNAzymes, Spiegelzymes and the antisense oligodeoxynucleotide ASO824 are:

| | |
|---|---|
| HHRz 1 (L-RNA): | $^{5'}$CCUGGCUGAUGAGGCCGAAAGGCCGAAACUCCU$^{3'}$ |
| HHRz 2 (L-RNA): | $^{5'}$UGGGGCUGAUGAGGCCGAAAGGCCGAAACAAAC$^{3'}$ |
| HHRz 3 (L-RNA): | $^{5'}$GUGGUCUGAUGAGGCCGAAAGGCCGAAACUGUG$^{3'}$ |
| Dz 1 (L-DNA): | $^{5'}$CTGGGAGGCTAGCTACAACGATCCTTC$^{3'}$ |
| Dz 2 (L-DNA): | $^{5'}$GGGGGAGGCTAGCTACAACGAAAACAG$^{3'}$ |
| Dz 3 (L-DNA): | $^{5'}$TGGTGAGGCTAGCTACAACGATGTGTG$^{3'}$ |
| Dz736: | $^{5'}$GGCCCCCCAGGCTAGCTACAACGACACTGCCCC$^{3'}$ |
| Dz736_6/7: | $^{5'}$CCCCCAGGCTAGCTACAACGACACTGCC$^{3'}$ |
| Dz839: | $^{5'}$TTGGGGTAAGGCTAGCTACAACGAGGTGCATGT$^{3'}$ |
| Dz824: | $^{5'}$ATGTTTTCAGGCTAGCTACAACGAGATAGTAAC$^{3'}$ |
| Dz824_10/11: | $^{5'}$CATGTTTTCAGGCTAGCTACAACGAGATAGTAACGG$^{3'}$ |
| Dz824_10/11 scramble: | $^{5'}$ACTTAGATCAGGCTAGCTACAACGATAGTGGTATCG$^{3'}$ |
| ASO824_10/11: | $^{5'}$CATGTTTTCACGATAGTAACGG$^{3'}$ |
| Dz733: | $^{5'}$CCCCCACCAGGCTAGCTACAACGATGCCCCAGC$^{3'}$ |
| Dz2577: | $^{5'}$TACATGAAAGGCTAGCTACAACGAGATTCAGTG$^{3'}$ |

For cell culture experiments, the DNAzymes were modified with two L-dT nucleotides at their 3' ends. Dz839(FAM) is identical in sequence to Dz839 and is labelled with a fluorescein molecule at its 5' end.

**Target RNA sequences:**

RNA substrates are labelled with a fluorescein molecule at their 5' end. T839FRET is labelled with a fluorescein molecule at its 5' end and a BHQ-1 molecule at its 3' end, respectively. The sequences of the different RNA substrates are:

Target 1 (D- or L-RNA): $^{5'}$GAAGGAGUCCCAGG$^{3'}$
Target 2 (D- or L-RNA): $^{5'}$CUGUUUGUCCCCCA$^{3'}$
Target 3 (D- or L-RNA): $^{5'}$CACACAGUCACCAC$^{3'}$
T736: $^{5'}$GCUGGGGCAGUGGUGGGGGGCCUUG$^{3'}$
T839: $^{5'}$AAAACAUGCACCGUUACCCCAACCA$^{3'}$
T839FRET: $^{5'}$ACAUGCACCGUUACCCCAA$^{3'}$
T824: $^{5'}$ACCGUUACUAUCGUGAAAACAUGCA$^{3'}$
T733: $^{5'}$GCAGCUGGGGCAGUGGUGGGGGGCC$^{3'}$

**siRNA sequences:**

Pre-annealed siRNAs that were used for cell culture experiments were acquired from QIAGEN GmbH (Hilden, Germany). The sequences for these siRNAs are denoted with $+$ for sense and $-$ for antisense strands:

siRNA736 $+$: $^{5'}$GGGGCAGUGGUGGGGGGCCTT$^{3'}$
$-$: $^{5'}$GGCCCCCCACCACUGCCCCAG$^{3'}$
siRNA839 $+$: $^{5'}$ACAUGCACCGUUACCCCAATT$^{3'}$
$-$: $^{5'}$UUGGGGUAACGGUGCAUGUTT$^{3'}$
siRNA2577 $+$: $^{5'}$GAAUCGUUUCAUGUAAGAATT$^{3'}$
$-$: $^{5'}$UUCUUACAUGAAACGAUUCAG$^{3'}$

**shRNA sequences:**

The shRNA constructs used in this work were designed using the BLOCK-iT™ RNAi Designer (ThermoFisher Scientific, Waltham, Massachusetts, USA). The expression plasmids were produced by annealing and cloning the following sequences into the pENTR™ U6 vector using the BLOCK-iT™ U6 RNAi Entry Vector Kit (ThermoFisher Scientific) according to the manufacturer's instructions:

shRNA1042 (top):
$^{5'}$CACCGCCTATTACCAGAGAGGATCG
CGAACGATCCTCTCTGGTAATAGGC$^{3'}$
shRNA1042 (bottom):
$^{5'}$AAAAGCCTATTACCAGAGAGGATCG
TTCGCGATCCTCTCTGGTAATAGGC$^{3'}$

shRNA1416 (top):
$^{5'}$CACCGGACTTAGTGCAACAGGTTGA
CGAATCAACCTGTTGCACTAAGTCC$^{3'}$
shRNA1416 (bottom):
$^{5'}$AAAAGGACTTAGTGCAACAGGTTGA
TTCGTCAACCTGTTGCACTAAGTCC$^{3'}$

shRNAlacZ (top):
$^{5'}$CACCGCTACACAAATCAGCGAT
TTCGAAAAATCGCTGATTTGTGTAG$^{3'}$
shRNAlacZ (bottom):
$^{5'}$AAAACTACACAAATCAGCGATT
TTTCGAAATCGCTGATTTGTGTAGC$^{3'}$

Transient expression in cells produces the respective shRNA molecules that are complementary and antiparallel to the bottom strand. Expression is driven by a U6 pol III type promoter. The plasmid sequence and map are shown in the following section for the pENTR™ U6 vector containing the shRNA1042 construct. The vectors for shRNA1416 and shRNAlacZ only differ in the sequence of the insert. For reasons of clarity only the U6 promoter, the insert for shRNA expression, the origin of replication (ori), and the kanamycin resistance gene (KanR, codes for aminoglycoside phosphotransferase), which was used for cloning, are shown in the map.

pENTR/U6 + shRNA1042 plasmid sequence:

```
   1 CTTTCCTGCG TTATCCCCTG ATTCTGTGGA TAACCGTATT ACCGCCTTTG AGTGAGCTGA TACCGCTCGC
  71 CGCAGCCGAA CGACCGAGCG CAGCGAGTCA GTGAGCGAGG AAGCGGAAGA GCGCCCAATA CGCAAACCGC
 141 CTCTCCCCGC GCGTTGGCCG ATTCATTAAT GCAGCTGGCA CGACAGGTTT CCCGACTGGA AAGCGGGCAG
 211 TGAGCGCAAC GCAATTAATA CGCGTACCGC TAGCCAGGAA GAGTTTGTAG AAACGCAAAA AGGCCATCCG
 281 TCAGGATGGC CTTCTGCTTA GTTTGATGCC TGGCAGTTTA TGGCGGGCGT CCTGCCCGCC ACCCTCCGGG
 351 CCGTTGCTTC ACAACGTTCA AATCCGCTCC CGGCGGATTT GTCCTACTCA GGAGAGCGTT CACCGACAAA
 421 CAACAGATAA AACGAAAGGC CCAGTCTTCC GACTGAGCCT TTCGTTTTAT TTGATGCCTG GCAGTTCCCT
 491 ACTCTCGCGT TAACGCTAGC ATGGATGTTT TCCCAGTCAC GACGTTGTAA AACGACGGCC AGTCTTAAGC
 561 TCGGGCCCCA AATAATGATT TTATTTTGAC TGATAGTGAC CTGTTCGTTG CAACAAATTG ATGAGCAATG
 631 CTTTTTTATA ATGCCAACTT TGTACAAAAA AGCAGGCTTT AAAGGAACCA ATTCAGTCGA CTGGATCCGG
 701 TACCAAGGTC GGGCAGGAAG AGGGCCTATT TCCCATGATT CCTTCATATT TGCATATACG ATACAAGGCT
 771 GTTAGAGAGA TAATTAGAAT TAATTTGACT GTAAACACAA AGATATTAGT ACAAAATACG TGACGTAGAA
 841 AGTAATAATT TCTTGGGTAG TTTGCAGTTT TAAAATTATG TTTTAAAATG GACTATCATA TGCTTACCGT
 911 AACTTGAAAG TATTTCGATT TCTTGGCTTT ATATATCTTG TGGAAAGGAC GAAACACCGC CTATTACCAG
 981 AGAGGATCGC GAACGATCCT CTCTGGTAAT AGGCTTTTTT CTAGACCCAG CTTTCTTGTA CAAAGTTGGC
1051 ATTATAAGAA AGCATTGCTT ATCAATTTGT TGCAACGAAC AGGTCACTAT CAGTCAAAAT AAAATCATTA
1121 TTTGCCATCC AGCTGATATC CCCTATAGTG AGTCGTATTA CATGGTCATA GCTGTTTCCT GGCAGCTCTG
1191 GCCCGTGTCT CAAAATCTCT GATGTTACAT TGCACAAGAT AAAAATATAT CATCATGAAC AATAAAACTG
1261 TCTGCTTACA TAAACAGTAA TACAAGGGGT GTTATGAGCC ATATTCAACG GGAAACGTCG AGGCCGCGAT
1331 TAAATTCCAA CATGGATGCT GATTTATATG GGTATAAATG GGCTCGCGAT AATGTCGGGC AATCAGGTGC
1401 GACAATCTAT CGCTTGTATG GGAAGCCCGA TGCGCCAGAG TTGTTTCTGA AACATGGCAA AGGTAGCGTT
1471 GCCAATGATG TTACAGATGA GATGGTCAGA CTAAACTGGC TGACGGAATT TATGCCTCTT CCGACCATCA
1541 AGCATTTTAT CCGTACTCCT GATGATGCAT GGTTACTCAC CACTGCGATC CCCGGAAAAA CAGCATTCCA
1611 GGTATTAGAA GAATATCCTG ATTCAGGTGA AAATATTGTT GATGCGCTGG CAGTGTTCCT GCGCCGGTTG
1681 CATTCGATTC CTGTTTGTAA TTGTCCTTTT AACAGCGATC GCGTATTTCG TCTCGCTCAG GCGCAATCAC
1751 GAATGAATAA CGGTTTGGTT GATGCGAGTG ATTTTGATGA CGAGCGTAAT GGCTGGCCTG TTGAACAAGT
1821 CTGGAAAGAA ATGCATAAAC TTTTGCCATT CTCACCGGAT TCAGTCGTCA CTCATGGTGA TTTCTCACTT
1891 GATAACCTTA TTTTTGACGA GGGGAAATTA ATAGGTTGTA TTGATGTTGG ACGAGTCGGA ATCGCAGACC
1961 GATACCAGGA TCTTGCCATC CTATGGAACT GCCTCGGTGA GTTTTCTCCT TCATTACAGA AACGGCTTTT
2031 TCAAAAATAT GGTATTGATA ATCCTGATAT GAATAAATTG CAGTTTCATT TGATGCTCGA TGAGTTTTTC
2101 TAATCAGAAT TGGTTAATTG GTTGTAACAC TGGCAGAGCA TTACGCTGAC TTGACGGGAC GGCGCAAGCT
2171 CATGACCAAA ATCCCTTAAC GTGAGTTACG CGTCGTTCCA CTGAGCGTCA GACCCCGTAG AAAAGATCAA
2241 AGGATCTTCT TGAGATCCTT TTTTTCTGCG CGTAATCTGC TGCTTGCAAA CAAAAAAACC ACCGCTACCA
2311 GCGGTGGTTT GTTTGCCGGA TCAAGAGCTA CCAACTCTTT TTCCGAAGGT AACTGGCTTC AGCAGAGCGC
2381 AGATACCAAA TACTGTCCTT CTAGTGTAGC CGTAGTTAGG CCACCACTTC AAGAACTCTG TAGCACCGCC
2451 TACATACCTC GCTCTGCTAA TCCTGTTACC AGTGGCTGCT GCCAGTGGCG ATAAGTCGTG TCTTACCGGG
2521 TTGGACTCAA GACGATAGTT ACCGGATAAG GCGCAGCGGT CGGGCTGAAC GGGGGGTTCG TGCACACAGC
2591 CCAGCTTGGA GCGAACGACC TACACCGAAC TGAGATACCT ACAGCGTGAG CATTGAGAAA GCGCCACGCT
2661 TCCCGAAGGG AGAAAGGCGG ACAGGTATCC GGTAAGCGGC AGGGTCGGAA CAGGAGAGCG CACGAGGGAG
2731 CTTCCAGGGG GAAACGCCTG GTATCTTTAT AGTCCTGTCG GGTTTCGCCA CCTCTGACTT GAGCGTCGAT
2801 TTTTGTGATG CTCGTCAGGG GGGCGGAGCC TATGGAAAAA CGCCAGCAAC GCGGCCTTTT TACGGTTCCT
2871 GGCCTTTTGC TGGCCTTTTG CTCACATGTT
```

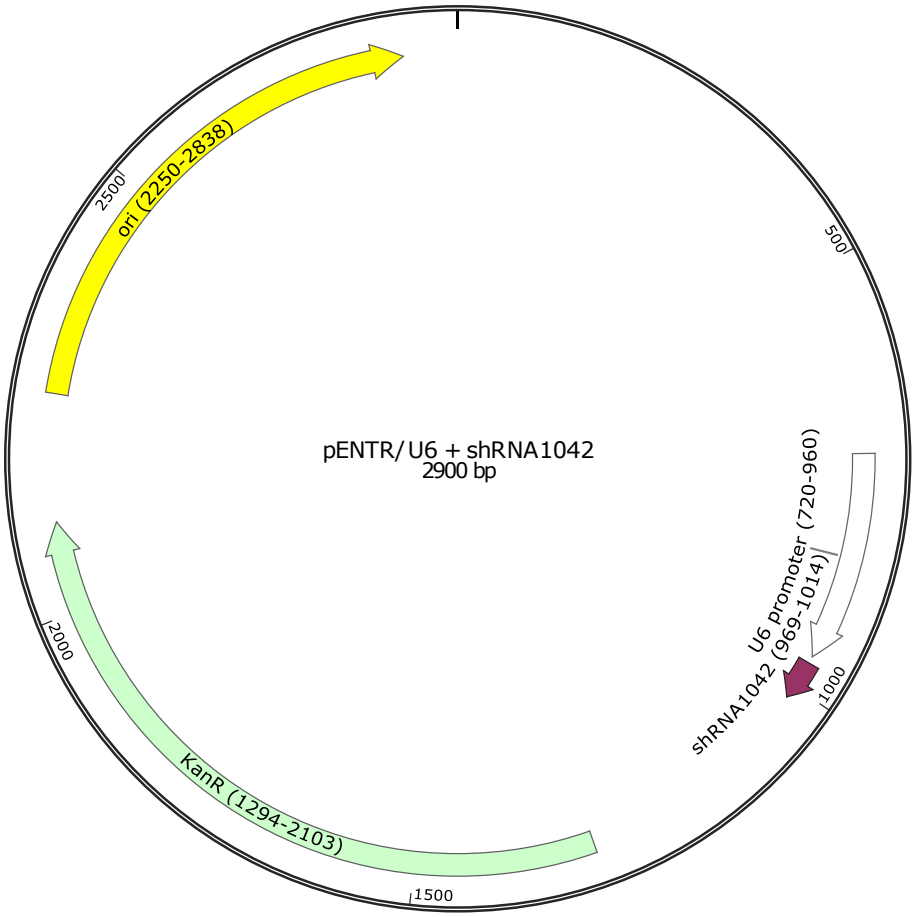


**Figure 4.1 – Vector map of pENTR/U6 + shRNA1042.** Only relevant features are displayed. ori = origin of replication (high-copy-number pUC); KanR = kanamycin resistance cassette, codes for aminoglycoside phosphotransferase

For *in vitro* transcription experiments the pET11a vector containing the human PrP amino acid 23-230 coding sequence was used as a template. The plasmid map only shows relevant features.

pET11a + huPrP23-230 CDS plasmid sequence:

```
   1 TATGAAGAAG CGCCCGAAGC CTGGAGGATG GAACACTGGG GGCAGCCGAT ACCCGGGGCA GGGCAGCCCT
  71 GGAGGCAACC GCTACCCACC TCAGGGCGGT GGTGGCTGGG GGCAGCCTCA TGGTGGTGGC TGGGGGCAGC
 141 CTCATGGTGG TGGCTGGGGG CAGCCCCATG GTGGTGGCTG GGGACAGCCT CATGGTGGTG GCTGGGGTCA
 211 AGGAGGTGGC ACCCACAGTC AGTGGAACAA GCCGAGTAAG CCAAAAACCA ACATGAAGCA CATGGCTGGT
 281 GCTGCAGCAG CTGGGGCAGT GGTGGGGGGC CTTGGCGGCT ACATGCTGGG AAGTGCCATG AGCAGGCCCA
 351 TCATACATTT CGGCAGTGAC TATGAGGACC GTTACTATCG TGAAAACATG CACCGTTACC CCAACCAAGT
 421 GTACTACAGG CCCATGGATG AGTACAGCAA CCAGAACAAC TTTGTGCACG ACTGCGTCAA TATCACAATC
 491 AAGCAGCACA CGGTCACCAC AACCACCAAG GGGGAGAACT TCACCGAGAC CGACGTTAAG ATGATGGAGC
 561 GCGTGGTTGA GCAGATGTGT ATCACCCAGT ACGAGAGGGA ATCTCAGGCC TATTACCAGA GAGGATCGTG
 631 ATAAGGATCC GGCTGCTAAC AAAGCCCGAA AGGAAGCTGA GTTGGCTGCT GCCACCGCTG AGCAATAACT
 701 AGCATAACCC CTTGGGGCCT CTAAACGGGT CTTGAGGGGT TTTTTGCTGA AAGGAGGAAC TATATCCGGA
 771 TATCCCGCAA GAGGCCCGGC AGTACCGGCA TAACCAAGCC TATGCCTACA GCATCCAGGG TGACGGTGCC
```

```
 841 GAGGATGACG ATGAGCGCAT TGTTAGATTT CATACACGGT GCCTGACTGC GTTAGCAATT TAACTGTGAT
 911 AAACTACCGC ATTAAAGCTT ATCGATGATA AGCTGTCAAA CATGAGAATT CTTGAAGACG AAAGGGCCTC
 981 GTGATACGCC TATTTTTATA GGTTAATGTC ATGATAATAA TGGTTTCTTA GACGTCAGGT GGCACTTTTC
1051 GGGGAAATGT GCGCGGAACC CCTATTTGTT TATTTTTCTA AATACATTCA AATATGTATC CGCTCATGAG
1121 ACAATAACCC TGATAAATGC TTCAATAATA TTGAAAAAGG AAGAGTATGA GTATTCAACA TTTCCGTGTC
1191 GCCCTTATTC CCTTTTTTGC GGCATTTTGC CTTCCTGTTT TTGCTCACCC AGAAACGCTG GTGAAAGTAA
1261 AAGATGCTGA AGATCAGTTG GGTGCACGAG TGGGTTACAT CGAACTGGAT CTCAACAGCG GTAAGATCCT
1331 TGAGAGTTTT CGCCCCGAAG AACGTTTTCC AATGATGAGC ACTTTTAAAG TTCTGCTATG TGGCGCGGTA
1401 TTATCCCGTG TTGACGCCGG GCAAGAGCAA CTCGGTCGCC GCATACACTA TTCTCAGAAT GACTTGGTTG
1471 AGTACTCACC AGTCACAGAA AAGCATCTTA CGGATGGCAT GACAGTAAGA GAATTATGCA GTGCTGCCAT
1541 AACCATGAGT GATAACACTG CGGCCAACTT ACTTCTGACA ACGATCGGAG GACCGAAGGA GCTAACCGCT
1611 TTTTTGCACA ACATGGGGGA TCATGTAACT CGCCTTGATC GTTGGGAACC GGAGCTGAAT GAAGCCATAC
1681 CAAACGACGA GCGTGACACC ACGATGCCTG CAGCAATGGC AACAACGTTG CGCAAACTAT TAACTGGCGA
1751 ACTACTTACT CTAGCTTCCC GGCAACAATT AATAGACTGG ATGGAGGCGG ATAAAGTTGC AGGACCACTT
1821 CTGCGCTCGG CCCTTCCGGC TGGCTGGTTT ATTGCTGATA AATCTGGAGC CGGTGAGCGT GGGTCTCGCG
1891 GTATCATTGC AGCACTGGGG CCAGATGGTA AGCCCTCCCG TATCGTAGTT ATCTACACGA CGGGGAGTCA
1961 GGCAACTATG GATGAACGAA ATAGACAGAT CGCTGAGATA GGTGCCTCAC TGATTAAGCA TTGGTAACTG
2031 TCAGACCAAG TTTACTCATA TATACTTTAG ATTGATTTAA AACTTCATTT TTAATTTAAA AGGATCTAGG
2101 TGAAGATCCT TTTTGATAAT CTCATGACCA AAATCCCTTA ACGTGAGTTT TCGTTCCACT GAGCGTCAGA
2171 CCCCGTAGAA AAGATCAAAG GATCTTCTTG AGATCCTTTT TTTCTGCGCG TAATCTGCTG CTTGCAAACA
2241 AAAAAACCAC CGCTACCAGC GGTGGTTTGT TTGCCGGATC AAGAGCTACC AACTCTTTTT CCGAAGGTAA
2311 CTGGCTTCAG CAGAGCGCAG ATACCAAATA CTGTCCTTCT AGTGTAGCCG TAGTTAGGCC ACCACTTCAA
2381 GAACTCTGTA GCACCGCCTA CATACCTCGC TCTGCTAATC CTGTTACCAG TGGCTGCTGC CAGTGGCGAT
2451 AAGTCGTGTC TTACCGGGTT GGACTCAAGA CGATAGTTAC CGGATAAGGC GCAGCGGTCG GGCTGAACGG
2521 GGGGTTCGTG CACACAGCCC AGCTTGGAGC GAACGACCTA CACCGAACTG AGATACCTAC AGCGTGAGCT
2591 ATGAGAAAGC GCCACGCTTC CCGAAGGGAG AAAGGCGGAC AGGTATCCGG TAAGCGGCAG GGTCGGAACA
2661 GGAGAGCGCA CGAGGGAGCT TCCAGGGGGA AACGCCTGGT ATCTTTATAG TCCTGTCGGG TTTCGCCACC
2731 TCTGACTTGA GCGTCGATTT TTGTGATGCT CGTCAGGGGG GCGGAGCCTA TGGAAAAACG CCAGCAACGC
2801 GGCCTTTTTA CGGTTCCTGG CCTTTTGCTG GCCTTTTGCT CACATGTTCT TTCCTGCGTT ATCCCCTGAT
2871 TCTGTGGATA ACCGTATTAC CGCCTTTGAG TGAGCTGATA CCGCTCGCCG CAGCCGAACG ACCGAGCGCA
2941 GCGAGTCAGT GAGCGAGGAA GCGGAAGAGC GCCTGATGCG GTATTTTCTC CTTACGCATC TGTGCGGTAT
3011 TTCACACCGC ATATATGGTG CACTCTCAGT ACAATCTGCT CTGATGCCGC ATAGTTAAGC CAGTATACAC
3081 TCCGCTATCG CTACGTGACT GGGTCATGGC TGCGCCCCGA CACCCGCCAA CACCCGCTGA CGCGCCCTGA
3151 CGGGCTTGTC TGCTCCCGGC ATCCGCTTAC AGACAAGCTG TGACCGTCTC CGGGAGCTGC ATGTGTCAGA
3221 GGTTTTCACC GTCATCACCG AAACGCGCGA GGCAGCTGCG GTAAAGCTCA TCAGCGTGGT CGTGAAGCGA
3291 TTCACAGATG TCTGCCTGTT CATCCGCGTC CAGCTCGTTG AGTTTCTCCA GAAGCGTTAA TGTCTGGCTT
3361 CTGATAAAGC GGGCCATGTT AAGGGCGGTT TTTTCCTGTT TGGTCACTGA TGCCTCCGTG TAAGGGGGAT
3431 TTCTGTTCAT GGGGGTAATG ATACCGATGA AACGAGAGAG GATGCTCACG ATACGGGTTA CTGATGATGA
3501 ACATGCCCGG TTACTGGAAC GTTGTGAGGG TAAACAACTG GCGGTATGGA TGCGGCGGGA CCAGAGAAAA
3571 ATCACTCAGG GTCAATGCCA GCGCTTCGTT AATACAGATG TAGGTGTTCC ACAGGGTAGC CAGCAGCATC
3641 CTGCGATGCA GATCCGGAAC ATAATGGTGC AGGGCGCTGA CTTCCGCGTT TCCAGACTTT ACGAAACACG
3711 GAAACCGAAG ACCATTCATG TTGTTGCTCA GGTCGCAGAC GTTTTGCAGC AGCAGTCGCT TCACGTTCGC
3781 TCGCGTATCG GTGATTCATT CTGCTAACCA GTAAGGCAAC CCCGCCAGCC TAGCCGGGTC CTCAACGACA
3851 GGAGCACGAT CATGCGCACC CGTGGCCAGG ACCCAACGCT GCCCGAGATG CGCCGCGTGC GGCTGCTGGA
3921 GATGGCGGAC GCGATGGATA TGTTCTGCCA AGGGTTGGTT TGCGCATTCA CAGTTCTCCG CAAGAATTGA
3991 TTGGCTCCAA TTCTTGGAGT GGTGAATCCG TTAGCGAGGT GCCGCCGGCT TCCATTCAGG TCGAGGTGGC
4061 CCGGCTCCAT GCACCGCGAC GCAACGCGGG GAGGCAGACA AGGTATAGGG CGGCGCCTAC AATCCATGCC
```

```
4131 AACCCGTTCC ATGTGCTCGC CGAGGCGGCA TAAATCGCCG TGACGATCAG CGGTCCAGTG ATCGAAGTTA
4201 GGCTGGTAAG AGCCGCGAGC GATCCTTGAA GCTGTCCCTG ATGGTCGTCA TCTACCTGCC TGGACAGCAT
4271 GGCCTGCAAC GCGGGCATCC CGATGCCGCC GGAAGCGAGA AGAATCATAA TGGGGAAGGC CATCCAGCCT
4341 CGCGTCGCGA ACGCCAGCAA GACGTAGCCC AGCGCGTCGG CCGCCATGCC GGCGATAATG GCCTGCTTCT
4411 CGCCGAAACG TTTGGTGGCG GGACCAGTGA CGAAGGCTTG AGCGAGGGCG TGCAAGATTC CGAATACCGC
4481 AAGCGACAGG CCGATCATCG TCGCGCTCCA GCGAAAGCGG TCCTCGCCGA AAATGACCCA GAGCGCTGCC
4551 GGCACCTGTC CTACGAGTTG CATGATAAAG AAGACAGTCA TAAGTGCGGC GACGATAGTC ATGCCCCGCG
4621 CCCACCGGAA GGAGCTGACT GGGTTGAAGG CTCTCAAGGG CATCGGTCGA GATCCCGGTG CCTAATGAGT
4691 GAGCTAACTT ACATTAATTG CGTTGCGCTC ACTGCCCGCT TTCCAGTCGG GAAACCTGTC GTGCCAGCTG
4761 CATTAATGAA TCGGCCAACG CGCGGGGAGA GGCGGTTTGC GTATTGGGCG CCAGGGTGGT TTTTCTTTTC
4831 ACCAGTGAGA CGGGCAACAG CTGATTGCCC TTCACCGCCT GGCCCTGAGA GAGTTGCAGC AAGCGGTCCA
4901 CGCTGGTTTG CCCCAGCAGG CGAAAATCCT GTTTGATGGT GGTTAACGGC GGGATATAAC ATGAGCTGTC
4971 TTCGGTATCG TCGTATCCCA CTACCGAGAT ATCCGCACCA ACGCGCAGCC CGGACTCGGT AATGGCGCGC
5041 ATTGCGCCCA GCGCCATCTG ATCGTTGGCA ACCAGCATCG CAGTGGGAAC GATGCCCTCA TTCAGCATTT
5111 GCATGGTTTG TTGAAAACCG GACATGGCAC TCCAGTCGCC TTCCCGTTCC GCTATCGGCT GAATTTGATT
5181 GCGAGTGAGA TATTTATGCC AGCCAGCCAG ACGCAGACGC GCCGAGACAG AACTTAATGG GCCCGCTAAC
5251 AGCGCGATTT GCTGGTGACC CAATGCGACC AGATGCTCCA CGCCCAGTCG CGTACCGTCT TCATGGGAGA
5321 AAATAATACT GTTGATGGGT GTCTGGTCAG AGACATCAAG AAATAACGCC GGAACATTAG TGCAGGCAGC
5391 TTCCACAGCA ATGGCATCCT GGTCATCCAG CGGATAGTTA ATGATCAGCC CACTGACGCG TTGCGCGAGA
5461 AGATTGTGCA CCGCCGCTTT ACAGGCTTCG ACGCCGCTTC GTTCTACCAT CGACACCACC ACGCTGGCAC
5531 CCAGTTGATC GGCGCGAGAT TTAATCGCCG CGACAATTTG CGACGGCGCG TGCAGGGCCA GACTGGAGGT
5601 GGCAACGCCA ATCAGCAACG ACTGTTTGCC CGCCAGTTGT TGTGCCACGC GGTTGGGAAT GTAATTCAGC
5671 TCCGCCATCG CCGCTTCCAC TTTTTCCCGC GTTTTCGCAG AAACGTGGCT GGCCTGGTTC ACCACGCGGG
5741 AAACGGTCTG ATAAGAGACA CCGGCATACT CTGCGACATC GTATAACGTT ACTGGTTTCA CATTCACCAC
5811 CCTGAATTGA CTCTCTTCCG GGCGCTATCA TGCCATACCG CGAAAGGTTT TGCGCCATTC GATGGTGTCC
5881 GGGATCTCGA CGCTCTCCCT TATGCGACTC CTGCATTAGG AAGCAGCCCA GTAGTAGGTT GAGGCCGTTG
5951 AGCACCGCCG CCGCAAGGAA TGGTGCATGC AAGGAGATGG CGCCCAACAG TCCCCCGGCC ACGGGGCCTG
6021 CCACCATACC CACGCCGAAA CAAGCGCTCA TGAGCCCGAA GTGGCGAGCC CGATCTTCCC CATCGGTGAT
6091 GTCGGCGATA TAGGCGCCAG CAACCGCACC TGTGGCGCCG GTGATGCCGG CCACGATGCG TCCGGCGTAG
6161 AGGATCGAGA TCTCGATCCC GCGAAATTAA TACGACTCAC TATAGGGGAA TTGTGAGCGG ATAACAATTC
6231 CCCTCTAGAA ATAATTTTGT TTAACTTTAA GAAGGAGATA TACA
```

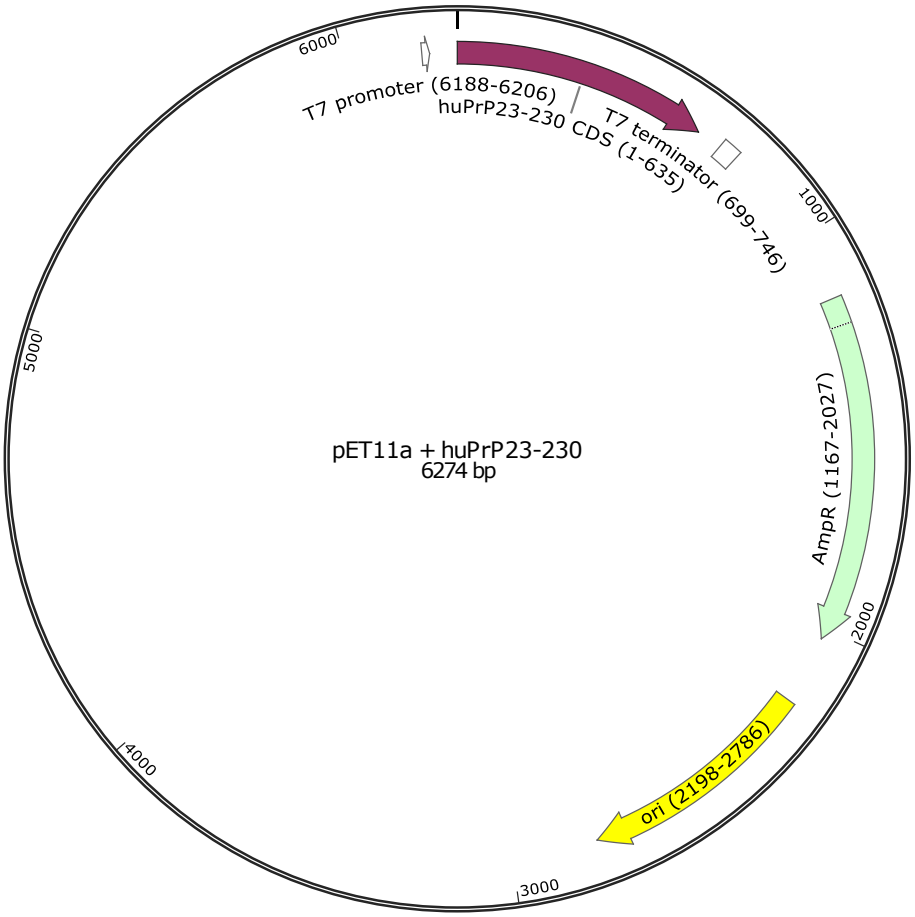


**Figure 4.2 – Vector map of pET11a + huPrP23-230 CDS.** Only relevant features are displayed. ori = origin of replication (high-copy-number pBR322); AmpR = ampicillin resistance cassette, codes for $\beta$-lactamase

## 4.8 Equipment and consumables

| | |
|---|---|
| ChemiDoc™ MP System | Bio-Rad Laboratories (Hercules, California, USA) |
| Spark® 10M microplate reader | Tecan Group AG (Männedorf, Switzerland) |
| Leica TCS SP5 confocal microscope | Leica Microsystems (Wetzlar, Germany) |
| Thermomixer comfort | Eppendorf AG (Hamburg, Germany) |
| Mini-PROTEAN® Tetra Vertical Electrophoresis Cell | Bio-Rad Laboratories (Hercules, California, USA) |

| | |
|---|---|
| Mini Trans-Blot® Cell | Bio-Rad Laboratories (Hercules, California, USA) |
| EPS 3501 XL Electrophoresis Power Supply | Amersham Pharmacia (Little Chalfont, United Kingdom) |
| PowerPac™ Basic Power Supply | Bio-Rad Laboratories (Hercules, California, USA) |
| 5415 R Microcentrifuge | Eppendorf AG (Hamburg, Germany) |
| Biosphere® SafeSeal Tube 1.5 ml | Sarstedt AG & Co (Nümbrecht, Germany) |
| Biosphere® Filter pipette tips | Sarstedt AG & Co (Nümbrecht, Germany) |
| Cell scraper 16 cm | Sarstedt AG & Co (Nümbrecht, Germany) |
| Disposable serological pipettes | Sarstedt AG & Co (Nümbrecht, Germany) |
| Falcon® 24 Multiwell Cell Culture Plates | Corning (New York, USA) |
| TC Flask T75, with ventilation cap | Sarstedt AG & Co (Nümbrecht, Germany) |
| Microplate 384-well (non-binding, flat bottom, black) | Greiner Bio-One GmbH (Essen, Germany) |
| Menzel™ square glass coverslips, 12 mm | ThermoFisher Scientific (Waltham, Massachusetts, USA) |
| Microscope slides (ground edges, frosted) | VWR International GmbH (Langenfeld, Germany) |
| Slide-A-Lyzer™ MINI Dialysis Device (7 kDa MWCO) | ThermoFisher Scientific (Waltham, Massachusetts, USA) |

| | |
|---|---|
| Hettich EBA 12 Centrifuge | Hettich Lab Technology (Tuttlingen, Germany) |
| $CO_2$ incubator | Binder GmbH (Tuttlingen, Germany) |
| Conical centrifuge tubes, 15 and 50 ml (Polypropylene) | Sarstedt AG & Co (Nümbrecht, Germany) |

# List of Figures

# List of abbreviations

| | | |
|---|---|---|
| 5-HT | — | 5-hydroxytryptamine |
| AD | — | Alzheimer's disease |
| AS-ODN | — | Antisense oligodeoxynucleotide |
| CDP | — | Chronic demyelinating polyneuropathy |
| CJD | — | Creutzfeldt-Jakob disease |
| CuAAC | — | Copper(I)-catalyzed azide-alkyne cycloaddition |
| fCJD | — | familial Creutzfeldt-Jakob disease |
| iCJD | — | iatrogenic Creutzfeldt-Jakob disease |
| sCJD | — | sporadic Creutzfeldt-Jakob disease |
| vCJD | — | variant Creutzfeldt-Jakob disease |
| CMV | — | Cytomegalovirus |
| CNS | — | Central nervous system |
| CPP | — | Cell-penetrating peptide |
| DABCO | — | 1,4-diazabicyclo-(2,2,2)octan |
| DAPI | — | 4',6-diamidino-2-phenylindole |
| DNA | — | Deoxyribonucleic acid |
| GSS | — | Gerstmann-Sträussler-Scheinker syndrome |
| FFI | — | Fatal familial insomnia |
| BSE | — | bovine spongiform encephalopathy |
| CDS | — | Coding sequence |
| CWD | — | Chronic wasting disease |
| dsDNA | — | Double-stranded deoxribonucleic acid |
| dsRNA | — | Double-stranded ribonucleic acid |
| DTT | — | Dithiothreitol |
| ECM | — | Extracellular matrix |
| EDTA | — | Ethylenediaminetetraacetic acid |
| Egr-1 | — | Early growth response factor-1 |
| EGTA | — | ethylene glycol-bis($\beta$-aminoethyl ether)-N,N,N',N'-tetraacetic acid |
| FFI | — | Fatal familial insomnia |
| FRET | — | Förster radius energy transfer |
| GATA3 | — | Transcription factor GATA3 |
| GLE | — | Graphics Layout Engine |
| GPI | — | Glycosyl-phosphatidylinositol |
| IV | — | Intravenous |
| IVT | — | *in vitro* transcription |
| JCV | — | John Cunningham virus |

| | | |
|---|---|---|
| LSM | — | Laser scanning microscopy |
| LSTc | — | Lactoseries tetrasaccharide c |
| Tat | — | Trans-activator of transcription |
| $T_h2$ | — | Type 2 helper T cell |
| Tris | — | Tris(hydroxymethyl)-aminomethan |
| TSE | — | Transmissible spongiform encephalopathy |
| (L)ADME | — | (Liberation), absorption, distribution, metabolism, excretion |
| LNA | — | Locked nucleic acid |
| ORF | — | Open reading frame |
| PAGE | — | Polyacrylamide gel electrophoresis |
| PBS | — | Phosphate-buffered saline |
| PEG | — | Polyethylene glycol |
| PCR | — | Polymerase chain reaction |
| PPS | — | Pentosan polyphosphate |
| PML | — | Progressive multifocal leukoencephalopathy |
| PTGS | — | Post-transcriptional gene silencing |
| PVDF | — | Polyvinylidene fluoride |
| RNA | — | Ribonucleic acid |
| RNAi | — | RNA interference |
| RVG | — | Rabies virus glycoprotein |
| scFv | — | Single-chain variable fragment |
| SELEX | — | Systematic evolution of ligands by exponential enrichment |
| siRNA | — | Small interfering ribonucleic acid |
| shRNA | — | Short hairpin ribonucleic acid |
| ssDNA | — | Single-stranded deoxyribonucleic acid |
| ssRNA | — | Single-stranded ribonucleic acid |
| SMC | — | Smooth muscle cell |
| SNALP | — | Stable nucleic acid lipid particle |
| SPAAC | — | Strain-promoted azide-alkyne cycloaddition |
| miRNA | — | microRNA |
| mRNA | — | Messenger ribonucleic acid |
| nt | — | Nucleotide(s) |
| VLP | — | Virus-like particle |
| WGA | — | Wheat germ agglutinin |

# Nucleotide ambiguity code

In this work nucleotides and nucleosides are denoted by the symbols recommended by the Nomenclature Committee of the International Union of Pure and Applied Chemistry - International Union of Biochemistry (IUPAC-IUB). Although not all symbols are used throughout the work the entire nucleotide ambiguity code is included for reasons of completeness. Also, the ribonucleotide uridine is present in the list for the sake of clarity although the original recommendations only comprised deoxyribonucleotides. The symbols can refer to either nucleosides, nucleotides or nucleobases which will be clear from the text.

**Table 4.2** – Nucleotide ambiguity code

| Code | Nucleobase | Complement |
|---|---|---|
| A | Adenine | T or U |
| G | Guanine | C |
| C | Cytosine | G |
| T | Thymine | A |
| U | Uracil | U |
| R | Purine (A or G) | Y |
| Y | Pyrimidine (C or T or U) | R |
| W | Weak pairing (A or T or U) | W |
| S | Strong pairing (G or C) | S |
| K | Keto (T or G) | M |
| M | Amino (C or A) | K |
| H | Not G | D |
| D | Not C | H |
| V | Not T | B |
| B | Not A | V |
| N | Any | N |

# Danksagung

Mein Dank gilt Herrn Professor Riesner, der mir als Mentor die Anfertigung dieser Arbeit ermöglichte, für seinen unermüdlichen Einsatz und die wissenschaftlichen Freiheiten, die er mir gewährte. Ich danke Gerhard Steger, der mich stets mit Rat und Tat unterstützte und seinem Sohn Matthias für die Hilfe mit PYTHON. Prof. Dieter Willbold möchte ich dafür danken, dass ich die Arbeiten an diesem Thema in seiner Arbeitsgruppe durchführen durfte. Außerdem danke ich Prof. Volker Erdmann, der leider inzwischen verstorben ist. Er war es, dessen ursprüngliche Idee meine Arbeit überhaupt erst möglich gemacht hat.
Mein besonderer Dank gilt meiner Freundin Katharina für die mittlerweile mehr als sieben Jahre an meiner Seite. Mit ihrer grenzenlosen Untertützung ist sie ein fester Punkt in meinem Leben. Ich danke meinen Eltern Christa und Klaus, die mich immer dabei unterstützten, meinen eigenen Weg zu finden. Meinen Schwestern Anna und Rebekka danke ich für die vielen gemeinsamen Jahre.
Ich danke allen Mitgliedern des Instituts für Physikalische Biologie für gemeinsame Abende, interessante Gespräche und die außergewöhnliche Atmosphäre. Ich danke Manuel, Ingrid, Aldino, Jan und Hannah für die tolle Zusammenarbeit, die meiner Arbeit im Institut eine zweite Richtung gegeben hat.
Insbesondere erwähnen möchte ich Michael und Hannah, neben tollen Kollegen habe ich in ihnen wahre Freunde gefunden.

# Bibliography


Aaldering L, Tayeb H, Krishnan S, Fletcher S, Wilton S, Veedu R (2015) Smart functional nucleic acid chimeras: enabling tissue specific RNA targeting therapy. RNA Biol **12**:412–425, http://doi.org/10.1080/15476286.2015.1017234

Agard N, Baskin J, Prescher J, Lo A, Bertozzi C (2006) A comparative study of bioorthogonal reactions with azides. ACS Chemical Biology **1**(10):644–648, https://doi.org/10.1021/cb6003228

Alper T, Haig D, Clarke M (1978) The scrapie agent: evidence against its dependence for replication on intrinsic nucleic acid. J Gen Virol **3**:503–516, http://doi.org/10.1099/0022-1317-41-3-503

Asanuma H, Hayashi H, Zhao J, Liang X, Yamazawa A, Kuramochi T, Matsunaga D, Aiba Y, Kashida H, Komiyama M (2006) Enhancement of rna cleavage activity of 10-23 dnazyme by covalently introduced intercalator. Chemical communications (Cambridge, England) **5**:5062–5064, https://doi.org/10.1039/b611078a

Ashley G (1992) Modeling, synthesis, and hybridization properties of (L)-ribonucleic acid. J Am Chem Soc **114**:9731–9736, http://doi.org/10.1021/ja00051a001

Assetta B, Maginnis MS, Gracia Ahufinger I, Haley SA, Gee GV, Nelson CDS, O'Hara BA, Allen Ramdial SaA, Atwood WJ (2013) 5-ht2 receptors facilitate jc polyomavirus entry. Journal of virology **87**:13,490–13,498, https://doi.org/10.1128/JVI.02252-13

Bender H, Kane S, Zabel M (2016) Delivery of Therapeutic siRNA to the CNS Using Cationic and Anionic Liposomes. J Vis Exp **113**:e54106, http://dx.doi.org/10.3791/54106

Berry D, Lu D, Geva M, Watts J, Bhardwaj S, Oehler A, Renslo A, DeArmond S, Prusiner S, Gilesa K (2013) Drug resistance confounding prion therapeutics. Proc Natl Acad Sci USA **44**:E4160 – E416, http://dx.doi.org/10.1073/pnas.1317164110

Birmingham A, Anderson E, Sullivan K, Reynolds A, Boese Q, Leake D, Karpilow J, Khvorova A (2007) A protocol for designing siRNAs with high functionality and specificity. Nat Protoc **2**:2068–2078, http://dx.doi.org/10.1038/nprot.2007.278

Bitko V, Musiyenko A, Shulyayeva O, Barik S (2005) Inhibition of respiratory viruses by nasally administered siRNA. Nat Med **11**:50–55, http://doi.org/10.1038/nm1164

Bockman J, Kingsbury D, McKinley M, Bendheim P, Prusiner S (1985) Creutzfeldt-Jakob disease prion proteins in human brains. N Engl J Med **312**:73–78, https://doi.org/10.1056/NEJM198501103120202

Bolton D, McKinley M, Prusiner S (1982) Identification of a protein that purifies with the scrapie prion. Science **218**:1309–1311, http://10.1126/science.6815801

Bone I, Belton L, Walker A, Darbyshire J (2008) Intraventricular pentosan polyphosphate in human prion diseases: an observational study in the UK. Eur J Neurol **15**:458–464, http://doi.org/10.1111/j.1468-1331.2008.02108.x

Breaker R, Joyce G (1994) A DNA enzyme that cleaves RNA. Chemistry & Biology **1**(4):223–229, https://doi.org/10.1016/1074-5521(94)90014-0

Breaker R, Emilsson G, Lazarev D, Nakamura S, Puskarz I, Roth A, Sudarsan N (2003) A common speed limit for RNA-cleaving ribozymes and deoxyribozymes. RNA **9**:949–957, http://doi.org/10.1261/rna.5670703

Bremer J, Baumann F, Tiberi C, Wessig C, Fischer H, Schwarz P, Steele A, Toyka K, Nave K, Weis J, Aguzzi A (2010) Axonal prion protein is required for peripheral myelin maintenance. Nat Neurosci **13**:310–318, https://doi.org/10.1038/nn.2483

Brown P, Coker-Vann M, Pomeroy K, Franko M, Asher D, Gibbs CJ, Gajdusek D (1986) Diagnosis of Creutzfeldt-Jakob disease by Western blot identification of marker protein in human brain tissue. N Engl J Med **314**:547–551, https://doi.org/10.1056/NEJM198602273140904

Büeler H, Fischer M, Lang Y, Bluethmann H, Lipp H, DeArmond S, Prusiner S, Aguet M, Weissmann C (1992) Normal development and behaviour of mice lacking the neuronal cell-surface PrP protein. Nature **356**:577–582, http://dx.doi.org/10.1038/356577a0

Büeler H, Aguzzi A, Sailer A, Greiner R, Autenried P, Aguet M, Weissmann C (1993) Mice devoid of PrP are resistant to scrapie. Cell **73**:1339–1347, http://doi.org/10.1016/0092-8674(93)90360-3

Cairns MJ, Hopkins TM, Witherington C, Wang L, Sun LQ (1999) Target site selection for an rna-cleaving catalytic dna. Nature biotechnology **17**:480–486, https://doi.org/10.1038/8658

Cairns MJ, Hopkins TM, Witherington C, Sun LQ (2000) The influence of arm length asymmetry and base substitution on the activity of the 10-23 dna enzyme. Antisense & nucleic acid drug development **10**:323–332, https://doi.org/10.1089/oli.1.2000.10.323

Chang C, Wang M, Ou W, Chen P, Shen C, Lin P, Fang C, Chang D (2011) Human JC virus-like particles as a gene delivery vector. Expert Opin Biol Ther **11**:1169–1175, http://doi.org/10.1517/14712598.2011.583914

Chen L, Wang M, Ou W, Fung C, Chen P, Chang C, Huang W, Wang J, Lin P, Chang D (2010) Efficient gene transfer using the human JC virus-like particle that inhibits human colon adenocarcinoma growth in a nude mouse model. Gene Ther **17**:1033–1041, http://doi.org/10.1038/gt.2010.50

Cho E, Moloney F, Cai H, Au-Yeung A, China C, Scolyer R, Yosufi B, Raftery M, Deng J, Morton S, Hammond P, Arkenau H, Damian D, Francis D, Chesterman C, Barnetson R, Halliday G, Khachigian L (2013) Safety and tolerability of an intratumorally injected DNAzyme, Dz13,

in patients with nodular basal-cell carcinoma: A phase 1 first-in-human trial (DISCOVER). Lancet **381**:1835–1843, http://doi.org/10.1016/S0140-6736(12)62166-7

Cieslak M, Szymanski J, Adamiak RW, Cierniewski CS (2003) Structural rearrangements of the 10-23 dnazyme to beta 3 integrin subunit mrna induced by cations and their relations to the catalytic activity. The Journal of biological chemistry **278**:47,987–47,996, https://doi.org/10.1074/jbc.M300504200

Collinge J (2001) Prion diseases of humans and animals: Their causes and molecular basis. Annual Review of Neuroscience **24**(1):519–550, https://doi.org/10.1146/annurev.neuro.24.1.519

Come J, Fraser P, Lansbury PJ (1993) A kinetic model for amyloid formation in the prion diseases: importance of seeding. Proc Natl Acad Sci USA **90**:5959–5963

Creutzfeldt H (1920) Über eine eigenartige herdförmige Erkrankung des Zentralnervensystems. Z ges Neurol Psychiat **57**:1–18

Cuenoud B, Szostak J (1995) A DNA metalloenzyme with DNA ligase activity. Nature **375**(6532):611–614, https://doi.org/10.1038/375611a0

Daude N, Marella M, Chabry J (2003) Specific inhibition of pathological prion protein accumulation by small interfering RNAs. Journal of Cell Science **116**:2775–2779, http://doi.org/10.1242/jcs.00494

Dovydenko I, Venyaminova A, Pyshnyi D, Tarassov I, Entelis N (2016) Modifications in Therapeutic Oligonucleotides Improving the Delivery. RNA Technologies: Modified Nucleic Acids in Biology and Medicine pp 319–337, http://doi.org/10.1007/978-3-319-34175-0

Eigen M (1996) Prionics or The Kinetic basis of prion diseases. Biophys Chem **63**:A1–A18, https://doi.org/10.1016/S0301-4622(96)02250-8

Ellington A, Szostak J (1990) In vitro selection of RNA molecules that bind specific ligands. Nature **346**(6287):818–822, https://doi.org/10.1038/346818a0

Fedoruk-Wyszomirska A, Szymański M, Wyszko E, Barciszewska MZ, Barciszewski J (2009) Highly active low magnesium hammerhead ribozyme. Journal of biochemistry **145**:451–459, https://doi.org/10.1093/jb/mvn182

Fokina A, Meschaninova M, Durfort T, Venyaminova A, François J (2012) Targeting insulin-like growth factor I with 10-23 DNAzymes: 2'-O-methyl modifications in the catalytic core enhance mRNA cleavage. Biochemistry **51**:2181–2191, https://doi.org/10.1021/bi201532q

Fokina A, Stetsenko D, François J (2015) DNA enzymes as potential therapeutics: towards clinical application of 10-23 DNAzymes. Expert Opinion on Biological Therapy **15**(5):689–711, https://doi.org/10.1517/14712598.2015.1025048

Forloni G, Artuso V, Roiter I, Morbin M, Tagliavini F (2013) Therapy in prion diseases. Curr Top Med Chem **13**:2465–2476, http://doi.org/10.2174/15680266113136660173

de Fougerolles A, Novobrantseva T (2008) siRNA and the lung: research tool or therapeutic drug? Curr Opin Pharmacol **8**:280–285, http://doi.org/10.1016/j.coph.2008.04.005

Foust KD, Nurre E, Montgomery CL, Hernandez A, Chan CM, Kaspar BK (2009) Intravascular aav9 preferentially targets neonatal neurons and adult astrocytes. Nature biotechnology **27**:59–65, https://doi.org10.1038/nbt.1515

Friberg NK, Hung G, Wancewicz E, Giles K, Black C, Freier S, Bennett F, Dearmond S, Freyman Y, Lessard P, Ghaemmaghami S, Prusiner S (2012) Intracerebral Infusion of Antisense Oligonucleotides Into Prion-infected Mice. Mol Ther Nucleic Acids **1**:e9, http://dx.doi.org/10.1038/mtna.2011.6

Gajdusek D, Zigas V (1959) Kuru: Clinical, pathological and epidemiological study of an acute progressive degenerative disease of the central nervous system among natives of the eastern highlands of new guinea. The American Journal of Medicine **26**(3):442–469, https://doi.org/10.1016/0002-9343(59)90251-7

Gajdusek D, Gibbs C, Alpers M (1966) Experimental transmission of a kuru-like syndrome to chimpanzees. Nature **209**:794–796, http://doi.org/10.1038/209794a0

Garbesi A, Capobianco M, Colonna F, Tondelli L, Arcamone F, Manzini G, Hilbers C, Aelen J, Blommers M (1993) L-DNAs as potential antimessenger oligonucleotides: a reassessment. Nucleic Acids Res **21**:4159–4165

Gibbons R, Hunter G (1967) Nature of the Scrapie Agent. Nature **215**:1041–1043, http://doi.org/10.1038/2151041a0

Gibbs C, Gajdusek D, Asher D, Alpers M, Beck E, Daniel P, Matthews W (1968) Creutzfeldt-Jakob Disease (Spongiform Encephalopathy): Transmission to the Chimpanzee. Science **161**:388–389, http://doi.org/10.1126/science.161.3839.388

Gibbs CJ, Gajdusek D, Latarjet R (1978) Unusual resistance to ionizing radiation of the viruses of kuru, Creutzfeldt-Jakob disease, and scrapie. Proc Natl Acad Sci USA **12**:6268–6270

Griffith J (1967) Nature of the Scrapie Agent: Self-replication and Scrapie. Nature **215**:1043–1044, http://doi.org/10.1038/2151043a0

Hadlow W (1959) SCRAPIE AND KURU. The Lancet **274**(7097):289–290, https://doi.org/10.1016/s0140-6736(59)92081-1

Haïk S, Marcon G, Mallet A, Tettamanti M, Welaratne A, Giaccone G, Azimi S, Pietrini V, Fabreguettes J, Imperiale D, Cesaro P, Buffa C, Aucan C, Lucca U, Peckeu L, Suardi S, Tranchant C, Zerr I, Houillier C, Redaelli V, Vespignani H, Campanella A, Sellal F, Krasnianski A, Seilhean D, Heinemann U, Sedel F, Canovi M, Gobbi M, Di Fede G, Laplanche J, Pocchiari M,

Salmona M, Forloni G, Brandel J, Tagliavini F (2014) Doxycycline in Creutzfeldt-Jakob disease: a phase 2, randomised, double-blind, placebo-controlled trial. Lancet Neurol **2**:150–158, http://doi.org/10.1016/S1474-4422(13)70307-7

Hoehlig K, Bethge L, Klussmann S (2015) Stereospecificity of oligonucleotide interactions revisited: no evidence for heterochiral hybridization and ribozyme/DNAzyme activity. PLoS One **10**:e0115,328, https://doi.org/10.1371/journal.pone.0115328

Hoffmann D, Böker K, Schneider S, Eckermann-Felkl E, Schuder A, Komrakova M, Sehmisch S, Gruber J (2016) In Vivo siRNA Delivery Using JC Virus-like Particles Decreases the Expression of RANKL in Rats. Mol Ther Nucleic Acids **5**:e298, http://doi.org/10.1038/mtna.2016.15

Houseley J, Tollervey D (2009) The Many Pathways of RNA Degradation. Cell **136**:763–776, http://doi.org/10.1016/j.cell.2009.01.019

Hoyer J, Neundorf I (2012) Peptide vectors for the nonviral delivery of nucleic acids. Acc Chem Res **45**:1048–1056, http://doi.org/10.1021/ar2002304

Hörnlimann B, Riesner D, Kretzschmar H (2001) Prionen und Prionkrankheiten. De Gruyter, URL http://www.ebook.de/de/product/1417563/beat_hoernlimann_detlev_riesner_hans_kretzschmar_prionen_und_prionkrankheiten.html

Jakob A (1921) Über eigenartige Erkrankungen des Zentralnervensystems mit bemerkenswerten anatomischen Befunden (spastische Pseudosklerose-Encephalomyelopathie mit disseminierten Degenerationsherden). Z ges Neurol Psychiat **64**:147–228

Kanasty R, Dorkin J, Vegas A, Anderson D (2013) Delivery materials for siRNA therapeutics. Nat Mater **12**:967–977, http://doi.org/10.1038/nmat3765

Kawasaki Y, Kawagoe K, Chen C, Teruya K, Sakasegawa Y, Doh-ura K (2007) Orally administered amyloidophilic compound is effective in prolonging the incubation periods of animals cerebrally infected with prion diseases in a prion strain-dependent manner. J Virol **81**:12,889–12,898, http://doi.org/10.1128/JVI.01563-07

Kellings K, Meyer N, Mirenda C, Prusiner S, Riesner D (1992) Further analysis of nucleic acids in purified scrapie prion preparations by improved return refocusing gel electrophoresis. J Gen Virol **73**:1025–1029, https://doi.org/10.1099/0022-1317-73-4-1025

Khvorova A, Watts J (2017) The chemical evolution of oligonucleotide therapies of clinical utility. Nat Biotechno **35**:238–248, https://doi.org/10.1038/nbt.3765

Khvorova A, Lescoute A, Westhof E, Jayasena SD (2003) Sequence elements outside the hammerhead ribozyme catalytic core enable intracellular activity. Nature structural biology **10**:708–712, https://doi.org/10.1038/nsb959

Klussmann S, Nolte A, Bald R, Erdmann V, Fürste J (1996) Mirror-image RNA that binds D-adenosine. Nat Biotechnol **14**:1112–1115, http://doi.org/10.1038/nbt0996-1112

Kordasiewicz H, Stanek L, Wancewicz E, Mazur C, McAlonis M, Pytel K, Artates J, Weiss A, Cheng S, Shihabuddin L, Hung G, Bennett C, Cleveland D (2012) Sustained therapeutic reversal of Huntington's disease by transient repression of huntingtin synthesis. Neuron **74**:1031–1044, http://doi.org/10.1016/j.neuron.2012.05.009

Kore A, Vaish N, Kutzke U, Eckstein F (1998) Sequence specificity of the hammerhead ribozyme revisited; the NHH rule. Nucleic Acids Res **26**:4116–4120, https://doi.org/10.1093/nar/26.18.4116

Korth C, Peters P (2006) Emerging pharmacotherapies for Creutzfeldt-Jakob diseases. Arch Neurol **63**:497–501, http://doi.org/10.1001/archneur.63.4.497

Škrlj N, Drevenšek G, Hudoklin S, Romih R, Šerbec VČ, Dolinar M (2013) Recombinant Single-Chain Antibody with the Trojan Peptide Penetratin Positioned in the Linker Region Enables Cargo Transfer Across the Blood–Brain Barrier. Appl Biochem Biotechnol **1**:159–169, http://doi.org/10.1007/s12010-012-9962-7

Krug N, Hohlfeld J, Kirsten A, Kornmann O, Beeh K, Kappeler D, Korn S, Ignatenko S, Timmer W, Rogon C, Zeitvogel J, Zhang N, Bille J, Homburg U, Turowska A, Bachert C, Werfel T, Buhl R, Renz J, Garn H, Renz H (2015) Allergen-induced asthmatic responses modified by a GATA3-specific DNAzyme. N Engl J Med **372**:1987–1995, http://doi.org/10.1056/NEJMoa1411776

Kumar P, Wu H, McBride J, Jung K, Kim M, Davidson B, Lee S, Shankar P, Manjunath N (2007) Transvascular delivery of small interfering RNA to the central nervous system. Nature **448**:39–43, http://doi.org/10.1038/nature05901

Kurreck J, Bieber B, Jahnel R, Erdmann V (2002) Comparative study of DNA enzymes and ribozymes against the same full-length messenger RNA of the vanilloid receptor subtype I. J Biol Chem **277**:7099–7107, http://doi.org/10.1074/jbc.M107206200

Latarjet R, Muel B, Haig D, Clarke M, Alper T (1970) Inactivation of the Scrapie Agent by Near Monochromatic Ultraviolet Light. Nature **227**:1341–1343, http://doi.org/10.1038/2271341a0

Laurén J, Gimbel D, Nygaard H, Gilbert J, Strittmatter S (2009) Cellular prion protein mediates impairment of synaptic plasticity by amyloid-beta oligomers. Nature **457**:1128–1132, http://dx.doi.org/10.1038/nature07761

Lehmann S, Relano-Gines A, Resina S, Brillaud E, Casanova D, Vincent C, Hamela C, Poupeau S, Laffont M, Gabelle A, Delaby C, Belondrade M, Arnaud J, Alvarez M, Maurel J, Maurel P, Crozet C (2014) Systemic delivery of siRNA down regulates brain prion protein and ameliorates neuropathology in prion disorder. PLoS One **2**:e8879–e8879, http://doi.org/10.1371/journal.pone.0088797

Li Y, Breaker R (1999) Kinetics of RNA Degradation by Specific Base Catalysis of Transesterification Involving the 2'-Hydroxyl Group. J Am Chem Soc **121**:5364–5372, http://doi.org/10.1021/ja990592p

Lu ZX, Ma XQ, Yang LF, Wang ZL, Zeng L, Li ZJ, Li XN, Tang M, Yi W, Gong JP, Sun LQ, Cao Y (2008) Dnazymes targeted to ebv-encoded latent membrane protein-1 induce apoptosis and enhance radiosensitivity in nasopharyngeal carcinoma. Cancer letters **265**:226–238, https://doi.org/10.1016/j.canlet.2008.02.019

Mallucci G, Dickinson A, Linehan J, Klöhn P, Brandner S, J C (2003) Depleting neuronal PrP in prion infection prevents disease and reverses spongiosis. Science **302**:871–874, http://doi.org/10.1126/science.1090187

Masel J, Jansen V, Nowak M (1999) Quantifying the kinetic parameters of prion replication. Biophys Chem **77**:139–152, https://doi.org/10.1016/S0301-4622(99)00016-2

Masters C, Gajdusek D, Gibbs C (1981) Creutzfeldt-Jakob disease virus isolations from the Gerstmann-Sträussler syndrome with an analysis of the various forms of amyloid plaque deposition in the virus-induced spongiform encephalopathies. Brain **104**:559–588, http://doi.org/10.1093/brain/104.3.559

Mendell JR, Al-Zaidy S, Shell R, Arnold WD, Rodino-Klapac LR, Prior TW, Lowes L, Alfano L, Berry K, Church K, Kissel JT, Nagendran S, L'Italien J, Sproule DM, Wells C, Cardenas JA, Heitzer MD, Kaspar A, Corcoran S, Braun L, Likhite S, Miranda C, Meyer K, Foust KD, Burghes AHM, Kaspar BK (2017) Single-dose gene-replacement therapy for spinal muscular atrophy. The New England journal of medicine **377**:1713–1722, https://doi.org/10.1056/NEJMoa1706198

Nair J, Willoughby J, Chan A, Charisse K, Alam M, Wang Q, Hoekstra M, Kandasamy P, Kel'in A, Milstein S, Taneja N, O'Shea J, Shaikh S, Zhang L, van der Sluis R, Jung M, Akinc A, Hutabarat R, Kuchimanchi S, Fitzgerald K, Zimmermann T, van Berkel T, Maier M, Rajeev K, Manoharan M (2014) Multivalent N-Acetylgalactosamine-Conjugated siRNA Localizes in Hepatocytes and Elicits Robust RNAi-Mediated Gene Silencing. J Am Chem Soc **136**:16,958–16,961, http://doi.org/10.1021/ja505986a

Nawrot B, Widera K, Wojcik M, Rebowska B, Nowak G, Stec W (2007) Mapping of the functional phosphate groups in the catalytic core of deoxyribozyme 10-23. FEBS Journal **274**(4):1062–1072, https://doi.org/10.1111/j.1742-4658.2007.05655.x

Neu U, Maginnis MS, Palma AS, Ströh LJ, Nelson CDS, Feizi T, Atwood WJ, Stehle T (2010) Structure-function analysis of the human jc polyomavirus establishes the lstc pentasaccharide as a functional receptor motif. Cell host & microbe **8**:309–319, https://doi.org/10.1016/j.chom.2010.09.004

Niu X, Peng Z, Duan W, Wang H, Wang P (2006) Inhibition of HPV 16 E6 oncogene expression by RNA interference in vitro and in vivo. Int J Gynecol Cancer **16**:743–751, http://doi.org/10.1111/j.1525-1438.2006.00384.x

Nowakowski J, Shim P, Prasad G, Stout C, Joyce G (1999) Crystal structure of an 82-nucleotide RNA-DNA complex formed by the 10-23 DNA enzyme. Nat Struct Biol **6**:151–156, https://doi.org/10.1038/5839

Ortigão J, Rösch H, Selter H, Fröhlich A, Lorenz A, Montenarh M, Seliger H (1992) Antisense effect of oligodeoxynucleotides with inverted terminal internucleotidic linkages: a minimal modification protecting against nucleolytic degradation. Antisense Res Dev **2**:129–146, http://doi.org/10.1089/ard.1992.2.129

Otto M, Cepek L, Ratzka P, Doehlinger S, Boekhoff I, Wiltfang J, Irle E, Pergande G, Ellers-Lenz B, Windl O, Kretzschmar H, Poser S, Prange H (2004) Efficacy of flupirtine on cognitive function in patients with CJD: A double-blind study. Neurology **62**:714–718

Pan K, Baldwin M, Nguyen J, Gasset M, Serban A, Groth D, Mehlhorn I, Huang Z, Fletterick R, Cohen F, Prusiner S (1993) Conversion of alpha-helices into beta-sheets features in the formation of the scrapie prion proteins. Proc Natl Acad Sci USA **90**:10,962–10,966, https://doi.org/10.1073/pnas.90.23.10962

Pattison I, Jones K (1967) The possible nature of the transmissible agent of scrapie. Veterinary Record **80**:2–9, http://dx.doi.org/10.1136/vr.80.1.2

Pfeifer A, Eigenbrod S, Al-Khadra S, Hofmann A, Mitteregger G, Moser M, Bertsch U, Kretzschmar H (2006) Lentivector-mediated RNAi efficiently suppresses prion protein and prolongs survival of scrapie-infected mice. J Clin Invest **116**:3204–3210, http://dx.doi.org/10.1172/JCI29236

Poland D (1974) Recursion relation generation of probability profiles for specific-sequence macromolecules with long-range correlations. Biopolymers **13**:1859–1871, https://doi.org/10.1002/bip.1974.360130916

Prakash T, Graham M, Yu J, Carty R, Low A, Chappell A, Schmidt K, Zhao C, Aghajan M, Murray H, Riney S, Booten S, Murray S, Gaus H, Crosby J, Lima W, Guo S, Monia B, Swayze E, Seth P (2014) Targeted delivery of antisense oligonucleotides to hepatocytes using triantennary N-acetyl galactosamine improves potency 10-fold in mice. Nucleic Acids Res **42**:8796–8807, http://doi.org/10.1093/nar/gku531

Prusiner S (1982) Novel proteinaceous infectious particles cause scrapie. Science **216**:136–144, http://doi.org/10.1126/science.6801762

Prusiner S (1998) Prions. Proc Natl Acad Sci USA **95**:13,363–13,383, http://doi.org/10.1073/pnas.95.23.13363

Prusiner S, McKinley M, Groth D, Bowman K, Mock N, Cochran S, Masiarz F (1981) Scrapie agent contains a hydrophobic protein. Proc Natl Acad Sci USA **78**:6675–6679

Prusiner S, Bolton D, DF G, Bowman K, Cochran S, McKinley M (1982) Further purification and characterization of scrapie prions. Biochemistry **21**:6942–6950, http://doi.org/10.1021/bi00269a050

Prusiner S, Groth D, Bolton D, Kent S, Hood L (1984) Purification and structural studies of a major scrapie prion protein. Cell **38**:127–134, https://doi.org/10.1016/0092-8674(84)90533-6

Pulford B, Reim N, Bell A, Veatch J, Forster G, Bender H, Meyerett C, Hafeman S, Michel B, Johnson T, Wyckoff A, Miele G, Julius C, Kranich J, Schenkel A, Dow S, Zabel M (2010) Liposome-siRNA-peptide complexes cross the blood-brain barrier and significantly decrease PrP on neuronal cells and PrP in infected cell cultures. PLoS One **5**:e11,085, http://dx.doi.org/10.1371/journal.pone.0011085

Raouane M, Desmaële D, Urbinati G, Massaad-Massade L, Couvreur P (2012) Lipid conjugated oligonucleotides: a useful strategy for delivery. Bioconjug Chem **23**:1091–1104, http://doi.org/10.1021/bc200422w

Robaldo L, Izzo F, Dellafiore M, Proietti C, Elizalde P, JMontserrat J, Iribarren A (2012) Influence of conformationally restricted pyrimidines on the activity of 10–23 DNAzymes. Bioorganic & Medicinal Chemistry **20**(8):2581–2586, https://doi.org/10.1016/j.bmc.2012.02.047

Romani A (2011) Cellular magnesium homeostasis. Arch Biochem Biophys **512**:1–23, https://doi.org/10.1016/j.abb.2011.05.010

Romani A, Scarpa A (1992) Regulation of cell magnesium. Arch Biochem Biophys **298**:1–12

Roucou X, Gains M, LeBlanc A (2004) Neuroprotective functions of prion protein. J Neurosci Res **75**:153–161, https://doi.org/10.1002/jnr.10864

Safar J, Kellings K, Serban A, Groth D, Cleaver J, Prusiner S, Riesner D (2005) Search for a prion-specific nucleic acid. J Virol **79**:10,796–10,806, https://doi.org/10.1128/JVI.79.16.10796-10806.2005

Santiago FS, Lowe HC, Kavurma MM, Chesterman CN, Baker A, Atkins DG, Khachigian LM (1999) New dna enzyme targeting egr-1 mrna inhibits vascular smooth muscle proliferation and regrowth after injury. Nature medicine **5**:1264–1269, https://doi.org/10.1038/15215

Santoro S, Joyce G (1997) A general purpose RNA-cleaving DNA enzyme. Proc Natl Acad Sci USA **94**:4262–4266, http://doi.org/10.1073/pnas.94.9.4262

Santoro S, Joyce G (1998) Mechanism and utility of an RNA-cleaving DNA enzyme. Biochemistry **37**:13,330–13,342, http://doi.org/10.1021/bi9812221

Sawa H, Komagome R (2005) The jc virus-like particle overlay assay. Methods in molecular biology (Clifton, NJ) **292**:175–186

Schubert S, Gül D, Grunert H, Zeichhardt H, Erdmann V, Kurreck J (2003) RNA cleaving '10-23' DNAzymes with enhanced stability and activity. Nucleic Acids Res **31**:5982–5992

Schubert S, Fürste J, Werk D, Grunert H, Zeichhardt H, Erdmann V, Kurreck J (2004) Gaining target access for deoxyribozymes. J Mol Biol **339**:355–363, http://dx.doi.org/10.1016/j.jmb.2004.03.064

Sel S, Wegmann M, Dicke T, Sel S, Henke W, Yildirim AO, Renz H, Garn H (2008) Effective prevention and therapy of experimental allergic asthma using a gata-3-specific dnazyme. The Journal of allergy and clinical immunology **121**:910–916.e5, https://doi.org/10.1016/j.jaci.2007.12.1175

Sigurdsson B (1954) RIDA, a chronic encephalitis of sheep. British Veterinary Journal **110**(9):341–354, https://doi.org/10.1016/s0007-1935(17)50172-4

Silverman S (2005) In vitro selection, characterization, and application of deoxyribozymes that cleave RNA. Nucleic Acids Res **33**:6151–6163, http://dx.doi.org/10.1093/nar/gki930

Silverman S (2016) Catalytic DNA: Scope, Applications, and Biochemistry of Deoxyribozymes. Trends Biochem Sci **41**:595–609, http://dx.doi.org/10.1016/j.tibs.2016.04.010

Smuga D, Majchrzak K, Sochacka E, Nawrot B (2010) Rna-cleaving 10-23 deoxyribozyme with a single amino acid-like functionality operates without metal ion cofactors. New J Chem **34**:934–948, https://doi.org/10.1039/B9NJ00705A

Steger G (1994) Thermal denaturation of double-stranded nucleic acids: prediction of temperatures critical for gradient gel electrophoresis and polymerase chain reaction. Nucleic acids research **22**:2760–2768

Sugimoto N, Nakano S, Katoh M, Matsumura A, Nakamuta H, Ohmichi T, Yoneyama M, Sasaki M (1995) Thermodynamic parameters to predict stability of rna/dna hybrid duplexes. Biochemistry **34**:11,211–11,216

Sun L, Cairns M, Gerlach W, Witherington C, Wang L, King A (1999) Suppression of smooth muscle cell proliferation by a c-myc RNA-cleaving deoxyribozyme. J Biol Chem **274**:17,236–41, http://doi.org/10.1074/jbc.274.24.17236

Sunshine J, Bishop C, Green J (2011) Advances in polymeric and inorganic vectors for nonviral nucleic acid delivery. Ther Deliv **2**:493–521

Suzuki S, Sawa H, Komagome R, Orba Y, Yamada M, Okada Y, Ishida Y, Nishihara H, Tanaka S, Nagashima K (2001) Broad distribution of the jc virus receptor contrasts with a marked cellular restriction of virus replication. Virology **286**:100–112, https://doi.org/10.1006/viro.2001.0972

Szabat M, Gudanis D, Kotkowiak W, Gdaniec Z, Kierzek R, Pasternak A (2016) Thermodynamic Features of Structural Motifs Formed by b-L-RNA. PLoS One **11**:e0149,478, https://doi.org/10.1371/journal.pone.0149478

Tafer H, Ameres S, Obernosterer G, Gebeshuber C, Schroeder R, Martinez J, Hofacker I (2008) The impact of target site accessibility on the design of effective siRNAs. Nature biotechnology **26**:578–83, http://doi.org/10.1038/nbt1404

Tilly G, Chapuis J, Vilette D, Laude H, Vilotte J (2003) Efficient and specific down-regulation of prion protein expression by RNAi. Biochem Biophys Res Commun **305**:548–551, http://doi.org/10.1016/S0006-291X(03)00805-2

Tram K, Xia J, Gysbers R, Li Y (2015) An efficient catalytic dna that cleaves l-rna. PloS one **10**:e0126,402, https://10.1371/journal.pone.0126402

Tuerk C, Gold L (1990) Systematic evolution of ligands by exponential enrichment: RNA ligands to bacteriophage t4 DNA polymerase. Science **249**(4968):505–510, https://doi.org/10.1126/science.2200121

Um J, Nygaard H, Heiss J, Kostylev M, Stagi M, Vortmeyer A, Wisniewski T, Gunther E, Strittmatter S (2012) Alzheimer amyloid-$\beta$ oligomer bound to postsynaptic prion protein activates Fyn to impair neurons. Nat Neurosci **15**:1227–1235, http://dx.doi.org/10.1038/nn.3178

Valori CF, Ning K, Wyles M, Mead RJ, Grierson AJ, Shaw PJ, Azzouz M (2010) Systemic delivery of scaav9 expressing smn prolongs survival in a model of spinal muscular atrophy. Science translational medicine **2**:35ra42, https://doi.org/10.1126/scitranslmed.3000830

Vater A, Klussmann S (2015) Turning mirror-image oligonucleotides into drugs: the evolution of Spiegelmer(®) therapeutics. Drug Discov Today :147–155, http://doi.org/10.1016/j.drudis.2014.09.004

Vester B, Hansen L, Lundberg L, Babu B, Sørensen M, Wengel J, Douthwaite S (2006) Locked nucleoside analogues expand the potential of DNAzymes to cleave structured RNA targets. BMC Mol Biol **7**:19, http://dx.doi.org/10.1186/1471-2199-7-19

Victor J, Steger G, Riesner D (in press) Inability of DNAzymes to cleave RNA *in vivo* is due to limited $Mg^{2+}$ concentration in cells. European Biophysical Journal

Wagner J, Ryazanov S, Leonov A, Levin J, Shi S, Schmidt F, Prix C, Pan-Montojo F, Bertsch U, Mitteregger-Kretzschmar G, Geissen M, Eiden M, Leidel F, Hirschberger T, Deeg A, Krauth J, Zinth W, Tavan P, Pilger J, Zweckstetter M, Frank T, Bähr M, Weishaupt J, Uhr M, Urlaub H, Teichmann U, Samwer M, Bötzel K, Groschup M, Kretzschmar H, Griesinger C, Giese A (2013) Anle138b: a novel oligomer modulator for disease-modifying therapy of neurodegenerative diseases such as prion and Parkinson's disease. Acta Neuropathol **6**:795–813, http://doi.org/10.1007/s00401-013-1114-9

Wang B, Cao L, Chiuman W, Li Y, Xi Z (2010) Probing the function of nucleotides in the catalytic cores of the 8-17 and 10-23 DNAzymes by abasic nucleotide and c3 spacer substitutions. Biochemistry **49**(35):7553–7562, https://doi.org/10.1021/bi100304b

Watson S, Chang Y, O'Connell D, Weigand L, Ringquist S, Parma D (2000) Anti-L-selectin aptamers: binding characteristics, pharmacokinetic parameters, and activity against an intravascular target in vivo. Antisense Nucleic Acid Drug Dev **10**:63–75, https://doi.org/10.1089/oli.1.2000.10.63

Wender P, Mitchell D, Pattabiraman K, Pelkey E, Steinman L, Rothbard J (2000) The design, synthesis, and evaluation of molecules that enable or enhance cellular uptake: peptoid molecular transporters. Proc Natl Acad Sci USA **97**:13,003–13,008, http://doi.org/10.1073/pnas.97.24.13003

White A, Enever P, Tayebi M, Mushens R, Linehan J, Brandner S, Anstee D, Collinge J, Hawke S (2003) Monoclonal antibodies inhibit prion replication and delay the development of prion disease. Nature **422**:80–83, http://doi.org/10.1038/nature01457

White M, Farmer M, Mirabile I, Brandner S, Collinge J, Mallucci G (2008) Single treatment with RNAi against prion protein rescues early neuronal dysfunction and prolongs survival in mice with prion disease. Proc Natl Acad Sci USA **29**:10,238–10,243, http://doi.org/10.1073/pnas.0802759105

Whitehead K, Langer R, Anderson D (2009) Knocking down barriers: advances in siRNA delivery. Nat Rev Drug Discov **8**:129–138, https://doi.org/10.1038/nrd2742

Whittle I, Knight R, Will R (2006) Unsuccessful intraventricular pentosan polysulphate treatment of variant Creutzfeldt-Jakob disease. Acta Neurochir (Wien) **6**:677–679, http://doi.org/10.1007/s00701-006-0772-y

Williams G, Fischer A, Fischer J, Kurland L (1964) An evaluation of the kuru genetic hypothesis. J Genet Hum **13**:11–21

Wilson D, Szostak J (1999) In vitro selection of functional nucleic acids. Annual Review of Biochemistry **68**(1):611–647, https://doi.org/10.1146/annurev.biochem.68.1.611

Wu Y, Yu L, McMahon R, Rossi JJ, Forman SJ, Snyder DS (1999) Inhibition of bcr-abl oncogene expression by novel deoxyribozymes (dnazymes). Human gene therapy **10**:2847–2857, https://doi.org/10.1089/10430349950016573

Wyszko E, Mueller F, Gabryelska M, Bondzio A, Popenda M, Barciszewski J, Erdmann V (2014) Spiegelzymes® mirror-image hammerhead ribozymes and mirror-image DNAzymes, an alternative to siRNAs and microRNAs to cleave mRNAs in vivo? PloS One **9**:e86,673, http://dx.doi.org/10.1371/journal.pone.0086673

Yang X, Xiao Z, Zhu J, Li Z, He J, Zhang L, Yang Z (2016) Spatial conservation studies of nucleobases in 10–23 DNAzyme by 2′-positioned isonucleotides and enantiomers for increased activity. Organic & Biomolecular Chemistry **14**(17):4032–4038, https://doi.org/10.1039/c6ob00390g

Yen L, Strittmatter SM, Kalb RG (1999) Sequence-specific cleavage of huntingtin mrna by catalytic dna. Annals of neurology **46**:366–373

Young DD, Lively MO, Deiters A (2010) Activation and deactivation of dnazyme and antisense function with light for the photochemical regulation of gene expression in mammalian cells. Journal of the American Chemical Society **132**:6183–6193, https://doi.org/10.1021/ja100710j

Zhang L, Gasper WJ, Stass SA, Ioffe OB, Davis MA, Mixson AJ (2002) Angiogenic inhibition mediated by a dnazyme that targets vascular endothelial growth factor receptor 2. Cancer research **62**:5463–5469